NASA/TM—1999–209205

# Program for Arctic Regional Climate Assessment (PARCA)

## Greenland Science and Planning Meeting
## October 5–6, 1998
## Wallops Island, Virginia


*Program Scientist: Dr. Sivaprasad Gogineni*
*Project Scientist: Dr. Robert H. Thomas*
*Edited by: Dr. Waleed Abdalati*


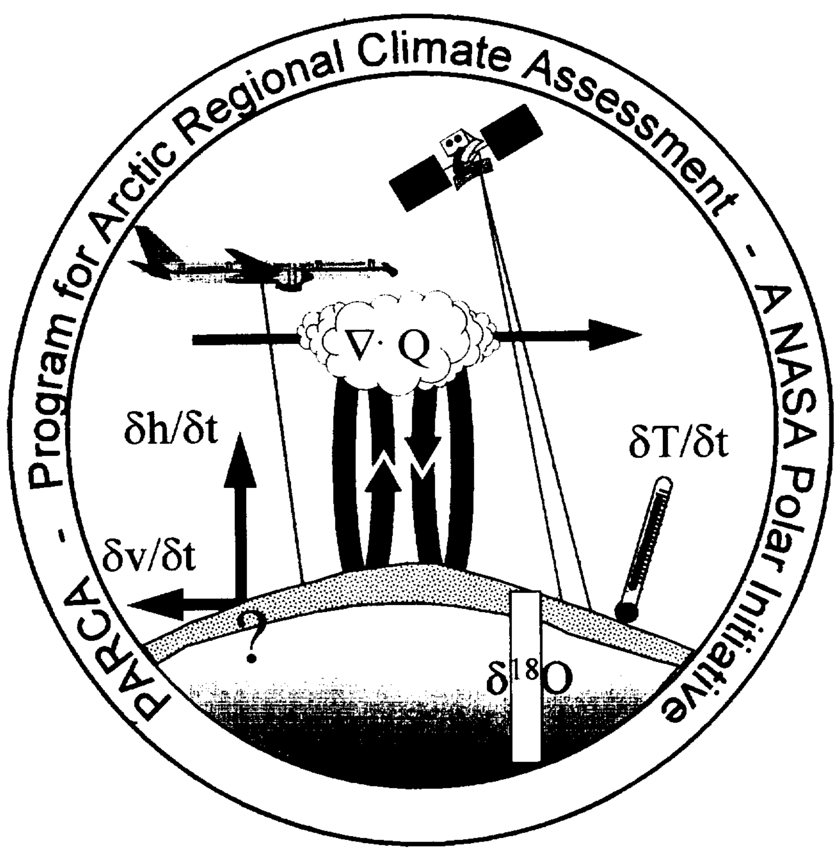



April 1999

## The NASA STI Program Office ... in Profile

Since its founding, NASA has been dedicated to the advancement of aeronautics and space science. The NASA Scientific and Technical Information (STI) Program Office plays a key part in helping NASA maintain this important role.

The NASA STI Program Office is operated by Langley Research Center, the lead center for NASA's scientific and technical information. The NASA STI Program Office provides access to the NASA STI Database, the largest collection of aeronautical and space science STI in the world. The Program Office is also NASA's institutional mechanism for disseminating the results of its research and development activities. These results are published by NASA in the NASA STI Report Series, which includes the following report types:

- TECHNICAL PUBLICATION. Reports of completed research or a major significant phase of research that present the results of NASA programs and include extensive data or theoretical analysis. Includes compilations of significant scientific and technical data and information deemed to be of continuing reference value. NASA's counterpart of peer-reviewed formal professional papers but has less stringent limitations on manuscript length and extent of graphic presentations.
- TECHNICAL MEMORANDUM. Scientific and technical findings that are preliminary or of specialized interest, e.g., quick release reports, working papers, and bibliographies that contain minimal annotation. Does not contain extensive analysis.
- CONTRACTOR REPORT. Scientific and technical findings by NASA-sponsored contractors and grantees.
- CONFERENCE PUBLICATION. Collected papers from scientific and technical conferences, symposia, seminars, or other meetings sponsored or cosponsored by NASA.
- SPECIAL PUBLICATION. Scientific, technical, or historical information from NASA programs, projects, and mission, often concerned with subjects having substantial public interest.
- TECHNICAL TRANSLATION. English-language translations of foreign scientific and technical material pertinent to NASA's mission.

Specialized services that complement the STI Program Office's diverse offerings include creating custom thesauri, building customized databases, organizing and publishing research results . . . even providing videos.

For more information about the NASA STI Program Office, see the following:

- Access the NASA STI Program Home Page at http://www.sti.nasa.gov/STI-homepage.html
- E-mail your question via the Internet to help@sti.nasa.gov
- Fax your question to the NASA Access Help Desk at (301) 621-0134
- Telephone the NASA Access Help Desk at (301) 621-0390
- Write to:
  NASA Access Help Desk
  NASA Center for AeroSpace Information
  7121 Standard Drive
  Hanover, MD 21076–1320

NASA/TM—1999-209205

# Program for Arctic Regional Climate Assessment (PARCA)

## Greenland Science and Planning Meeting
## October 5–6, 1998
## Wallops Island, Virginia

***Sivaprasad Gogineni, Polar Research Program Manager, NASA Headquarters***
*Department of Electrical Engineering and Computer Science, The University of Kansas*
*Lawrence, Kansas*

***Robert H. Thomas, Project Scientist***
*EG&G Services, Inc., NASA Wallops Flight Facility*
*Wallops Island, Virginia*

***Waleed Abdalati, Editor***
*Laboratory for Hydrospheric Processes, NASA Goddard Space Flight Center*
*Greenbelt, Maryland*

National Aeronautics and
Space Administration

**Goddard Space Flight Center**
Greenbelt, Maryland 20771

April 1999

Available from:

NASA Center for AeroSpace Information
7121 Standard Drive
Hanover, MD 21076–1320
Price Code: A17

National Technical Information Service
5285 Port Royal Road
Springfield, VA 22161
Price Code: A10

**The results presented in this document are preliminary and in largely unpublished.**

**Anyone interested in using any of these results or referring to them should contact the appropriate principal investigators**

# Table of Contents

Executive Summary ........ 1

Introduction ........ 4
*R.. Thomas*

Elevation Change of the Southern Greenland Ice Sheet: Update ........ 6
*C. Davis, C. Kluever, and B. Haines*

Large Ice Discharge from the Greenland Ice Sheet ........ 12
*E. Rignot*

Ice Flow in the North East Greenland Ice Stream ........ 16
*I. Joughin, M. Fahnestock, and D. MacAyael*

Satellite Observations of Ice Sheet Climate on Decadal Time Scales ........ 20
*D. Winebrenner and R. Arthern*

Airborne Resurveys of the Southern Greenland Ice Sheet ........ 22
*W. Krabill, E. Frederick, S. Manizade, C. Martin, J. Sonntag, R. Swift, R. Thomas, W. Wright, and J. Yungel*

Focused SAR Processing of Coherent Depth Sounder Data and Results from 1998 NGRIP Experiment .... 25
*J. Legarsky, and S. Gogineni*

Airborne Ice Thickness Measurement: Status Report and Future Work ........ 32
*T. Akins, S. Gogineni, P. Kanagaratnam, J. Legarsky, and A. Wong*

High Resolution Monitoring of Internal Layers at NGRIP ........ 35
*P. Kanagaratnam, S. Gogineni, J. Legarsky, and T. Akins*

Ultra-Wide Band Ground-Based Radar Measurements ........ 37
*F. Baumgartner and K. Jezek*

Mass Balance of the North and East Sides of the Ice Sheet ........ 38
*R. Thomas and B. Csatho*

Local Rates of Ice Sheet Thickness Change ........ 42
*G. Hamilton*

Absolute Gravity and GPS Measurements in Greenland ........ 45
*J. Wahr, T. van Dam, D. Robertson, K. Larson, and O. Francis*

Accumulation Estimates from Ice Cores ........ 48
*R. Bales, J. Burkhart, J. McConnel, and B. Snyder*

Greenland Net Annual Snow Accumulation: Temporal Perspective and Spatial Constraints .................. 54
*E. Mosley-Thompson*

Interdisciplinary Determination of Accumulation Patterns on the Greenland Ice Sheet: Combined Atmospheric Modeling, Field, and Remote Sensing Studies .............................................................. 60
*C. Shuman and R. Bindschadler*

Greenland Ice Sheet Climatology: GC-Net Status and Applications ................................................ 63
*K. Steffen, J. Box, J. Weber, and J. Estupinen*

Interpreting Aircraft-Derived Ice Sheet Changes Using Climate Station Data .................................. 71
*W. Abdalati, J. Box, and K. Steffen*

Evaluation of Recent Precipitation Studies for the Greenland Ice Sheet ........................................... 74
*D. Bromwich, and Q.S. Chen*

Development of Greenland GIS Database System (GGDS) ........................................................... 80
*B. Csatho, C. Kim, and J. Bolzan*

Software Development for Visualization and Analysis of Scanning Laser Altimetry Data ...................... 85
*S. Filin and B. Csatho*

Appendix I: Meeting Participants ................................................................................. 88

Appendix II: Listing of PARCA Publications ...................................................................... 90

# Executive Summary

The Program for Arctic Regional Climate Assessment (PARCA) is a NASA-sponsored initiative with the prime objective of understanding the mass balance of the Greenland ice sheet. In October, 1998, PARCA investigators met to review activities of the previous year, assess the program's progress, and plan future investigations directed at accomplishing that objective. Some exciting results were presented and discussed, including evidence of dramatic thinning of the ice sheet near the southeastern coast. Details of the investigations and many of the accomplishments are given in this report, but major highlights are given below:

### *Satellite observations*

- Radar altimetry data show an average of 1.6 ± 0.8 cm/yr thickening of the ice sheet in areas higher than 2000 meters.
- These same data also show a seasonal cycle of approximately ±10 cm amplitude.
- Interferometry is revealing unprecedented information on the dynamics of ice streams and outlet glaciers.
- Passive microwave data are providing a much-needed accumulation map of the ice sheet's dry snow regions.

### *Aircraft observations*

- Airborne laser elevation surveys show a major thinning of the ice sheet in the lower elevation regions near the east coast.
- For the first time, airborne radar has been used to map bedrock through 2000 meters of warm ice in the most temperate regions of the ice sheet, the southwestern flank.

### *Field observations*

- Radar imaging of the top 200 – 300 meters of firn successfully detected major volcanic eruptions with unprecedented spatial resolution.
- Comprehensive surface flow-rate measurements indicate that high regions of the ice sheet (above 2000 m) are roughly in balance in the north, but are thinning considerably (30 cm/yr) in the southeast.
- Vertical ice velocity measurements suggest thinning in East Greenland, thickening in the southwest, and balance at the summit.
- Absolute gravity and GPS measurements on the southwest and southeast coasts show rapid subsidence, bringing into question models of past deglaciation.
- Analyses of shallow ice cores are filling major gaps in the knowledge of ice sheet accumulation spatial and temporal characteristics
- Since 1994, 15 automatic weather stations have been established on the ice sheet to provide detailed information about sub- and near- surface processes in the major ice sheet climate zones. This network is the first of its kind in Greenland

### *Modeling*

- Unprecedented accuracy has been achieved in modeling the spatial and temporal characteristics of precipitation on the ice sheet using atmospheric fields.

The review indicated that PARCA has made considerable progress towards accomplishing its objectives. Many significant results have come out of the program as are evidenced by the nearly 80 peer-reviewed journal articles by PARCA investigators (Appendix II). We are rapidly gaining an understanding of the spatial characteristics of the ice sheet mass balance and the processes that affect them; major gaps in the data are being filled, either with in situ measurements, remote sensing observations, or modeling; and significant advances in the application of remote sensing technology to glaciological and climatological processes on the ice sheet have been made, which can also be extended to Antarctica. In its 4 years as a formal NASA program, PARCA has made significant contributions to our understanding of the mass balance of the Greenland ice sheet, and its response to a changing climate.

## INTRODUCTION

*Robert H. Thomas, EG&G Services, NASA Wallops Flight Facility, Code 972, Wallops Island, VA 23337, robert_thomas@hotmail.com*

The Program for Arctic Regional Climate Assessment (PARCA) is a NASA project that was formally initiated in 1995 by combining into one coordinated program various investigations associated with efforts, started in 1991, to assess whether airborne laser altimetry could be applied to measure ice-sheet thickness changes. It has the prime goal of measuring and understanding the mass balance of the Greenland ice sheet, with a view to assessing its present and possible future impact on sea level. Toward that end, the main components of the program are as follows:

- Airborne laser-altimetry surveys along precise repeat tracks across all major ice drainage basins, in order to measure changes in ice-surface elevation.
- Ice thickness measurements along the same flight lines.
- Shallow ice cores at many locations to infer snow-accumulation rates and their interannual variability, recent climate history, and atmospheric chemistry.
- Estimating snow-accumulation rates by climate-model analysis of column water vapor obtained from radiosondes, satellite atmospheric sounding observations, and European Center for Medium-Range Weather Forecasting (ECMWF) model data.
- Surface-based measurements of ice motion at 30-km intervals approximately along the 2000-m contour completely around the ice sheet, in order to calculate total ice discharge for comparison with total snow accumulation, and thus to infer the mass balance of most of the ice sheet.
- Local measurements of ice thickness changes in shallow drill holes.
- Investigations of individual glaciers and ice streams responsible for much of the outflow from the ice sheet.
- Monitoring of surface characteristics of the ice sheet using satellite radar altimetry, Synthetic Aperture Radar (SAR), passive-microwave, scatterometer and visible and infrared data.
- Investigations of surface energy balance and factors affecting snow accumulation and surface ablation.
- Continuous monitoring of crustal motion using global positioning system (GPS) receivers at coastal sites.

During 1998 major progress was made toward accomplishing the PARCA objective. The southern half of the ice sheet that was originally surveyed in 1993 using aircraft laser altimetry was resurveyed, and showed considerable changes, particularly near the eastern margins. Ice thickness was successfully measured in the thick temperate zones in the southwest, thus enabling the completion of flux estimates along the 2000 meter contour line. SAR interferometry and drainage basin thickness measurements have been used to estimate the balance and grounding line migrations of major glaciers in the northern and eastern regions of the ice sheet. Ice core data, atmospheric modeling, in situ climate data and remote sensing data are showing details on the history and spatial and temporal variability of accumulation on the ice sheet. The contributions in this report contain summaries of the 1998 field, modeling, and data analysis activities.

Through the combined techniques involving spaceborne, airborne, in situ and modeled data, NASA-funded researchers have partially answered this complex problem and are converging on the completion of the PARCA objective. Moreover, throughout the life of PARCA, considerable advances in technology have been made, as evidenced by the development of the ice-penetrating radar, major growth of SAR interferometry to the study of ice sheet dynamics, and innovative applications of remote sensing technology.

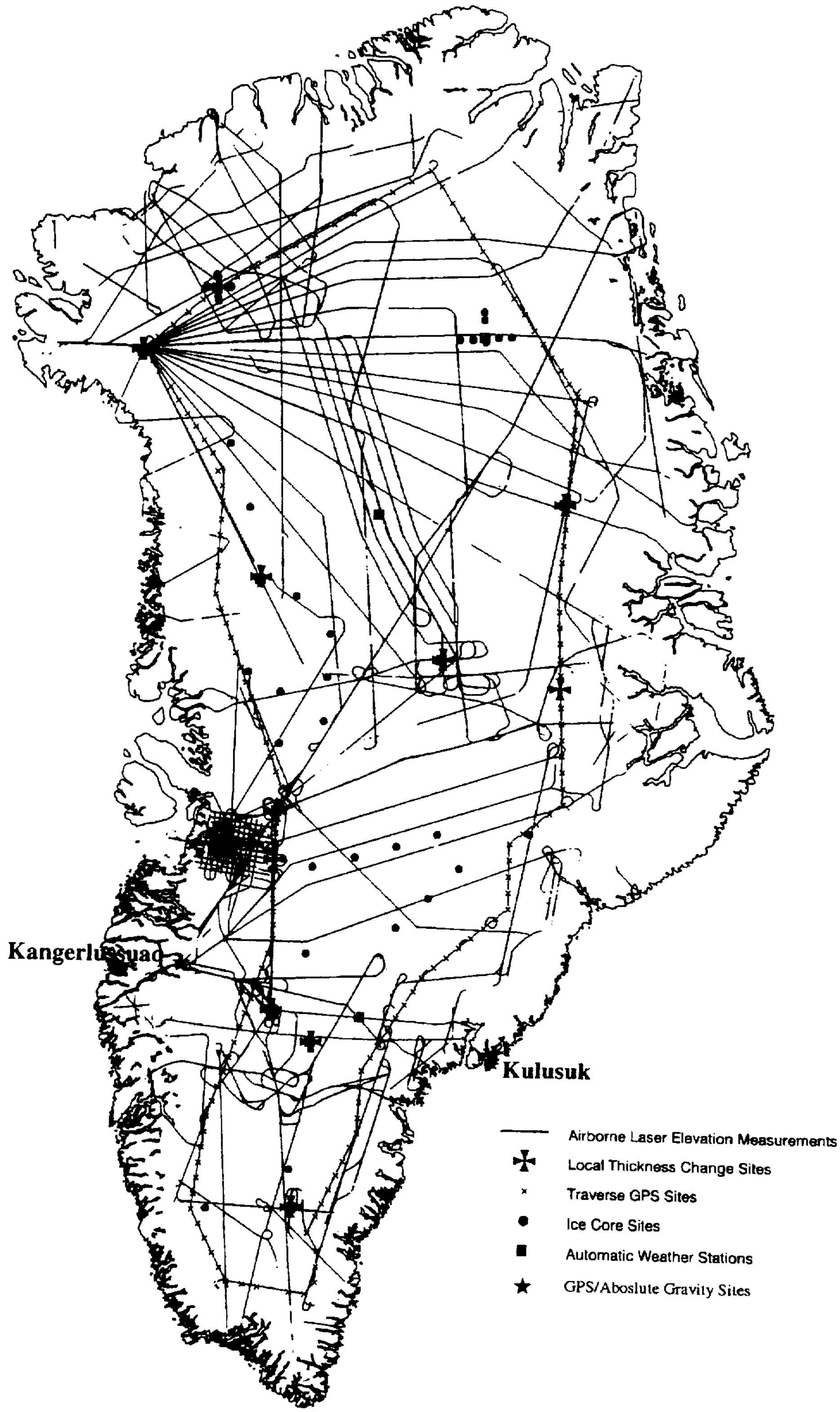


Figure 1. Location map of PARCA field activities on the Greenland ice sheet through 1998. For nearly all of areas for which airborne laser elevation surveys were made, ice thickness has also either been measured or will be measured in 1999.

PARCA has made significant progress towards its goals over the last 4 years, particularly in acquiring data needed both to measure ice-sheet mass balance and to understand key processes that determine the mass balance. The PARCA field program will culminate in 1999 with the laser-altimeter resurvey of the northern part of the ice sheet, and completion of many complementary field activities, with emphasis on ice coring. Our objectives thereafter will be to process and analyze the observations towards providing a rigorous assessment of the current state of balance of the Greenland ice sheet, with focused studies of key processes, such as the flow of outlet glaciers, that affect this balance.

The major result from resurvey of the southern part of the ice sheet is that most of the changes in the ice sheet occur at lower elevations, and particularly along east coast outlet glaciers. Another key PARCA finding concerns the large temporal variability in accumulation rates, which results in quite large changes in surface elevation solely from this effect. This information is extremely important to interpretation of time series of satellite-altimetry data, and we plan to compile maps of the magnitude of surface-elevation trends that could be caused by accumulation variability for various time intervals to help identify regions where observed changes exceed these values. The PARCA laser-altimetry surveys will provide estimates of elevation change over a 5-year period, and these will be extended by NASA's Geoscience Laser Altimeter System (GLAS) to be launched on ICESAT in 2001. The PARCA measurements will also provide baseline data sets for comparison with GLAS data to yield a total time series of elevation change from 1993/4 through the GLAS lifetime. We are also working on rigorous intercomparison of the laser-derived elevation-change rates with those from satellite radar altimetry (1978-1988), using the PARCA ice cores to infer elevation changes that occurred between the two time series. If successful, these data sets along with those from GLAS, will yield a time series of elevation changes over southern Greenland covering almost 30 years.

After 1999, we see the major PARCA activities as:

1. Interpretation of the observations
2. Increased emphasis on modeling studies
3. Continuation of studies using satellite data (passive-microwave time series; SAR etc)
4. Application of GLAS data to Greenland and other Arctic ice caps, including validation of GLAS against aircraft laser-altimetry data
5. Maintenance of the network of Automatic Weather Stations
6. Aircraft laser altimeter and radar sounding surveys of Canadian ice caps (first surveyed in 1995), and detailed surveys of key Greenland outlet glaciers towards understanding why they are rapidly thinning
7. Development and testing of new ice remote-sensing techniques in a comparatively low-cost location.

Finally, we believe that the approach adopted by PARCA – a focused, yet interdisciplinary effort strongly guided by clearly-stated goals and objectives, comprising an appropriate mix of in situ and remote sensing data acquisition, interpretation, and modeling - can be applied to the ice sheet in Antarctica. This will require interagency and international collaboration, which runs the risk of diluting the focus and weakening the guidance, but the key importance of GLAS and SAR data to this effort offers NASA the opportunity to provide the strong leadership needed to make such a program succeed.

# ELEVATION CHANGE OF THE SOUTHERN GREENLAND ICE SHEET: UPDATE

*C.H. Davis, UMKC Electrical Engineering, 5605 Troost Ave, Kansas City, MO 64110 curt@polar.cuep.umkc.edu*

*C.A. Kluever, UMKC Mechanical & Aerospace Engineering 5605 Troost Ave, Kansas City, MO 64110*

*B.J. Haines, JPL Earth Orbiter Systems Group, California Institute of Technology, 4800 Oak Grove Drive, M/S: 238-600, Pasadena, CA 91109-8099*

## Objectives

The overall focus of our research is to document long-term elevation change of the Greenland ice sheet using satellite altimeter data. In addition, we are investigating seasonal and interannual variations in the ice-sheet elevations to place the long-term measurements in context. Specific objectives of this research include:

1) Developing new techniques to significantly improve the accuracy of elevation-change estimates derived from satellite altimetry.

2) Measuring the elevation change of the Greenland ice sheet over a 10-year time period using Seasat (1978) and Geosat GM (1985-86) and Geosat ERM (1986-88) altimeter data.

3) Quantifying seasonal/interannual variations in the elevation-change estimates using the continuous time series of surface elevations from the Geosat GM and ERM datasets.

4) Extending the long-term elevation change analysis to two decades by incorporating data from the ERS-1/2 missions (1991-99) and, if available, the Geosat-Follow On (GFO) mission (1998-??).

## Progress & Results

*Geosat ERM x Seasat Elevation Change*

We recently completed a re-examination of elevation change over the southern Greenland ice sheet from 1978-88 using Seasat and Geosat ERM data [Davis *et al.*, 1998a]. This study incorporated technical advancements in ice-sheet retracking, orbit computation, orbit-error reduction, and inter-satellite bias estimation described in a previous PARCA report [Davis *et al.*, 1997]. A spatial average of the elevation change results for the ice sheet above 2000 m yielded a growth rate of only 2.0 ± 0.5 cm/yr (unadjusted for isostatic uplift). The ± 0.5 cm/yr uncertainty due to random error is an order of magnitude smaller than the ± 6 cm/yr uncertainty reported by Zwally *et al.* [1989]. In addition, the new elevation change result is significantly smaller than the 23 ± 6 cm/yr rate reported by Zwally *et al.* [1989].

While our average rate was close to zero, the new analysis revealed for the first time large regional variations in the elevation change estimates from -15 to +18 cm/yr. Changes in the northern interior of the ice sheet near the summit were -2 to +2 cm/yr and are consistent with estimates showing no significant change in mass balance for this region [Bolzan, 1993]. Thinning of 3 to 10 cm/yr was indicated for the lower elevations of the eastern and western flanks of the ice sheet between 70° to 72° N. The ice sheet west of the ice divide between 65° to 69° N increased in elevation by 10 to 15 cm/yr. This rate agrees with growth rates derived from a comparison of airborne laser altimeter and ground survey data from 1980 to 1994 [Krabill *et al.*, 1995].

In addition to the random measurement error of ± 0.5 cm/yr, uncertainties in 1) the rate of isostatic uplift 2) the inter-satellite bias 3) residual orbit errors and 4) the environmental corrections contribute to an overall error budget of ± 1-2 cm/yr [Davis *et al.*, 1998a]. Using a worst-case total error estimate of ± 2 cm/yr over the ten-year time period from Seasat to Geosat, the 2.0 cm/yr spatially averaged growth rate may not be significantly different than a null growth rate.

*Geosat-GM + ERM x Seasat Elevation Change*

Zwally *et al.* [1998] raised several issues regarding our results presented in the previous section. First they pointed out that the area coverage above 2000 m was roughly 70% and that much of the missing area was near changes of +5 to +18 cm/yr, which suggests that inclusion of the missing area could cause the overall rate to be significantly larger than our reported value of 2.0 cm/yr. Zwally *et al.* [1998] then reported elevation change results based on their analysis of Geosat-GM + ERM x Seasat data that showed growth of 6.2 ± 2.8 cm/yr for elevations > 700 m and 3.8 ± 0.2 cm/yr for elevations > 1700 m.

In our response, we pointed out that a majority of the missing area above 2000 m was in fact adjacent to areas of negative change [Davis *et al.*, 1998b]. We then updated our Geosat-ERM x Seasat analysis to include Geosat-GM data which increased our area coverage by 23% and filled in most of the missing area above 2000 m near the areas of large positive change noted by Zwally *et al.* [1998]. With the inclusion of the Geosat-GM data, we reported a preliminary result of 2.2 ± 0.9 cm/yr for the spatially averaged rate of change of the southern Greenland ice sheet > 2000 m [Davis *et al.*, 1998b]. The increase in spatial coverage included nearly equal areas of positive and negative change. Thus, the combined effect produced a net spatial average not significantly different than our earlier result. We reported the revised result as preliminary because of an unresolved 4-cm intra-satellite bias in the GM and ERM ocean data used to derive our orbit adjustments.

We have now completed an extensive analysis of Seasat, Geosat-GM, and Geosat-ERM orbit errors using a global ocean reference surface created from 4 years of Topex/Poseidon (T/P) altimeter data. We believe the T/P reference surface is superior to the 2-year Geosat-ERM reference surface used in our previous analyses for several reasons. First, the T/P data are accurate to better than 2 cm with respect to the geocenter. Second, the inclusion of 4 years of data for the T/P reference surface will minimize real inter-annual variations in the global oceans in comparison to the 2-year ERM reference surface which, for example, included the 1987 El Nino event. Finally, the environmental corrections (ionosphere, wet troposphere, etc.) applied to the T/P data are known to be significantly better than those currently available for Geosat. In evaluating the T/P orbit adjustments, we find that the time-varying (1/rev) portion of the adjustments are nearly identical to those derived from the ERM reference surface. However, the Geosat-Seasat inter-satellite bias increased to 32 cm compared to 27 cm in our previous analysis [Davis *et al.*, 1998a]. In addition, the 4-cm GM-ERM intra-satellite bias noted above was reduced to 1 cm, which is not significantly different than zero. Because of this and the reasons noted above, we believe the T/P orbit adjustments are the best that can be generated for comparing Seasat, Geosat-GM, and Geosat-ERM data to derive ice-sheet elevation change results.

Figure 1 shows our final result for the spatial distribution of ice-sheet elevation change from Geosat-GM+ERM x Seasat altimeter data utilizing the T/P orbit adjustments. The area coverage is virtually identical to that in our preliminary analysis [Davis *et al.*, 1998b]. A spatial average of the data yields a growth rate of only 1.6 ± 0.8 cm/yr, which is smaller than our preliminary result due to differences in the inter/intra-satellite bias estimates. The 3.8 ± 0.2 cm/yr result reported by Zwally *et al.* [1998] for elevations > 1700 m is in reasonable agreement with our final result when one considers that different methods are used for retracking, deriving orbit adjustments, and computing the spatial averages.

With regard to the 6.2 ± 2.8 cm/yr result reported by Zwally *et al.* [1998] for elevations > 700 m, we find that Geosat-Seasat crossover data below 1700 m are of extremely poor quality [Davis *et al.*, 1998b]. Moreover, these data are sparsely distributed over the ice sheet, representing only a few percent (no quality editing) of the total Geosat-Seasat crossover data. Because of this, we believe that these data cannot be reliably used to represent elevations from 700-1700 m which comprise approximately 25% of the southern Greenland ice sheet. This is especially true when one considers the large spatial variations in elevation change evident in Figure 1.


Fig.1 Spatial distribution of elevation change from 1978 to 1988 from an analysis of Geosat (GM + ERM) x Seasat altimeter data. The approximate location of the ice divide (stars) and 2000 m surface elevation contour (dots) are also shown. A spatial average of the data yields a growth rate of 1.6 +/- 0.8 cm/yr.

Finally, we note that our final dH/dt map for the southern Greenland ice sheet from 1978-88 (Fig. 1) is in very close agreement with the initial dH/dt map produced from a comparison of the airborne laser altimeter measurements from 1993-98 [Krabill, et al., this report]. This suggests that the spatial dH/dt pattern in our map is representative of long-term elevation change over a period of two decades (1978-98). The primary goal for the PARCA program is the measurement and understanding of the mass balance of the Greenland ice sheet [Thomas, 1996]. The combined radar and laser altimeter results demonstrate that a significant part of this goal has been achieved for the central southern Greenland ice sheet. Future work for the southern Greenland ice sheet should focus on understanding the cause of the spatial dH/dt variations evident in Fig. 1. This is a key requirement if we are to predict the future response of the ice sheet to global climate change.

*Seasonal/Interannual Elevation Change*

We are analyzing the continuous 3.5-year time series of surface elevations from the Geosat GM and ERM datasets to quantify seasonal/interannual variations in ice-sheet surface elevation. The seasonal elevation signal can provide important temporal information regarding the climatic processes that drive surface mass balance change. Precipitation/accumulation, snow compaction, snow melting, ice flow, and even seasonal variations in the surface penetration of the altimeter signal all will affect the apparent elevation change cycle observed in the altimetry data. The seasonal elevation signal over the two-year Geosat ERM data is approximately sinusoidal and repeatable from one year to the next. The amplitude of the seasonal signal varies between ±10 cm in 1987 and ±15 cm in 1988. The seasonal cycle in the 1.5-year Geosat GM data also has a ±15 cm, but it appears to be anomalous in comparison with the ERM data in that there is a large 30-cm negative trend in the data over the last 6-8 months. We are currently evaluating data from other PARCA investigators (AWS surface height, precipitation, etc.) in an attempt to understand the seasonal elevation signals. Given the large number of processes that affect the altimeter-derived elevation cycle and the limited amount of information available from the Geosat era, it may be difficult to completely unravel the different processes affecting the seasonal elevation signal.

Interannual variations were determined from the Geosat data by dividing each year of the seasonal elevation cycle into four 3-month seasons. Because we are interested in obtaining an estimate for the <u>random</u> component of interannual variations vs. those due to secular trends, we removed the large (anomalous?) negative elevation trend in the Geosat-GM noted above. Interannual variations were then computed by differencing the average dH values between different seasons. The results are summarized in Table 1. The year-to-year dH values are approximately Gaussian distributed with a mean of 0.6 cm and SD = 7.2 cm, which we feel is a reasonable estimate of the random component of the interannual variations. Note that the SD would be significantly larger if the linear trend in the GM data was not removed.

Table 1. Interannual Elevation Change from 3.5-Year Geosat Seasonal Cycle

| YEAR | WINTER dH (cm) | SPRING dH (cm) | SUMMER dH (cm) | FALL dH (cm) |
|---|---|---|---|---|
| 86 x 85 | -8.7 | --- | 4.6 | -8.2 |
| 87 x 86 | 6.2 | -4.7 | 5.9 | 12.1 |
| 88 x 87 | --- | 5.8 | -2.4 | -4.5 |

The interannual variations have important implications for the detection of long-term elevation trends. The uncertainty in long-term elevation change trends is directly related to the magnitude of interannual variations that represent the natural variability in the data. This is analogous to detecting long-term trends in accumulation rates derived from ice-cores which show substantial interannual variability. To quantify the uncertainty in long-term elevation change estimates, we simulated elevation change time series over periods of 3, 5, 10, 20 years using an SD for the interannual changes that varied from 1 to 20 cm. From these simulations, we can determine the likelihood that dH/dt results could be due solely to the cumulative effect of random year-to-year fluctuations. The results of the simulation are shown in Figure 2.

For interannual variations with an SD = 7 cm (from Geosat analysis), the results show a ±1 SD uncertainty of ±4.2, ±3.2, ±2.2, ±1.5 cm/yr for time spans of 3, 5, 10, and 20 years, respectively. Our Geosat x Seasat trends of 1.5-2 cm/yr over the ten-year period from 1978-88 are therefore not significant with respect to the ±2.2 cm/yr uncertainty due to the interannual variability in the elevation time series. Due to short (~ 3 - 4 yr) mission lifetimes, single satellite detection of elevation trends >5 cm/yr would be required for the observed trends to be significant. Also, it is important to note that our estimate for the interannual variability (SD = 7 cm) derived from the Geosat data is only applicable for data > 2000 m. For the lower elevations of the ice sheet, it is likely that larger accumulation and melting rates will lead to even greater interannual variability. This would then further increase the threshold which a long-term trend must exceed in order to be significant with respect to the natural variability in the data.

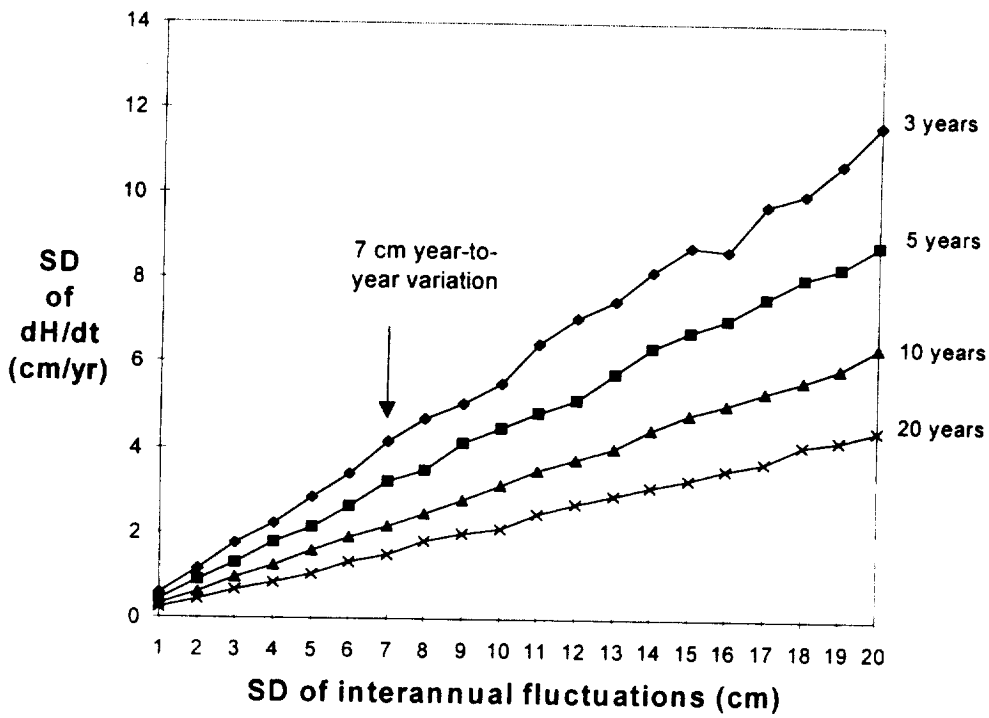


Figure 2. Uncertainty in dH/dt results associated with random interannual variations in surface elevation for time periods of 3 to 20 years. Results were derived from a Monte Carlo simulation.

## Future Work

First we plan to perform a rigorous comparison our dH/dt results in Fig. 1 with those derived from the airborne laser altimeter data for the period from 1993-1998 when they become available. We already know that the spatial dH/dt pattern is closely repeated in both the radar and laser altimeter results. Thus, we hope to synthesize the two datasets to derive an elevation change map for the central southern Greenland ice sheet that represents long-term change over the 20-year time period from 1978-98. As noted earlier, this would represent a major stride in documenting the mass-balance of the Greenland ice sheet, which is the primary objective of the PARCA program.

Next we plan to extend our radar altimeter results by including satellite altimeter data from the ERS-1/2 and GFO (if available) missions. Tnis has the potential for extending the radar altimeter time series of elevation-change estimates to over two decades. Because the altitude and inclination of the ERS satellites are substantially different from those of Seasat/Geosat/GFO, gravity-induced geographically correlated orbit errors (GCOE) will be very different in the ERS data, despite the fact that the same gravity model (JGM-3) is used to produce the orbit solutions. This introduces a new complication in trying to incorporate the ERS data into our existing Geosat/Seasat study. The T/P sea-height data are accurate to within 2 cm and the level of the GCOE is estimated to be <1 cm. As noted before, the T/P reference surface is also best suited for estimating inter-satellite systematic biases, which have already been shown to be quite large in the Seasat/Geosat studies. Thus, the T/P reference surface provides the ideal framework for blending data from diverse altimeter missions. By crossing the Seasat/Geosat/ERS/GFO datasets with respect to the precise T/P reference surface, the absolute levels of GCOE for each mission can be assessed along with the time-varying 1/rev orbit errors. We have already been successful in obtaining highly accurate estimates of the GCOE in the Seasat/Geosat data along with the time-varying 1/rev orbit errors.

**References**


Bolzan, J.F., 1995, A glaciological determination of the mass balance in central Greenland, *EOS Trans. Suppl.*, Vol. 73, No. 43, p. 203.

Davis, C.H., C.A. Kluever, and B.J. Haines, 1997, Elevation change of the southern Greenland ice sheet, *Program for Arctic Regional Climate Assessment (PARCA) - Report of the Greenland Science and Planning Meeting*, pp. 96-102, University of Arizona, Tucson, AZ, 15-16 Oct 1997.

Davis, C.H., C.A. Kluever, and B.J. Haines, 1998a, Elevation change of the southern Greenland ice sheet, *Science*, Vol. 279, 27 March 1998, pp. 2086-2088.

Davis, C.H., C.A. Kluever, and B.J. Haines, 1998b, Response: growth of the southern Greenland ice sheet, *Science*, Vol. 281, 28 August 1998, p. 1251a.

Krabill, W., R. Thomas, K. Jezek, K. Kuivinen, and S. Manizade, 1995, Greenland ice sheet thickness changes measured by laser altimetry, *Geophys. Res. Lett.*, Vol 22, No. 17, pp. 2341-2344.

Krabill, W., 1998, Airborne laser/GPS mapping of Arctic Regions, this report.

Thomas, R.H.,, 1996, Program for Arctic Regional Climate Assessment (PARCA): overview of the 1996 field season and plans for the future, *Program for Arctic Regional Climate Assessment (PARCA) - Report of the Greenland Science and Planning Meeting*, pp. 1-3, University of Colorado, Boulder, CO, 17-18 Sept 1996.

Zwally, H.J., A.C. Brenner, J.A. Major, R.A. Bindschadler, and J.G. Marsh, 1989, Growth of Greenland ice sheet: measurement, *Science*, Vol. 246, pp. 1587-1589.

Zwally, H.J., A.C. Brenner, J.P. DiMarzio, 1998, Technical comment: growth of the southern Greenland ice sheet, *Science*, Vol. 281, 28 August 1998, p. 1251.

# LARGE ICE DISCHARGE FROM THE GREENLAND ICE SHEET

*Eric Rignot, Jet Propulsion Laboratory, California Institute of Technology MS 300-235, 4800 Oak Grove Drive, Pasadena, CA 91109-8099, eric@adelie.jpl.nasa.gov*

## Objectives

The objectives of this work are to measure the ice discharge of the Greenland Ice Sheet close to the grounding line and/or calving front, and compare the results with mass accumulation and ablation in the interior to estimate the ice sheet mass balance.

## Approach

Multiple-pass ERS radar interferometry is combined with radar altimetry to measure the velocity, topography and grounding zones of outlet glaciers. Ice thickness is either derived from hydrostatic equilibrium at the grounding line, or from direct measurements by NASA/University of Kansas (UKANS) Ice Sounding Radar (ISR). Mass accumulation, formely from Ohmura and Reeh (1991), is now from PARCA (Bromwich and others, 1998). Surface ablation is from Reeh's degree day model (1991).

## Results

### *1997 results from North Greenland*

Using ERS data and a Digital Elevation Model (DEM) of north Greenland, we found that the grounding line ice discharge of north Greenland glaciers exceeds calf-ice production by a factor 3.5, because of pronounced basal melting at the underside of the glacier floating sections (Rignot and others, 1997a). The measured discharge exceeds mass accumulation and ablation in the interior, suggesting that the northern part of the ice sheet may be losing mass (Rignot and others, 1997b, Reeh and others, 1997).

Detection of the grounding line position of Petermann Gletscher between 1992-1996 suggests a grounding line retreat of about 270 ± 120 m in 4 years, which in turn implies a thinning rate of 78 ± 35 cm ice per year (Rignot, 1998).

### *1998 results from North Greenland*

Using an updated map of mass accumulation (Bromwich and others, 1998), which includes the PARCA cores and the 1993 German data (Friedman and others, 1995), we re-calculated mass accumulation and ablation in the north (Table 1). Total accumulation is 4% less than in Ohmura and Reeh (1991). Surface ablation is 9% higher (less snow to melt before melting ice) than the PARCA map and 18% higher due to a revision of our implementation of Reeh's model. The balance flux is 12% lower.

Combining the 1997 ISR data, with ascending/descending interferograms of north-east Greenland, we measured the ice flux of NioghalvfjerdBrae and Zachariae Isstrom above the grounding line and found results that were fairly consistent with the grounding line estimates. The mass budget of North Greenland glaciers however remains negative. This confirmation is consistent with historical records (Davis and Krinsley, 1962).

Table 1. Accumulation (Acc), Ablation (AB), Balance Flux (BF), and Grounding line Flux (GF) from *Science* publication and the most recent PARCA data sets. Units are in $km^3$ ice $yr^{-1}$ and values in parentheses were calculated with 2-d ice velocities rather than adjusting 1-d (across-satellite track) velocities for the flow direction.

| Glacier | Acc Science | Acc PARCA | AB Science | AB PARCA | BF Science | BF PARCA | GF Science |
|---|---|---|---|---|---|---|---|
| Petermann Gl. | 13.1 | 12.6 | 1.7 | 2.1 | 11.4 | 10.5 | 13.2 (12.1) |
| Steensby Gl. | 1.5 | 1.5 | 0.1 | 0.1 | 1.4 | 1.4 | 0.6 |
| Ryder Gl. | 5.6 | 5.5 | 1.0 | 1.1 | 4.6 | 4.4 | 2.4 |
| Ostenfeld Gl. | 2.8 | 2.8 | 1.8 | 1.9 | 1.0 | 0.9 | 3.7 |
| Jung. Nar. Hens. Gl. | 1.0 | 1.0 | 0.2 | 0.3 | 0.9 | 0.8 | 0.4 |
| Acad. MS. Hagen B. Gl. | 6.1 | 6.0 | 2.0 | 2.6 | 4.1 | 3.3 | 1.0 |
| NioghalvfjerdBrae | 18.1 | 17.0 | 3.6 | 5.3 | 14.4 | 11.7 | 14.9 (12.52) |
| Zachariae Isstrom | 8.7 | 8.2 | 5.0 | 5.7 | 3.7 | 2.4 | 12.6 (12.19) |
| Total | 57.0 | 54.5 | 15.3 | 19.2 | 41.6 | 35.3 | 48.7 (44.91) |

Several glaciers exhibit high temporal variability. Ryder Gl. (Joughin and others, 1996), Brikkerne Gl. (Higgins and Weidick, 1990) and Storstrommen Gl. (Reeh and others, 1994) surged in the past. Academy and Marie Sophie Gl. and Hagen Brae seem no longer active (Lauge, 1928; Davis and Krinsley, 1962).

Additional data have been processed along the north-west sector: 1) Tracy, Heilprin, Leidy, Mary and Harald Moltke Glaciers, north of Thule AF base; 2) Gade, Docker Smith, Rink, Peary, Kong Oscar and Nansen Glaciers in Melville Bay (Figure 1.). Floating sections are of limited extent in 1) and difficult to map in 2). We seek to obtain ice thickness data from UKANS' ISR in these sectors in 1999 to estimate ice discharge along the coast.

*1998 results from East Greenland*

With the help of one graduate student, G. Buscarlet, we processed ERS interferometric data along the entire coast of East Greenland (Figure 1). A time consuming process was to select appropriate image pairs. Ice velocity is large compared to north Greenland glaciers, and surface weathering is a significant problem in selecting good interferometric data pairs. We find no glacier floating section south of Storstrommen Gletscher, although the data could no longer be used for that purpose about south of Cecilia Nunatak (72N). The data were used to map the velocity and topography of the glaciers, and geocode the results. One remaining issue is the absolute geolocation accuracy of the data. We will use published maps and Airborne Topographic Mapper data to help refine the geocoding accuracy of the results.

To measure ice velocity in Terminal Valley, we employed a new feature tracking technique with the ERS data. The measurements are 2-d, but the precision is 5 times less in the across-track direction due to differences in spatial resolution. These velocities will be used to calculate ice discharge from the largest glaciers.

**1999 Planned Activities**

*New ISR Data*: We seek to collect new ice thickness data in the north-west Greenland sector (to measure ice flux at the coast), in Petermann's Fjord (to characterize its grounding zone more completely), across not-previously mapped areas in the north (Ostenfeld Gl., Hagen Brae in the north), and along the center line of NioghalvfjerdBrae and Zachariae Isstrom (to provide estimates of the longitudinal gradient in ice thickness at the grounding line).

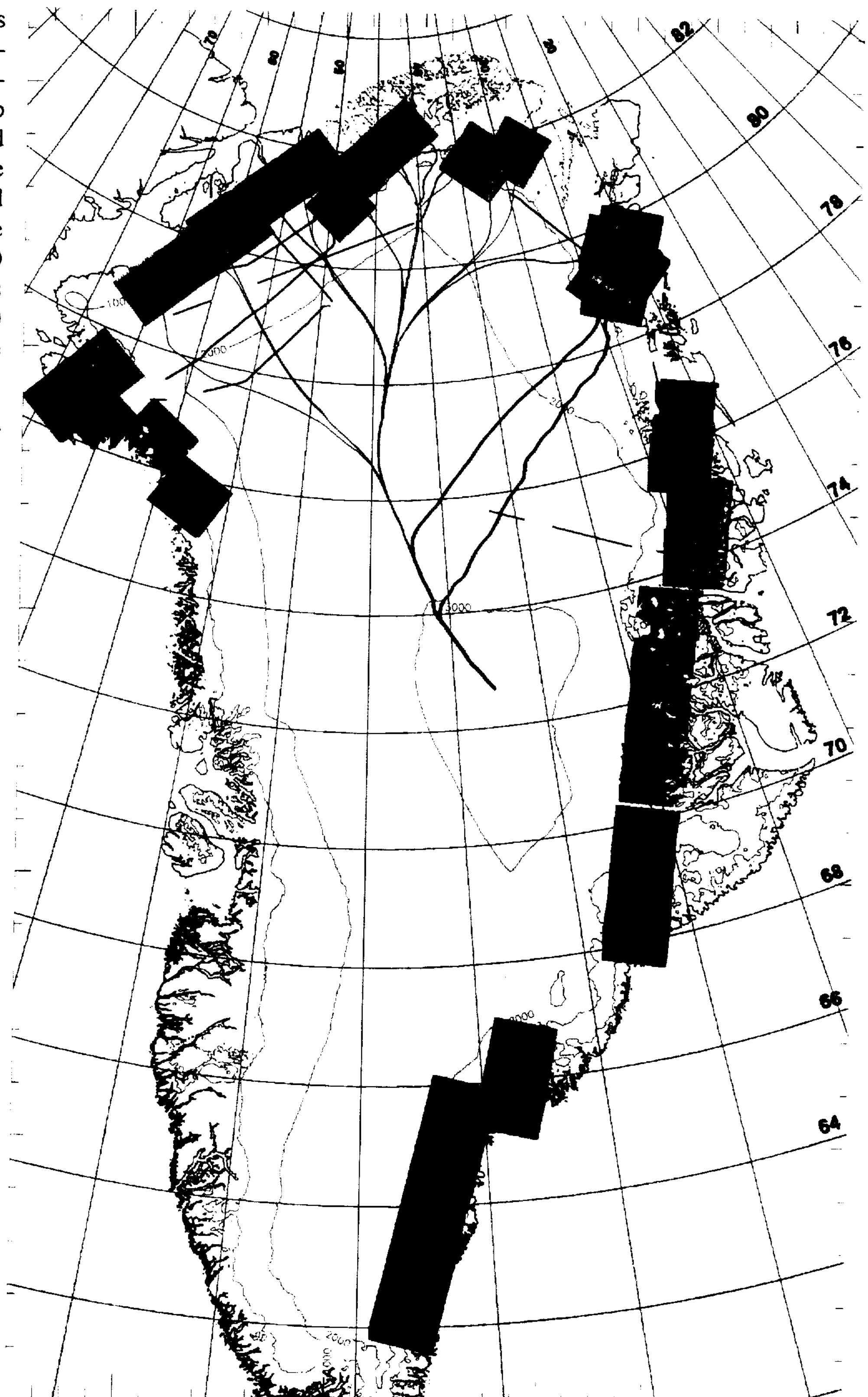


Fig. 1. ERS frames processed interferometrically (double-difference pairs to map both topography and velocity) along the coast of the Greenland ice sheet. Each frame is about 120 km x 120 km. Contour levels (1000, 2000, and 3000 m) of the ice sheet are from the Ekholm (1996) DEM. Drainage basins of individual glaciers and glacier systems are delineated as thin colored lines extending between the glacier grounding line and Greenland's summit. Ice sounding radar data collected by UKANS in 1997 are shown in thick green lines (data used in this study) and thick green/dark lines (data not yet used)

*New ERS Processing*: We will process additional data in the north-west sector to improve our current results, generate a three-dimensional velocity map of Petermann Gletscher, determine the grounding line stability of Ryder Gl., Ostenfeld Gl., HagenBrae and Storstrommen Gl. between 1992 and 1996 knowing that some of them underwent surges during that time.

*Calf-ice production*: In collaboration with A. Ohmura, ETH, we will estimate calf-ice flux along the east coast of Greenland combining geologic maps, ERS measurements of velocity, and proxy estimates of ice thickness from modeling inversion. The results will be used to refine past estimates of Greenland calf-ice production, the least well known component of its mass balance. These data will complement ice fluxes measured higher up along the east coast where ISR data can be collected, as well as measurements conducted during the NASA traverse.

## References


D. H. Bromwich, R. I. Cullather, Q-s Chen, B. M. Csatho, 1998. Evaluation of recent precipitation studies for the Greenland ice sheet. *J. Geophys. Res.*, Vol. 103, pp. 26007-26024.

Davies, W.E. and D. B. Krinsley. 1962. The recent regimen of the ice cap margin in North Greenland, *Symp. of Obergurgl, Austria 10-18 Sept. 1962*, Int. Ass. Sci. Hydrol., Pub. 58, 119-130.

Friedman and others. 1995. *Ann. Glaciol.*

Higgins, A.K. and A. Weidick. 1990. The World's northernmost surging glacier, *Z. Gletscherkde. Glazialgeol.* 24, 111-123.

Joughin, I., S. Tulaczyk, M. Fahnestock and R. Kwok. 1996. A mini-surge on the Ryder glacier, Greenland, observed by satellite radar interferometry. *Science}* 274(5285), 228-230.

Koch, L. 1928. Contributions to the glaciology of North Greenland, *Medd. Gronland*,65(2), 181-464.

Ohmura, A. and N. Reeh. 1991. New precipitation and accumulation maps for Greenland. *J. Glaciol.* 37(125), 140-148.

Reeh, N. 1991. Parametrization of melt rate and surface temperature on the Greenland Ice Sheet. *Polarforschung* 59(3), 1989, 113-128.

Reeh, N, H.H. Thomsen, O.B. Olesen, W. Starzer. 1997. Mass balance of north Greenland, Letter to *Science*, 278(5336).

Reeh, N, C.E. Boggild and H. Oerter. 1994. Surge of Storstrommen, a large outlet glacier from the inland ice of north-east Greenland. *Rep. GGU*, 162, 201-209.

Rignot, E., P. Gogineni, W.B. Krabill and S. Ekholm. 1997a. North and northeast Greenland Ice discharge from satellite radar interferometry, *Science*, 276, 934-937.

Rignot, E., P. Gogineni, W.B. Krabill and S. Ekholm. 1997b. Response to Mass balance of north Greenland, Letter to *Science*, 278(5336).

Rignot, E. 1998. Hinge-Line Migration of Petermann Gletscher, North Greenland, Detected Using Satellite Radar Interferometry, *J. Glaciol.*, in press.

# ICE FLOW IN THE NORTH EAST GREENLAND ICE STREAM

*Ian Joughin and Ron Kwok, Jet Propulsion Laboratory California Institute of Technology, 4800 Oak Grove Drive, Pasadena, CA 91109, ian@rgps1.jpl.nasa.gov*

*M. Fahnestock, JCESS, Dept. of Meteorology, University of Maryland, College Park, MD 20742*

*Doug MacAyeal, Department of Geosciences, The University of Chicago, Chicago, IL 60637*

## Objectives

Early observations with ERS-1 SAR image data revealed a large ice stream in North East Greenland (Fahnestock et al., 1993). The ice stream has a number of the characteristics of the more closely studied ice streams in Antarctica, including its large size and gross geometry. The onset of rapid flow close to the ice divide and the evolution of its flow pattern, however, make this ice stream unique. These features can be seen in the balance velocities for the ice stream (Joughin et al., 1997) and its outlets. The ice stream is identifiable for more than 700 km, making it much longer than any other flow feature in Greenland.

Our research goals are to gain a greater understanding of the ice flow in the northeast Greenland ice stream and its outlet glaciers in order to assess their impact on the past, present, and future mass balance of the ice sheet. We will accomplish these goals using a combination of remotely sensed data and ice sheet models. We are using satellite radar interferometry data to produce a complete maps of velocity and topography over the entire ice stream. We are in the process of developing methods to use these data in conjunction with existing ice sheet models similar to those that have been used to improve understanding of the mechanics of flow in Antarctic ice streams.

## Results

Figure 1 shows a map of the across-track component of velocity for the Northeast Greenland Ice Stream. We generated this map using data from several ascending ERS interferograms, which were collected during the ice and commissioning phases of ERS-1 and the tandem phase of ERS-1 and 2. The velocity data are plotted as contours over the associated amplitude imagery. The track headings differ for each strip, so the satellite across track-direction is slightly different for each strip. These directional differences are small enough that the data can be compared in the overlap regions as though they were acquired along the same track heading.

Most of the scenes contain no ice-free areas, so we had to rely entirely on ground-control points located on the ice sheet. The elevation control data were extracted from the Danish National Survey and Cadastre (KMS) DEM [Ekholm, 1996]. For the strip closest to the coast (far upper right strip), we used some control points from ice-free areas. The locations of the ground-control points are shown as black dots in Figure 1.

We generated a balance-velocity map of Greenland [Joughin and others, 1997] to provide velocity control on the ice sheet. Balance velocities are the depth-averaged velocities necessary to maintain the steady-state shape of the ice sheet and are estimated from surface slope ice, ice thickness, and accumulation data. The depth-averaged velocities were adjusted by a factor of 1.11 to obtain surface velocity estimates. Errors in the source data can lead to large errors in the balance-velocity estimates. To minimize the impact of balance-velocity errors on our baseline estimates, we selected control points in slow-moving areas, where the absolute

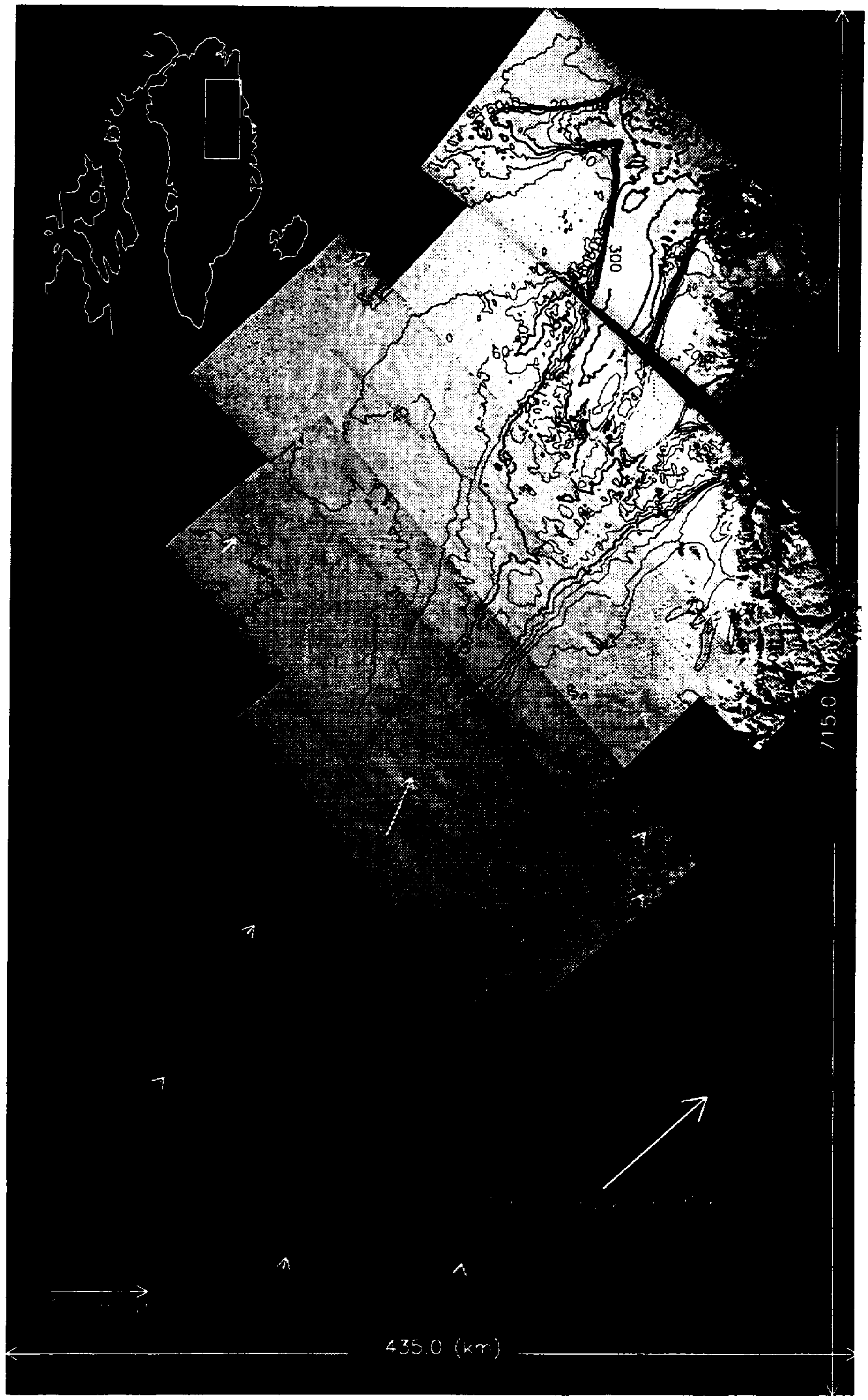


Figure 1. Interferometrically derived estimate of the across-track component of velocity (black contours) for the Northeast Greenland Ice Stream. Baselines were estimate using control points, which are shown as black dots. The thin white arrows show the velocity vectors measured using GPS. The indicated across track direction is only approximate, with the actual across-track direction varying slightly from strip to strip.

errors in the balance velocities are small. For example, if the velocity is 10 m/yr, then a 50 percent error leads to a balance-velocity error of only 5 m/yr. By selecting points in this manner, we anticipate control-point errors in the range of 1-10 m/yr. We used several dozen control points for each scene to reduce the random component of the control-point noise.

To compute our horizontal across-track velocity estimates, we used the KMS DEM to determine slope for removing the effect of vertical displacement [Joughin and others, 1996]. With the low resolution of the DEM, we were unable to compensate for short-wavelength components of vertical motion (i.e., less than 5 km). This results in errors equal to a few percent of the horizontal across-track velocity. Since the KMS DEM also was used to remove the direct effect of topography, there are additional errors caused by topographic fringes from short-scale topographic features. Ultimately, we will combine our data with descending passes and interferometrically derived DEMs to estimate the full 3-component velocity field using a surface-parallel flow assumption (Joughin and others, 1998).

GPS data were collected by NASA along the 2000-meter contour of Greenland to measure ice sheet outflow. Additional data were collected near the onset area of the Northeast Greenland Ice Stream for use as interferometric control points. The GPS points that fall within our velocity map are shown as white arrows in Figure 1. While we eventually plan to use these data as control, they were in no way used to control the velocity shown in Figure 1, which was derived using only balance velocities and the KMS DEM as sources of control data.

We projected the GPS measurements onto the across-track direction for comparison with the interferometric data. The GPS points were determined by repeat surveys of stakes separated by an interval of nearly one year so that the errors are well under a 1 m/yr. Thus, we assume that any difference between the GPS and interferometric data represents an error in the interferometric measurement.

Table 1 shows the difference between the 18 GPS points and the interferometric map shown in Figure 1 (entire map). Note that all of the strips used in this comparison were controlled solely with points from the ice sheet. The RMS difference is 3.14 m/yr with a maximum error of 6.7 m/yr. The results indicate that the balance velocities are a reasonable source of control. It is important to also note that some portion of the error can be attributed to uncompensated topography and vertical motion, which can be reduced with additional interferometric data and processing.

Table 1. Across-track velocity error for GPS points shown in Figure 1.

| Velocity Data | Error (m/yr) | | |
|---|---|---|---|
| | Mean | Std. Dev. | RMS |
| Entire Map | 2.08 | 2.42 | 3.14 |
| Tandem Data | 2.76 | 2.40 | 3.60 |
| Ice & Commissioning | 1.44 | 3.60 | 3.74 |

Three strips were from either the ice or commissioning phases (the first, third, and sixth strips from lower left to upper right) and have temporal separations of 6 days or more verses 1 day for the tandem data. Since the displacement is observed over a longer period the ice/commissioning data should be more accurate. Indeed, inspection of the velocity data reveals that these estimates are smoother and appear to have less noise, such as artifacts from residual topography. To quantify these differences we separately compared the tandem and ice/commissioning data with the GPS data and were surprised to find that the errors were similar. The largest differences for both phases occurred on the fastest moving areas and/or on the strips nearer the coast, where larger balance velocities had to be used. The larger balance velocities will tend to be less accurate, resulting in greater velocity errors over the entire strip for which they provided control. In the faster moving areas, the effects of uncompensated vertical displacement will be in greater velocity errors over the entire strip for which they provided control. In the faster moving areas, the effects of uncompensated vertical displacement will be greater, and this effect is insensitive to temporal separation. Thus, the errors for the different phases are probably similar because they are dominated by a few points where the sources of error are independent of temporal baseline. Over slower moving areas the ice/commissioning data should be more accurate. Note that the error for the total map is smaller than for the individual acquisition phases because accuracy is improved by the averaging that occurs in areas of overlap.

## Summary

Our results indicate that balance velocities can provide an acceptable substitute for in situ GPS measurement and that single-component velocity accuracies of just over 3 m/yr can be achieved. Some portion of the error is due to topography and vertical motion effects that can be removed to provide further improvement with a higher resolution DEM.

In the next year we plan to combine these results with data from descending orbits and detailed slope information to produce a 3-D velocity map over the full extent of the ice stream. We will use these data in conjunction with ice sheet models to determine the factors that control the fast flow within the icestream. The model development is well underway and testing of model inversions has begun using balance velocities as a proxy until the measured data are available.

## References

Ekholm S. A full coverage, high-resolution, topographic model of Greenland, computed from a variety of digital elevation data, *J. Geophys. Res.*, vol B10, no. 21, pp 961-972, 1996.

Fahnestock M., R. Bindschadler, R. Kwok, and K. Jezek. 1993. Greenland ice sheet surface properties and ice dynamics from ERS-1 SAR imagery, *Science*, vol. 262, pp. 1530-1534.

Joughin I., M. Fahnestock, S. Ekholm, and R. Kwok, Balance velocities for the Greenland Ice Sheet, *Geophys. Res. Lett.*, vol. 24, no. 23, pp 3045-3048, 1997.

Joughin I., R. Kwok, and M. Fahnestock, Interferometric estimation of three-dimensional ice flow using ascending and descending passes, *IEEE Trans. Geosci. Remote Sensing*, vol. 36, no. 1, pp 25-37.

Joughin I., R. Kwok, and M. Fahnestock, Estimation of ice sheet motion using satellite radar interferometry: method and error analysis with application to the Humboldt Glacier, Greenland, *J. Glaciology*, vol 42, no. 142, pp. 564-575, 1996.

# SATELLITE OBSERVATIONS OF ICE SHEET CLIMATE ON DECADAL TIME SCALES

*Dale P. Winebrenner and Robert J. Arthern, Polar Science Center Applied Physics Laboratory 1013 NE 40th Street University of Washington Seattle, WA 98105 dpw@apl.washington.edu*

## Objective

The objective of this work is to map accumulation rates and decadal variations in surface temperature in the dry snow zone in Greenland using spaceborne microwave observations, based on a quantitative understanding of the physics underlying those observations. We anticipate comparison of our results with corresponding estimates from ground observations and atmospheric modeling, and we will work toward improving accumulation rate parameterizations suitable for coupled ice sheet/atmosphere models.

## Methods

We have extended to Greenland our method for accumulation rate retrieval from 4.5 cm-wavelength (6.7 GHz) emission observations, by testing our method for Antarctica using Benson's extensive Greenland traverse observations. The relations between layering parameters and accumulation rate inferred from the latter differ slightly from, but are similar to, corresponding relations in Antarctica. A first-cut map of Greenland accumulation rates based on this update shows the theoretically expected accumulation rate/emission relationship, provided we assume a somewhat greater prevalence of snow crusts in Greenland firn, compared with Antarctic firn. We note that this is plausible in light of anecdotes from field investigators, and that, in contrast to Antarctica, a single crust appears to predominate over the whole of the dry snow zone.

The inclusion of field work in our methods this year, has had a profound effect on our understanding and certainty of our methods. We traveled to Summit in April and May, as pit-diggers with Chris Shuman. We dug a total of 5 2-m pits and 1 4-m pit, including two pits roughly 100 km from Summit; one was chosen to provide low-accumulation rate data, the other high-accumulation rate data. As discussed below, this experience and data have advanced our thinking on the density stratigraphy - accumulation rate connection, and led us to wavelet methods for analysis of density stratigraphy to quantify long- and short-scale components, both in terms of variance and the "shape" of their associated density variations (the latter being consequential for revised emission modeling).

## Results

The relationship we observe between emission (polarization) and accumulation in Greenland is consistent with that expected from earlier work in Antarctica, after allowing for a slightly different relationship between accumulation rate and "mean layer thickness" (cf. below), as estimated from Benson's data, and for apparently greater (but spatially invariant) crust parameters. Moreover, it appears that despite the coarse (150 km) spatial resolution of 6.7 GHz Scanning Multichannel Microwave Radiometer (SMMR) data, observations interpolated onto a 25 km grid usefully reflect true underlying emission and accumulation rate variations. We provided our first-cut Greenland accumulation rate map to the PARCA community in March 1998 to help in planning field data acquisition. We anticipate imminent comparison of our map with ground-based data from the 1998 field season.


Figure 1. Accumulation map derived from passive-microwave emission data.

The 1998 field season provided both first-hand familiarity with firn layering and a trove of much higher quality density profiles than were previously available to us. These in turn have modified our modeling of firn density stratification in relation to accumulation rate. It is now clear 1) that the annual cycle of density variation is the cause of the correlation we observed between estimated layering parameters and accumulation rate; 2) that density stratification consists additionally of a component with very short-scale (~1 cm) variability accounting for roughly half of the total variance in firn density stratigraphy; and 3) that these components together affect emission (on prior evidence) in such a way as to reproduce the accumulation rate - emission relationship we expected on the basis of a simpler firn stratigraphy model. So although we can now explain why our estimates of "mean layer thickness" correlate with accumulation rate, we must revise our understanding of stratigraphy parameterization and the relationship between stratigraphy and emission, to better explain our earlier, empirical success.

**Future Work**

Our next steps follow directly from the discussion above: 1) We are using wavelet methods to quantitatively decompose and estimate parameters for the two components of density stratification; 2) We will analyze as many data as are available to estimate, and understand, the relationships between spatial variations in those parameters and accumulation rate variations (for this task, we expect to collaborate with Shuman and use his isotope profiles to verify and understand annual density and accumulation rate information); and 3) we will use the resulting new stratigraphy model in conjuction with electrodynamic modeling of firn emission to understand the observed emission/accumulation relationships.

# Airborne Resurveys of the Southern Greenland Ice Sheet

*William B. Krabill, Code 972, NASA/GSFC Wallops Flight Facility, Wallops Island, VA, 23337 krabill@osb.wff.nasa.gov*

*Earl Frederick, Serdar Manizade, Chreston Martin, John Sonntag, Robert Swift, Robert Thomas, Wayne Wright, and Jim Yungel, EG&G, NASA Wallops Flight Facility, Wallops Island, VA 23337*

## Introduction

1998 was a milestone for PARCA, in that airborne laser-altimeter flight lines from 1993 over southern parts of the ice sheet were resurveyed with almost complete repeat coverage. In 1993 and 1994, NASA surveyed the entire Greenland ice sheet by airborne laser altimeter (Figure 1), obtaining surface-elevation profiles with root mean square (rms) accuracies of 10 cm or better (Krabill et al, 1995) along flight lines that crossed all the major catchment basins. In 1998, the ten flight lines flown in 1993 in the south of Greenland were resurveyed with about 99% repeat coverage; flight lines in the north will be resurveyed in 1999. Additional flights in 1998 were over glaciers, identified by E. Rignot, where existing SAR data give information on ice motion.

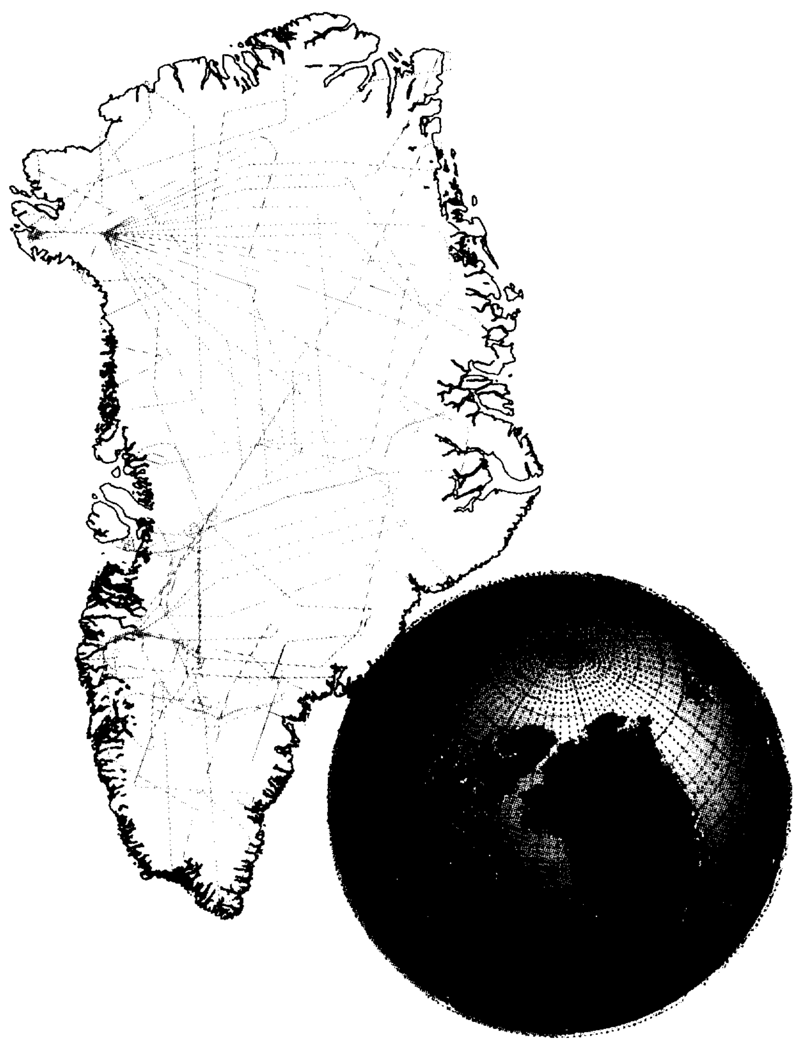

Figure 1. Airborne laser-altimeter flight lines from 1993 and 1994. The 1993 lines were resurveyed in 1998, and the 1994 lines will be resurveyed in 1999.

The Airborne Topographic Mapper (ATM-1) is a conical-scanning laser with a pulse repetition rate of 3 kHz (800 Hz in 1993) and scan rate of 10 Hz (5Hz), at an off-nadir angle of 10 degrees. Aircraft location is determined by kinematic Global Positioning System (GPS) techniques, and aircraft heading, pitch, and roll are measured by inertial navigation systems. At an aircraft altitude of 400 meters above the surface, a 140-m swath of data is acquired comprising a dense array of 1-m laser footprints. Instrument biases and overall performance are checked during each flight by overflying flat surface areas (such as sea ice or fjords) and precisely-surveyed portions of the runway. Additional checks are made on data consistency by comparing data at locations where flight lines cross and at stations on the ice sheet where surface-based GPS measurements were made. During repeat surveys, the airplane is navigated along the earlier flight lines by a GPS-guided autopilot, achieving cross-track separations typically less than 50 meters. A second version of the instrument (ATM-2) operated concurrently with ATM-1, with a 15 degrees off-nadir scan angle, yielding a swath width of about 200 meters, but with lower accuracy.

**Results**

Results of comparison between the 1993 and 1998 surveys are shown in Figure 2, where colors represent rates of elevation change along the survey flight lines. The error in change rates derived from a single flight line is about 2 cm/yr, so flight segments with changes of less than 2 cm/yr can be regarded as being in mass balance over the period, and are shown as pale gray. Figure 2 shows the rates of change in surface elevation that have occurred between June/July 1993 and June /July 1998. Because rock beneath the ice sheet is also moving vertically as a result of past and present changes in ice loading, these are not identical to ice thickening/thinning rates. Consequently, a rock uplift rate of approximately 5 mm/yr (Davis et al, 1998) should be subtracted from our elevation-change rates to yield estimated ice thickening and thinning rates.

Major features in Figure 2 are:

1. Three areas in the south that are thickening at rates up to 25 cm/yr.
2. Large, peripheral areas of thinning, with thinning rates increasing rapidly towards the ocean. Where the ice-sheet ridge runs north-south, it also marks a remarkably sharp transition between thickening to the west and thinning to the east.
3. Very high thinning rates (up to >1 m/yr) in the lower reaches of east-coast outlet glaciers. These observations represent the major new contribution of this work.

Our results give an average thinning, for elevations above 2000m, of 1mm/yr $\pm$ 7mm/yr for 1993-1998, which is close to the estimate of 15 mm/yr thickening between 1978 and 1988 from satellite radar-altimeter data for the same region (Davis et al, 1998). It would appear that these higher-elevation central regions have been almost exactly in balance for the past 20 years.

The lower-elevation, coastal regions are behaving differently. Extensive thinning in the east is consistent with observations of warmer-than-normal temperatures for 1993-1998, but we also find areas of thinning near the west coast, where temperatures were cooler than normal (Abdalati et al., this report). In general, the elevation changes along the west side of the ice sheet show good qualitative agreement with estimates of marginal activity between 1950 and 1985 based on comparison of aerial photographs (Weidick, 1991) but not along the east coast, where the earlier, rather sparse data suggest glacier advance.

These are the first observations of extensive, near-coastal thinning of the Greenland ice sheet, and they raise the importance of the detailed monitoring of these regions that will be provided by NASA's ICESAT, carrying a laser altimeter, scheduled for launch in 2001. Meanwhile, the aircraft measurements described here will provide baseline data for comparison with early ICESAT data to give 10-year trends in Greenland ice thickness.

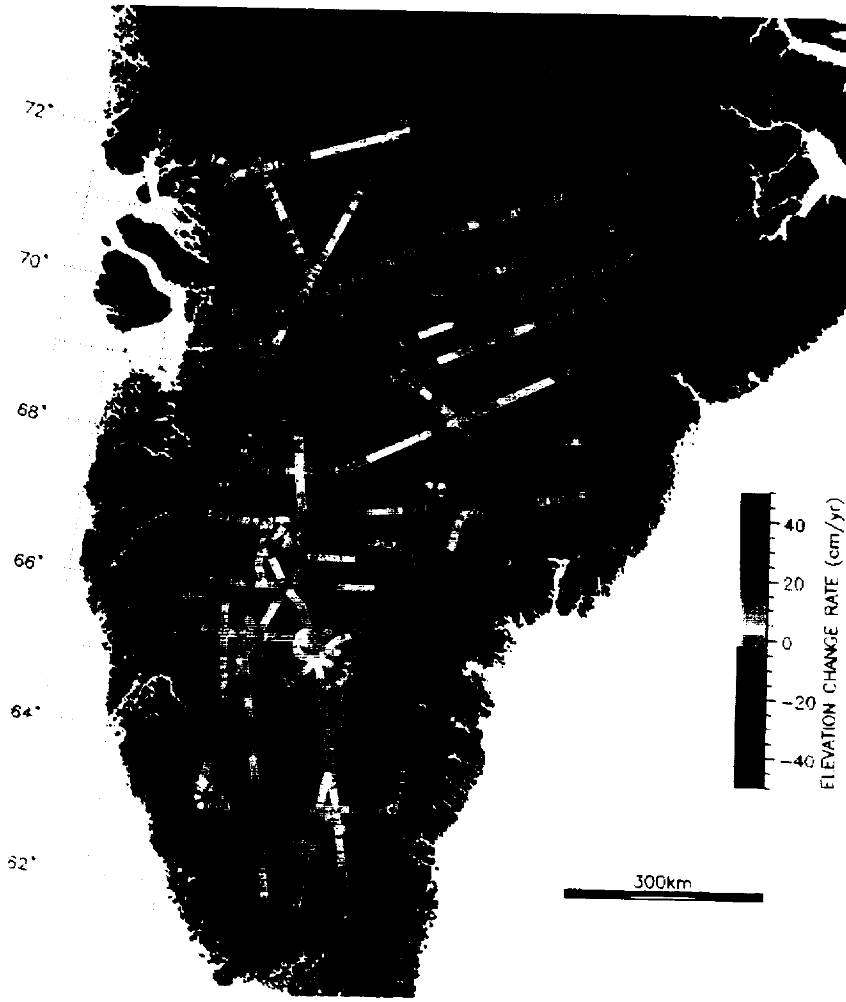


Figure 2. Greenland, showing flight tracks of laser-altimeter surveys color-coded according to the rate of surface elevation change. The pale gray segments are in balance to within the survey errors ($\pm 2$ cm/yr).

## References


C. H. Davis, C. A. Kluever, and B. Haines. 1998. Elevation change of the southern Greenland ice sheet. *Science*, 279, p. 2086-2088.

W. B. Krabill, R. H. Thomas, C. F. Martin, R. N. Swift, and E. B. Frederick. 1995. Accuracy of airborne laser altimetry over the Greenland ice sheet. *Int. J. Rem. Sens.*, 16, p. 1211-1222.

Weidick. A1991. Present-day expansion of the southern part of the Inland ice. *Rapp.Gronlands. Geol. Unders.*, 152, p. 73-79.

# FOCUSED SAR PROCESSING OF COHERENT DEPTH SOUNDER DATA AND RESULTS FROM 1998 NGRIP SURFACE EXPERIMENT

*J. Legarsky and S.P. Gogineni, The University of Kansas, 2291 Irving Hill Road, Lawrence, KS 66045, legarsky@rsl.ukans.edu*

## Project objectives

We have been performing airborne ice-thickness measurements using a coherent radar depth sounder [*Chuah*, 1997a; *Chuah*, 1997b] as part of the NASA PARCA program. The radar uses complementary Surface Acoustic Wave (SAW) devices for pulse expansion and compression. The system operates as an unfocussed SAR. We have used this system to collect a large volume of data over the last five years, obtaining clear echoes from the bottom as well as from layers to a depth of about 2.5 km over the new European deep drill site and several outlet glaciers.

## Tasks completed during 1997-1998

Tasks completed during the 1997-1998 year:
1. Collected ice thickness data
2. Redesigned antenna
3. Designed and tested an interferometric mode for NG-CORDS
4. Processed and published data from 1997 field season
5. Designed and tested an optical delay line for NG-CORDS
6. Tested new data acquisition system
7. Conducted NGRIP surface experiment

We collected radar data over the interior ice sheet, around the margin and over outlet glaciers using an Improved Coherent Radar Depth Sounder. Radar data are tagged with geolocation information obtained with GPS receivers onboard. In addition radar data were collected in conjunction with laser altimetric measurements of ice-surface elevation. We also developed the Next-Generation Coherent Radar Depth Sounder (NG-CORDS), which is capable of measuring polar ice-thickness to about 4000 m in colder ice and to lesser thicknesses in temperate glaciers using MIcrowave Monolithic Integrated Circuits (MIMICs). The ice thicknesses of Greenland's 2000-m contour line and summit (ice thickness of about 3200 meters) were measured during the recent field seasons; moreover, these measurements are being used in conjunction with models to estimate Greenland's mass balance.

These radar systems have measured the thickest ice in Greenland (about 3200-m thick) using unfocused processing; however, the unfocused images collected in a portion of southwestern Greenland showed weak bottom returns. We developed and implemented a new focusing algorithm for the coherent system, which increases the signal-to-noise ratio and sharpens the resolution as shown in Figure 1. Using these techniques, we successfully obtained the first high-quality ice thickness measurements in southwestern Greenland. Figure 2 shows an example of the focused bottom echoes in southwest Greenland. Figure 3 shows focused internal layers data collected over southwest Greenland.

In addition to the airborne experiment, We conducted a 1998 surface experiment at the North Greenland Ice core Project (NGRIP) ice camp. Radar measurements of the bedrock showed strong signal-to-noise ratios between 30 dB to 60 dB. Internal layers were imaged down to near the bedrock, deeper than those previously measured. Figure 4 shows a radio echogram of one of the NGRIP traverses. Figure 5 shows the deep internal layers that were imaged.

**Results**

We have successfully acquired radar depth-sounding data every year since 1993 and published several refereed papers based on our ice-thickness data; furthermore, we refined the radar to the level where we now routinely make field measurements. We have been providing routine ice-thickness measurements of the Greenland ice sheet to scientists worldwide. There are several papers partly based on the radar ice-thickness data, which have been or soon will be published [*Rignot et al.*, 1997; *Allen et al.*, 1997; *Dahl-Jensen et al.*, 1997; *Legarsky et al.*, 1998].

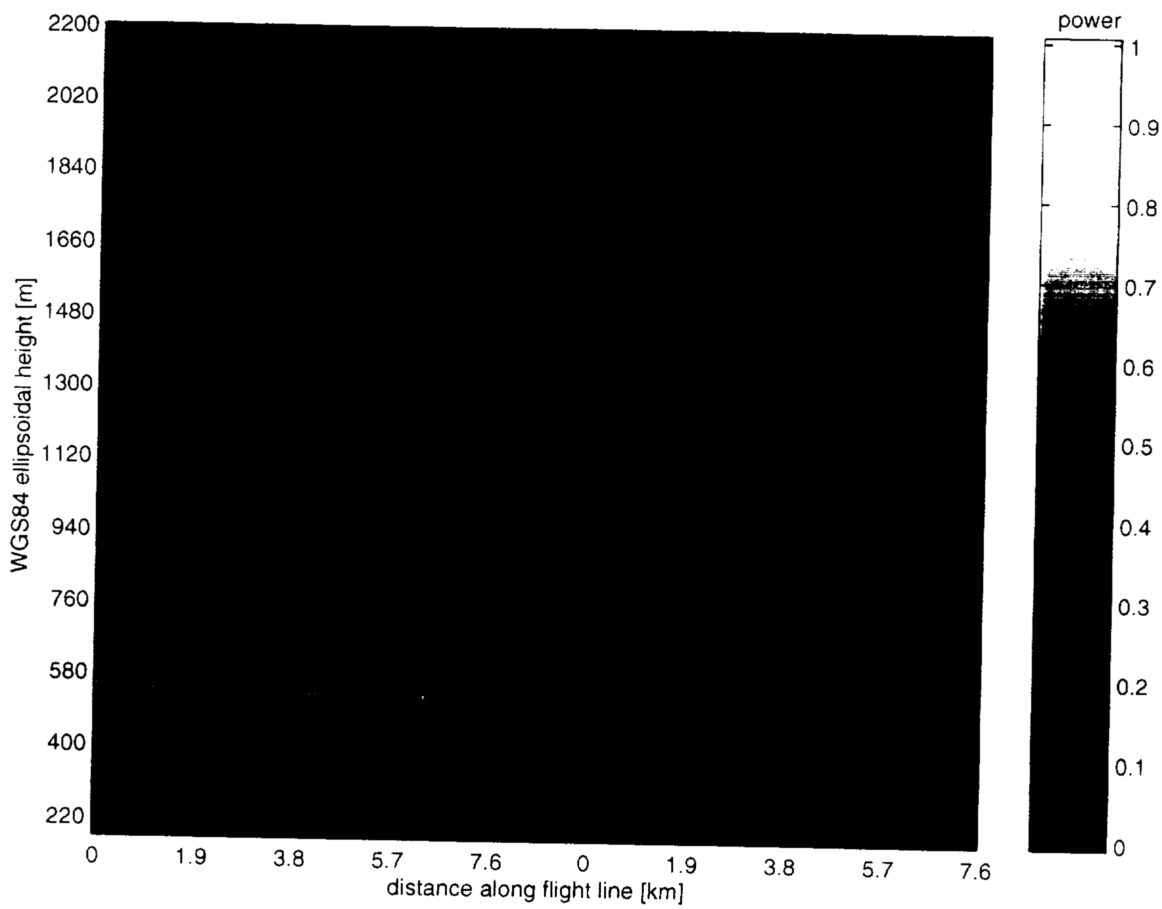


Figure 1. Left frame shows focused ice-sounding radar image. Right frame shows the unfocused ice-sounding radar image. Data were collected in Northwest Greenland.

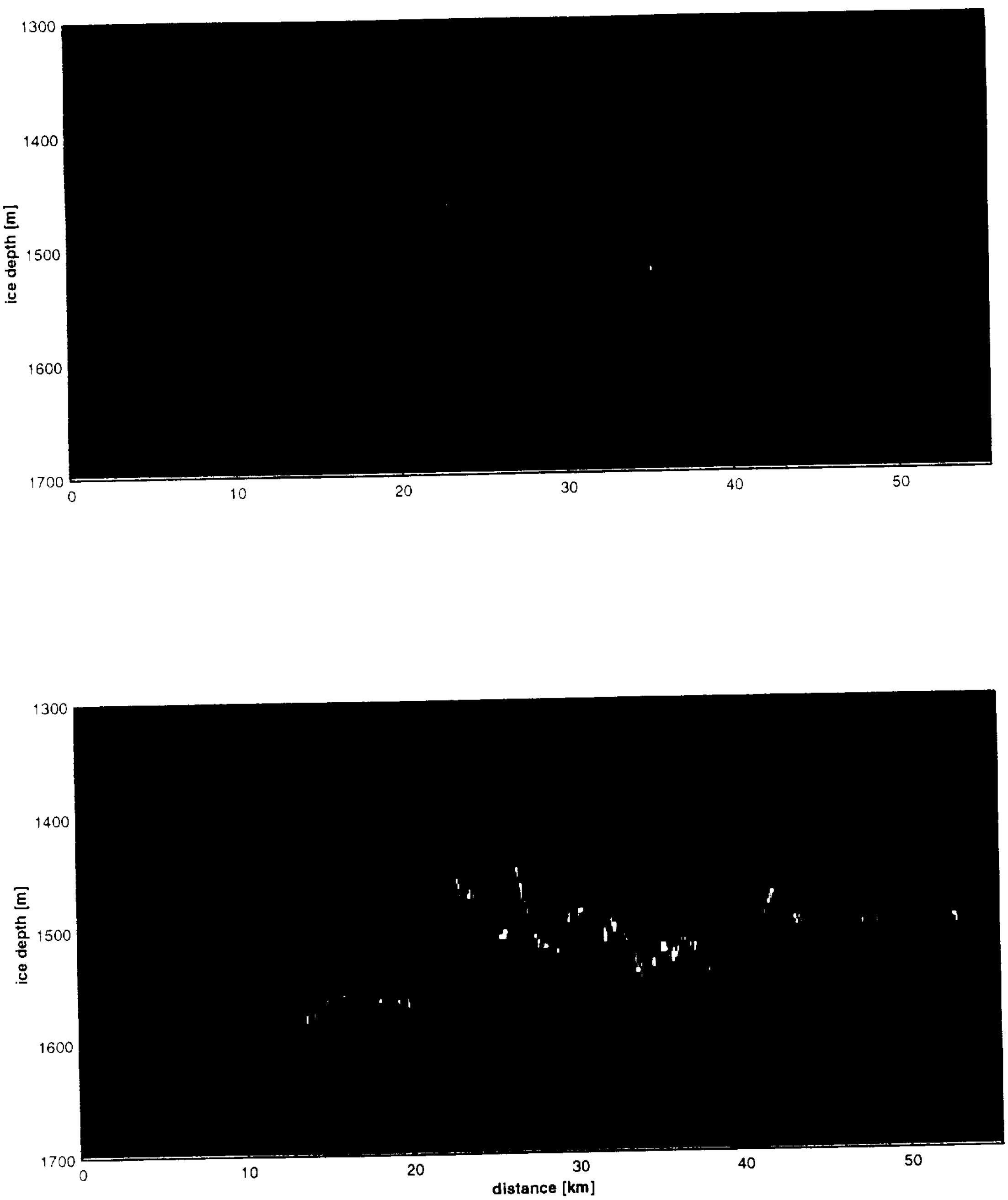


Figure 2. Top frame shows unfocused bottom return. Bottom frame shows focused bottom return. Data were collected over Southwest Greenland.

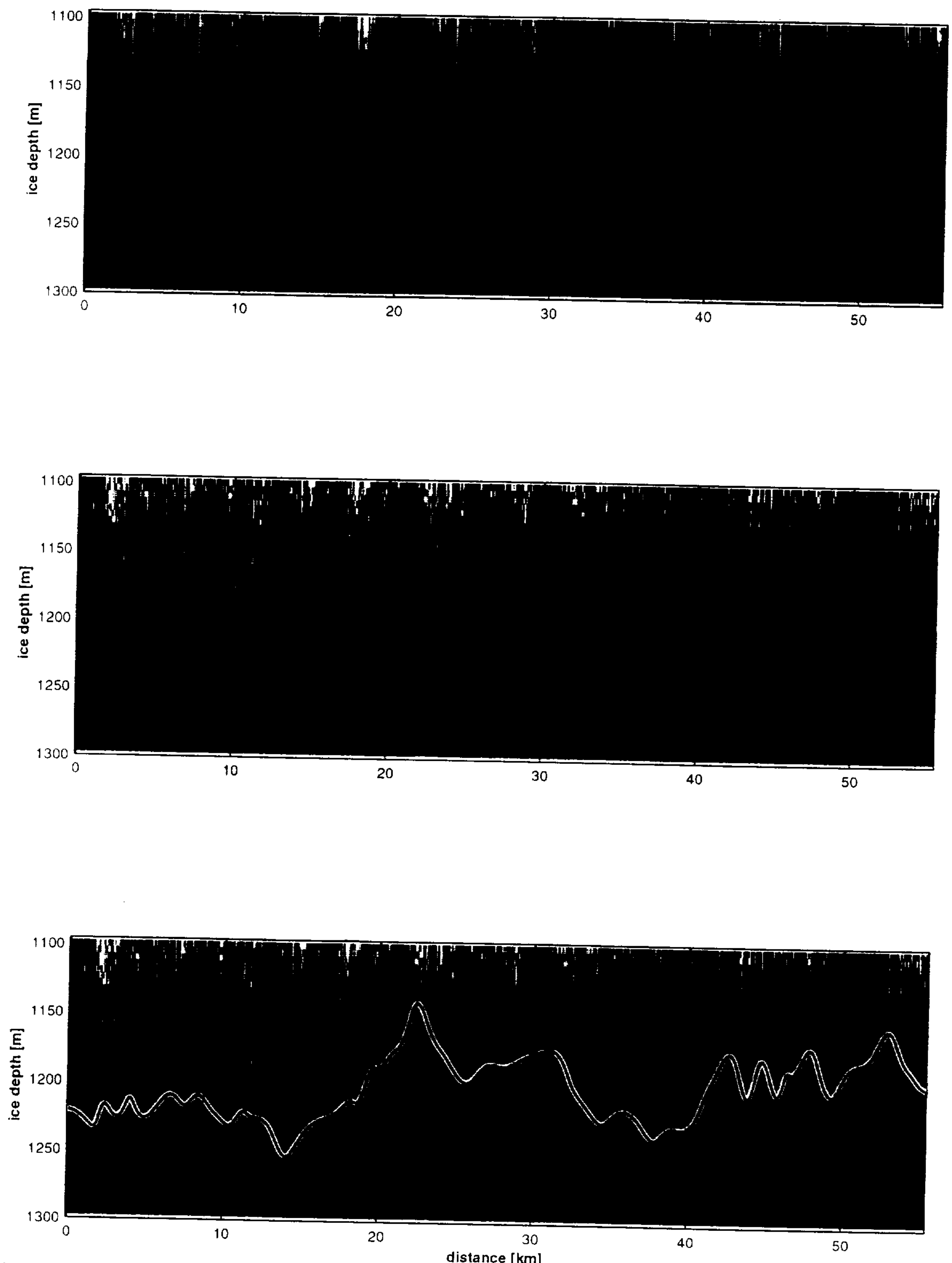


Figure 3. Top frame shows unfocused radar data. Middle frame shows focused radar data with a weak internal layer signal-to-noise ratio improved. Bottom frame shows the detected internal layer. Data were collected over Southwest Greenland.

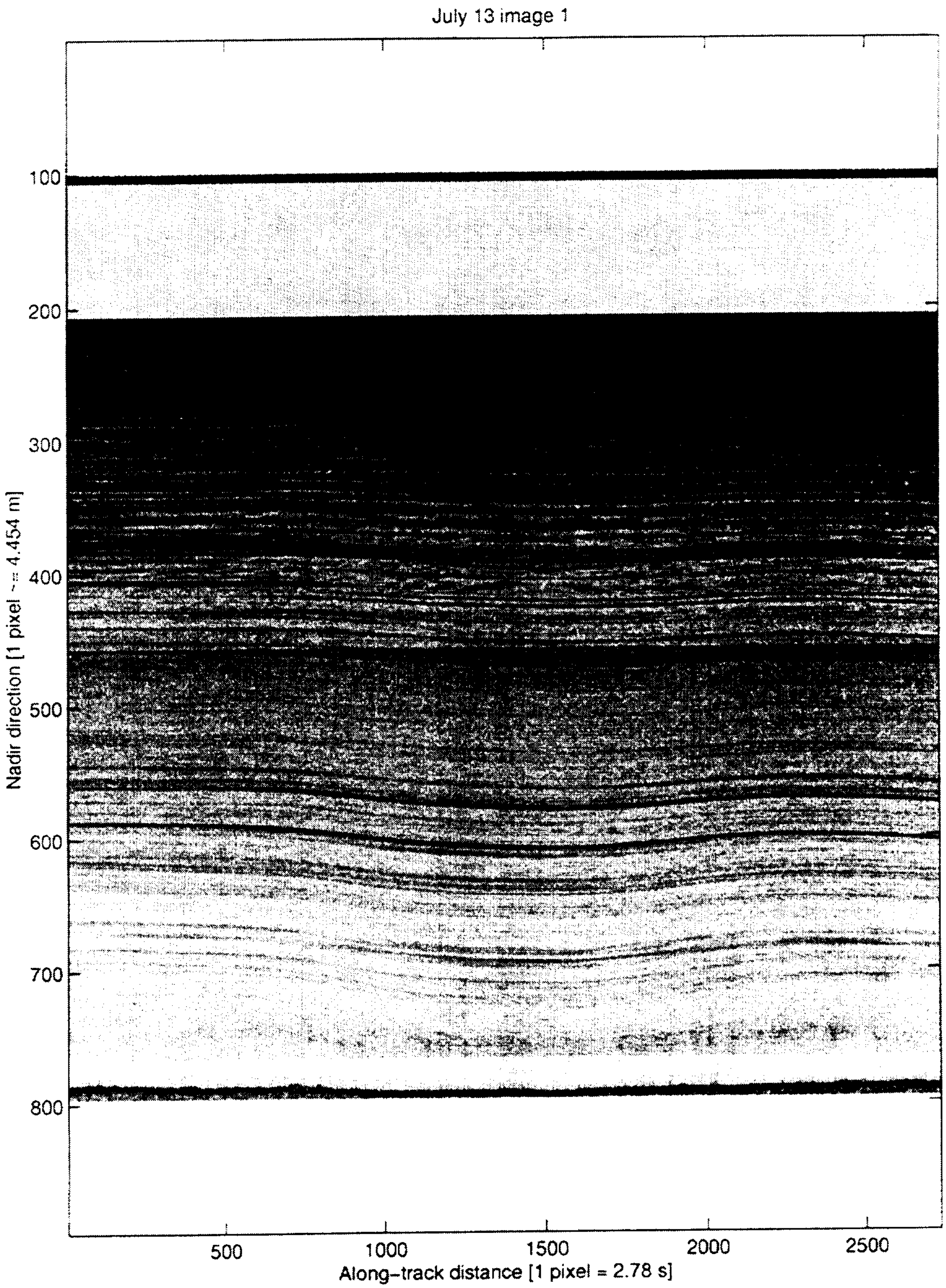


Figure 4. Radio echogram collected at NGRIP, Greenland.

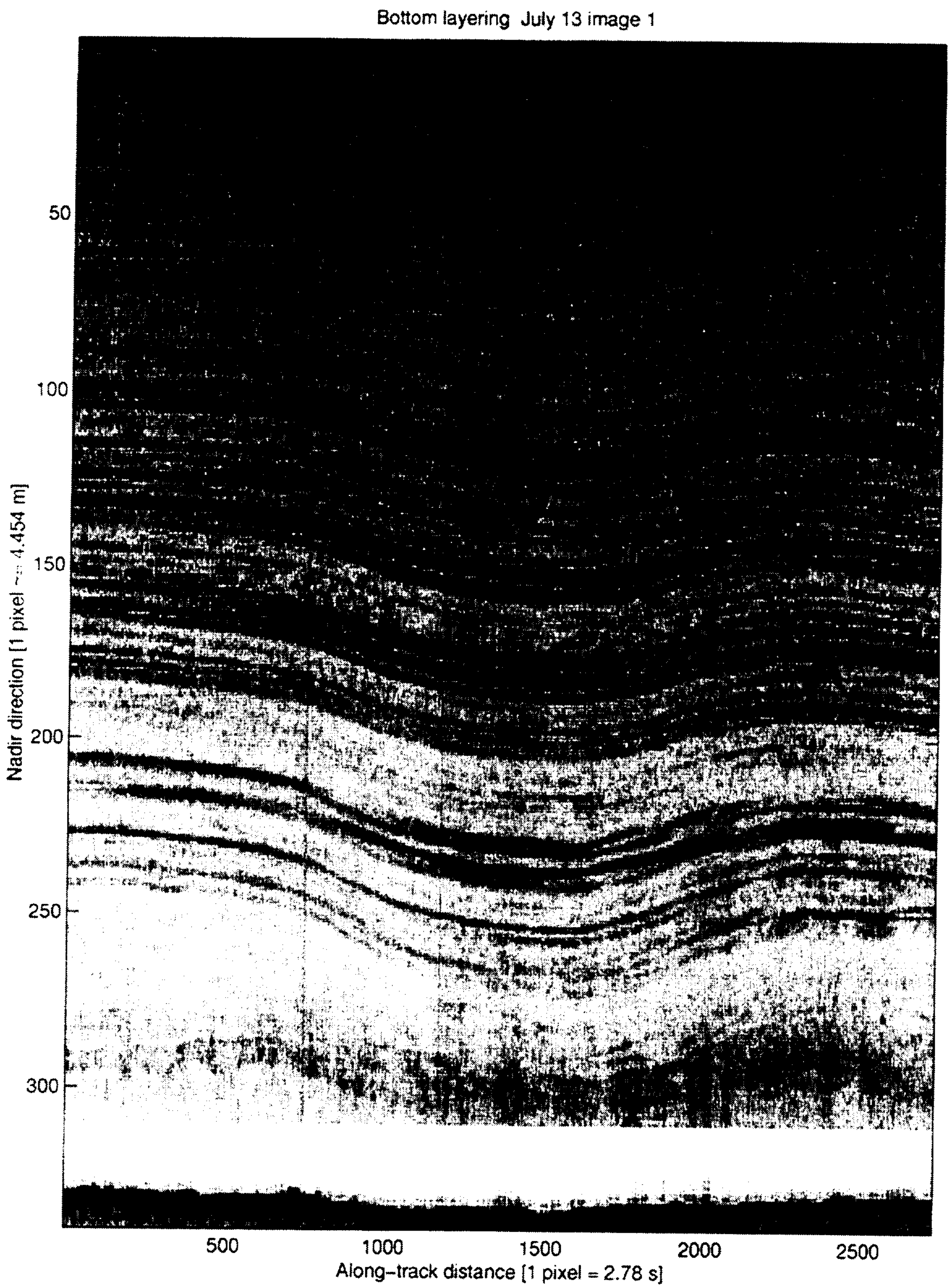


Figure 5. Expanded bottom view of the NGRIP radio echogram. Internal layer around pixel 300 is at a depth of about 2880 m. The bottom depth is about 3080 m at pixel 345.

**Plans for 1998-1999**

The main task of the 1999 field mission is to repeat the 1994 measurements over northern Greenland for a five-year comparison study.

**References**

Allen, C., S. Gogineni, B. Wohletz, K. Jezek and T. Chuah, Airborne radio echo sounding of outlet glaciers in Greenland, *International J. Remote Sensing Letters*, vol. 18, no. 14, pp. 3103-3107, 1997.

Chuah, T. S., Design and Development of a Coherent Radar Depth Sounder for Measurement of Greenland Ice Sheet Thickness, RSL Technical Report 10470-5, January 1997, 125 pages.

Chuah, T. S., Component characterization and data sheets for Design and Development of a Coherent Radar Depth Sounder for Measurement of Greenland Ice Sheet Thickness, RSL Technical Memorandum 10470-2, January 1997, 120 pages.

Dahl-Jensen, D., N. S. Gundestrup, K. Keller, S. J. Johnsen, S. P.Gogineni, C. T. Allen, T.S. Chuah, H. Miller, and S. Kipfstuhl, A search in north Greenland for a new ice core drill site, *Journal of Glaciology*, vol. 43, no. 14-, June, 1997.

Legarsky, J., V-antenna for coherent depth sounding radar: 1996 sled expedition, RSL Technical Memorandum 10470-1, June 1996.

Legarsky, J., A. Wong, T. Akins, and S. P. Gogineni, Detection of hills from radar data in central-northern Greenland, *Journal of Glaciology*, vol. 44, no. 146, 1998.

Rignot, E. J., S. P. Gogineni, W. B. Krabill, and S. Ekholm, North and northeast Greenland ice discharge from satellite radar interferometry, *Science*, vol. 276, pp. 934-937, 9 May 1997.

# AIRBORNE ICE-THICKNESS MEASUREMENT: STATUS REPORT AND FUTURE WORK

*Torry Akins, Sivaprasad Gogineni, Pannirselvam Kanagaratnam, Justin Legarsky and Anthony Wong, The University of Kansas, 2291 Irving Hill Road, Lawrence, KS 66045 takins@rsl.ukans.edu*

## Introduction

The University of Kansas has been participating in NASA's airborne remote sensing program for performing ice-thickness measurements using a coherent radar depth sounder. This depth sounder is capable of measuring ice thickness up to 4000 m in the colder ice of northern Greenland and lesser thickness in temperate ice. A large volume of data has been collected with this system over the past six years.

Many improvements have been made to the depth sounder's transmitter and receiver since its initial operation in 1993. The Next-Generation Coherent Radar Depth Sounder (NG-CORDS) is a compact version of the depth sounder that contains many of these improvements.

## Tasks completed during 1997-1998

During the 1997 field season, it became apparent that the depth sounder needed slightly more sensitivity to sound the southwestern contour line successfully. The following improvements were made to the depth-sounding system after the 1997 field season to enhance its performance for obtaining data in the Southwest:

- New Digital System
- Antenna Improvements

The new digital system shown in Figure 1 was designed and built at the University of Kansas. It was designed to improve the system. It accomplishes this by using 12-bit A/D converters instead of the 8-bit converters that were used in the original digital system. The new system can handle much higher data rates than the original system. This allows the system to do less data averaging and to record data that can be used in different types of post-processing algorithms.

The lengths of the cables that feed the individual dipoles of the antenna array were modified to steer the antenna beams. This technique was used to compensate for the tilt of the aircraft wings. The transmission lines that connect the depth sounder to the antennas were replaced with low-loss lines. These two antenna improvements removed approximately 9 dB of loss from the system.

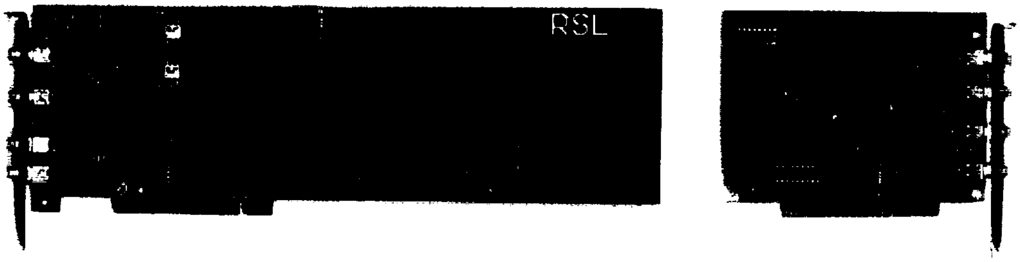


Figure 1: Improved Digital System

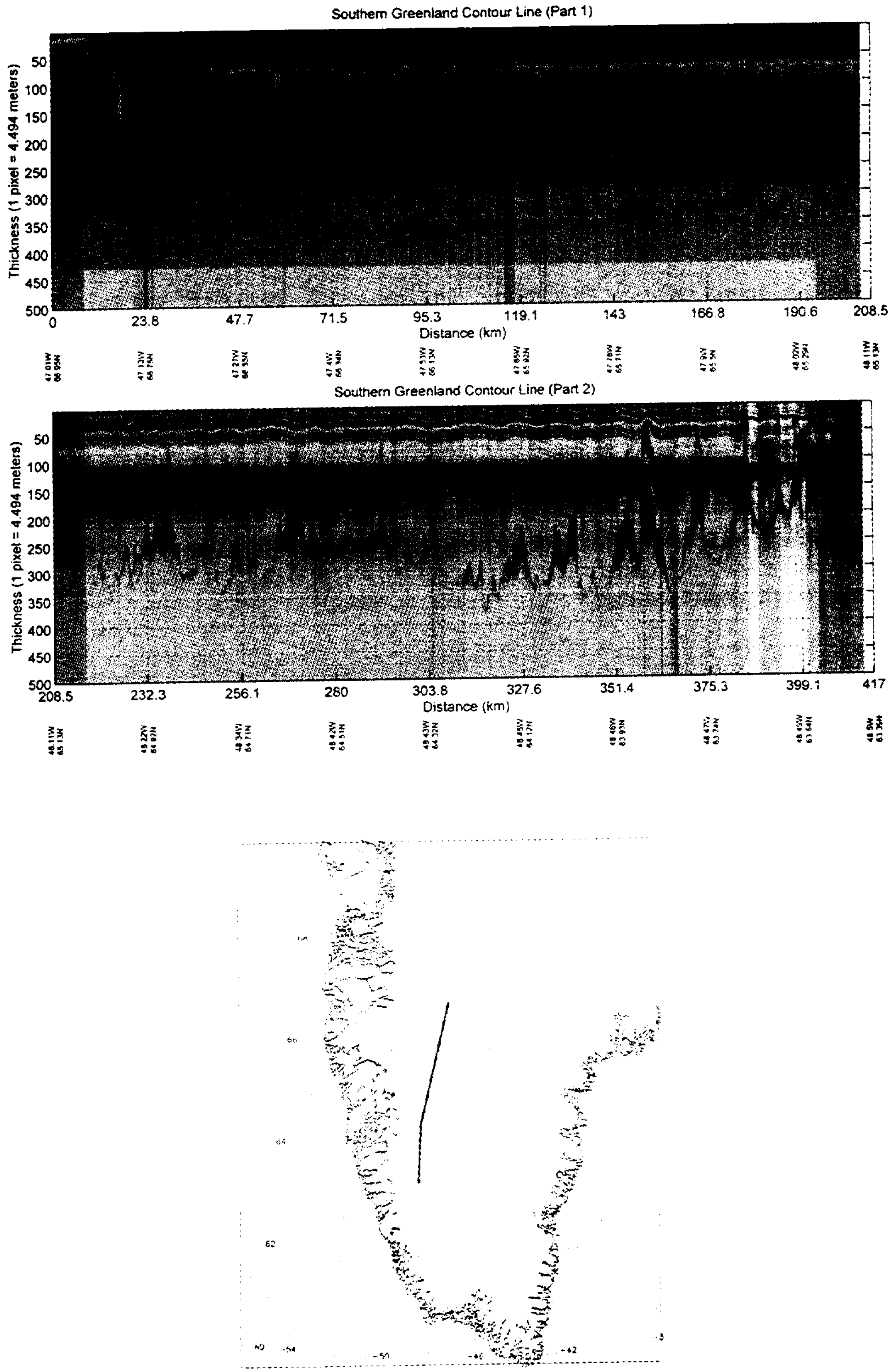


Figure 2 (top): radio echograms for a portion the southern Greenland 2000 m contour line. (bottom) Map of the Upper Section of the Southwest Contour Line from which the data in the top figure were collected

Using the depth sounder, we successfully collected ice thickness data on all the missions over Greenland during the 1998 field season, including the southwestern contour line that was unsuccessfully sounded in 1997. An echogram of the upper section of the southwestern contour line is shown in Figure 2(a). The flight line for this echogram is displayed in Figure 2(b).

The 1993, 1995, 1996 and 1997 data have been written to compact disc. These data are currently available to anyone upon request. Using our CD library, we can quickly meet user data requests by mail or ftp.

## Results

We have successfully acquired radar depth-sounding data every year since 1993, and have published several papers based on our ice-thickness data; furthermore, we refined the radar and its digital system to the level where we now routinely make field measurements. We have been providing routine ice-thickness measurements of the Greenland ice sheet to scientists world wide.

## Future work

Currently we are working on processing the remainder of the 1998 data and hope to release it by March of 1999. The main task of the 1999 field mission will be to repeat the 1994 measurements over northern Greenland for a five-year comparison study.

# HIGH-RESOLUTION MONITORING OF INTERNAL LAYERS AT NGRIP

*Pannirselvam Kanagaratnam, Sivaprasad Gogineni, Justin Legarsky and Torry Akins, The University of Kansas, 2291 Irving Hill Road, Lawrence, KS 66045, pkanagar @rsl.ukans.edu*

## Objective

One of the major goals of NASA's Office of Earth Science Polar Program is to determine the mass balance of the Greenland and Antarctic ice sheets. A key variable in assessing the mass balance of an ice sheet is accumulation rate. Currently, accumulation rate is determined from ice cores and pits. These data are sparse and there are large uncertainties in existing accumulation rate maps derived from sparely distributed ice cores and pits. There is an urgent need for developing remote sensing techniques for determining accumulation rate.

We developed an ultra wideband Frequency Modulated-Continuous Wave (FM-CW) radar system for determining the accumulation rate. The radar system operates over the frequency range from 100 to 2000 MHz, for imaging the top 200 to 300 meters of ice with high resolution using both echo amplitude and phase information. We performed shallow radar sounding experiments at the North Greenland Icecore Project (NGRIP) site during June and July of 1998. Preliminary results from our experiments are presented here.

## Approach

To obtain the accumulation rate data, we focus on the following tasks:

1. Obtain electrical record of ice cores.
2. Use the finite-difference time-domain (FDTD) technique to determine optimum radar parameters by simulating the scattering response of the ice sheet due to radar sounding.
3. Design a radar system based on the parameters obtained from the simulation.
4. Develop the system.
5. Make measurements using this system at the NGRIP site.
6. Analyze data and publish results.

We have completed tasks 1 through 5, and we are currently analyzing the data. We will reduce these data to determine amplitude and phase information as a function of depth for the top 200 to 300 meters of ice. By determining echo amplitude and phase, we can isolate the returns from known volcanic events from the returns from other events. This will help us to estimate the accumulation rate.European investigators have drilled a deep core at this site and have performed conductivity measurements on it. We will work with these investigators to analyze radar and conductivity data and will develop an algorithm for estimating the accumulation rate at this site.

## Results

The results are shown in Figure 1. The figures show the radar echogram of internal layers observed at NGRIP. We can see that some of the layers correspond to known volcanic events. The volcanic horizons were identified at the NGRIP site by scientists from the Alfred Wegner Institute (Germany) and the Department of Glaciology at the University of Copenhagen (Denmark). The layer depths measured with our radar are within +/- 2m of the volcanic layers obtained from icecore data.

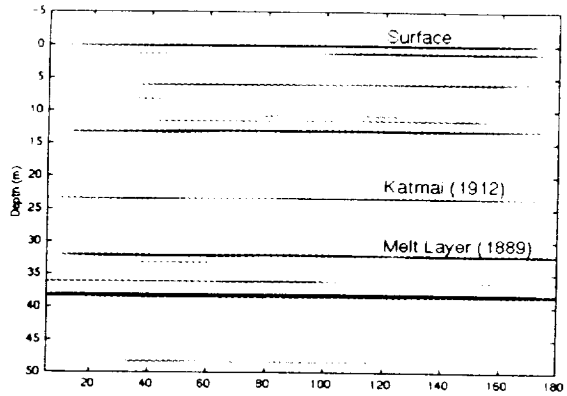


**Figure 1(a).** Radar echogram of internal layers observed at NGRIP (0-50m).

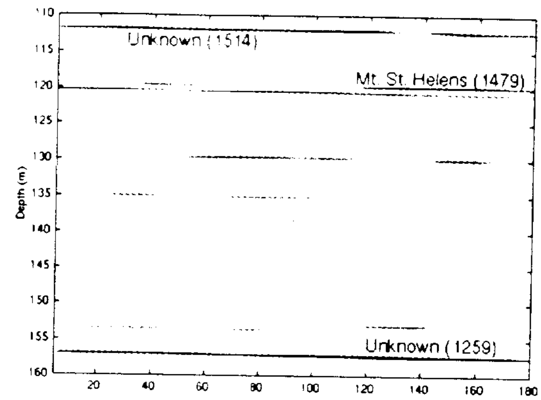


**Figure 1(b).** Radar echogram of internal layers observed at NGRIP (110-160m).

**Future work**

It has been reported that the real part of the acidic layer and background are the same and that the main cause of internal reflections from ice is change in conductivity resulting from acidic impurities embedded in ice during volcanic eruptions. The reflection coefficient resulting from a change in conductivity is purely imaginary, whereas the reflection coefficient caused by change in the real part of the permittivity is purely real. Therefore, by measuring both echo amplitude and phase, we can isolate the returns from known volcanic events from the returns from other events. Our next step will be to analyze the phase of the reflections from the internal layers in our measured data to determine the source of reflection.

We have also started to design a radar system for airborne measurements. The system will be a pulse radar operating from 350 MHz to 650 MHz. With this system we should be able to map internal layers at 50 cm resolution and also map the ice thickness.

# ULTRA WIDE BAND GROUND-BASED RADAR MEASUREMENTS

*Francois Baumgartner and Ken. Jezek, Byrd Polar Research Center, The Ohio State University, baum@iceberg.mps.ohio-state.edu*

## Summary

Radar remote sensing is an important and widely used tool for studying long term changes and seasonal dynamics of the Greenland Ice sheet. Still, there is a limited understanding of the relationship between regionally varying glaciological properties of firn conditions categorized across Greenland as diagenetic glacier facies. We present results from the dry-snow zone which demonstrate the ability to estimate accumulation rate from SAR backscatter. To investigate this relationship we compared co-registered backscatter and mean-annual accumulation rate data over the summit area, where accumulation is well constrained, and also through a large extent of the remaining dry-snow zone where accumulation is poorly constrained. In the summit area the C-band backscatter and mean-annual accumulation rate data for all four transects show that the backscatter increases as the accumulation rate decreases. This relationship extends many hundreds of kilometers throughout the dry snow zone, especially where the accumulation is low. The backscatter is less sensitive and the relationship appears to break-down at the higher accumulation rates. However, the results from the summit area indicate that at least the initial loss of sensitivity may result from the coarse resolution of accumulation data. The most probable mechanisms relating accumulation rate to backscatter in the dry snow zone are 1) volume scatter from the increase in grain size with depth as accumulation rate decreases, and 2) scattering from buried annual layers and depth hoar mechanisms could account for the decreased sensitivity with high accumulation.

To investigate the scattering sources we compare high-resolution ground-based radar returns with snow/firn stratigraphy from pits and cores. This data will also be used to constrain a coupled snow-metamorphose and back-scatter model which will lead to an inverse model for accumulation rate estimation from SAR backscatter.

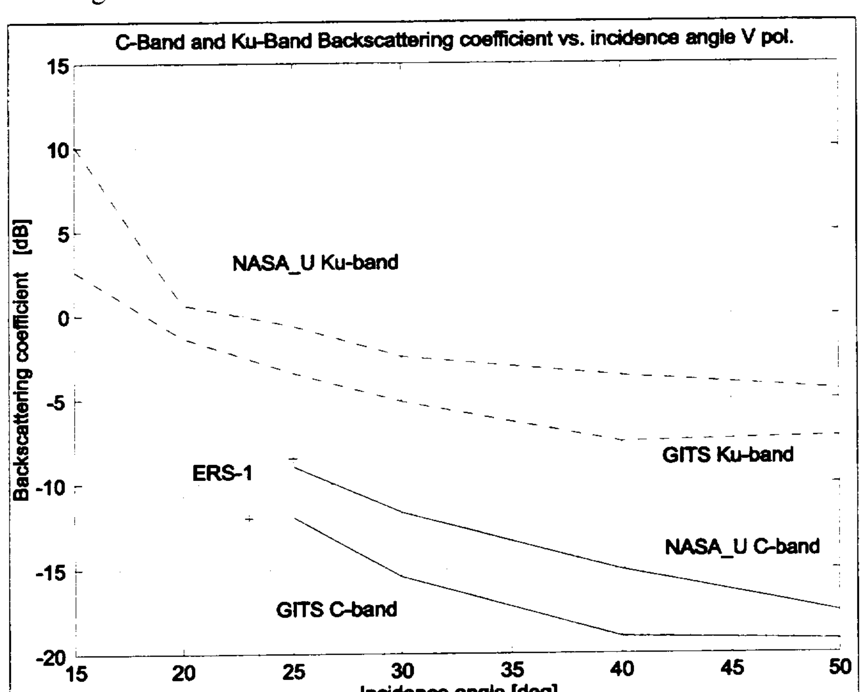


**Figure 1: Comparison between Ground-based and ERS-1 (C-band) backscattering coefficients.**

# MASS BALANCE OF THE NORTH AND EAST SIDES OF THE ICE SHEET

*Robert Thomas, EG&G Services, NASA Wallops Flight Facility, Code 972, Wallops Island, VA 23337*

*Bea Csathó, Byrd Polar Research Center, The Ohio State University, Columbus OH, 43210 csatho@ohglas.mps.ohio-state.edu*

## Introduction

During 1993 through 1997, ice motion was inferred from repeat GPS measurements at stations, shown in Figure 1, completely circumnavigating the ice sheet. Most of the stations lie close to the 2000-meter contour, apart from several in the south east which are significantly higher because of high mountains, crevasses and nunataks. The major goal of this work was to estimate the mass balance of the ice sheet lying within the traverse, by comparing total ice discharge with upstream snow accumulation. Last year, we presented results from part of the western side of the ice sheet and, over the past year, we have analyzed data from the north and east portions of the ice sheet, which we present here. Estimates of ice discharge require measurements of ice thickness from the University of Kansas group, and the 1997 measurements were not successful over portions of the stake traverse in the south and southwest which lie over ice that is warm and deep. In 1998, improvements in the U Kansas radar resulted in the first successful measurements of ice thickness over this entire region, but data processing will not be complete in time for us to fill the gaps in our mass-balance calculations for this report.

Details of the stake traverse, mass-balance analysis, and error assessment were provided in the 1997 PARCA Report, and in the resulting publication (Thomas et al, in press). Briefly, our approach is to:

1 Estimate ice discharge (Q) through gates, between adjacent traverse stations, by dividing the gate into small sections and adding the products of interpolated ice velocity, gate width normal to ice motion, ice thickness, and a correction factor R, which is equal to the column-averaged velocity divided by surface velocity.

2 Compare Q with the total volume (V) of ice accumulated as snow over the catchment region, with area S, corresponding to the gate, and estimate an average ice thickening rate T = (V-Q)/S.

## Results

Errors are quite large for gates between adjacent traverse stations (30-km apart), because of large percentage errors in S for the small associated catchment regions. Consequently, Figure 2 presents our results as values of T calculated for several adjacent traverse stations, such that their collective catchment area is approximately 30,000 sq km. The group of gates was shifted, one traverse station at a time, to give values of T plotted in Figure 2 at positions corresponding to the centers of the groups of gates. Errors here are dominated by uncertainty in the accumulation rate (A) and in R, and are equal to about 0.15A. For this analysis, we used values of A from Ohmura and Reeh (1991), and we know, from German and PARCA ice cores, of significant errors in parts of the ice sheet. As these new data become available, we shall include them in our analysis. Meanwhile, the information in Figure 2, together with known deficiencies in the Ohmura and Reeh data set, suggest the following:

1 The catchment region corresponding to the stations between Camp Century and the northeast corner of the traverse (AB in Figure 1) is very close to balance.

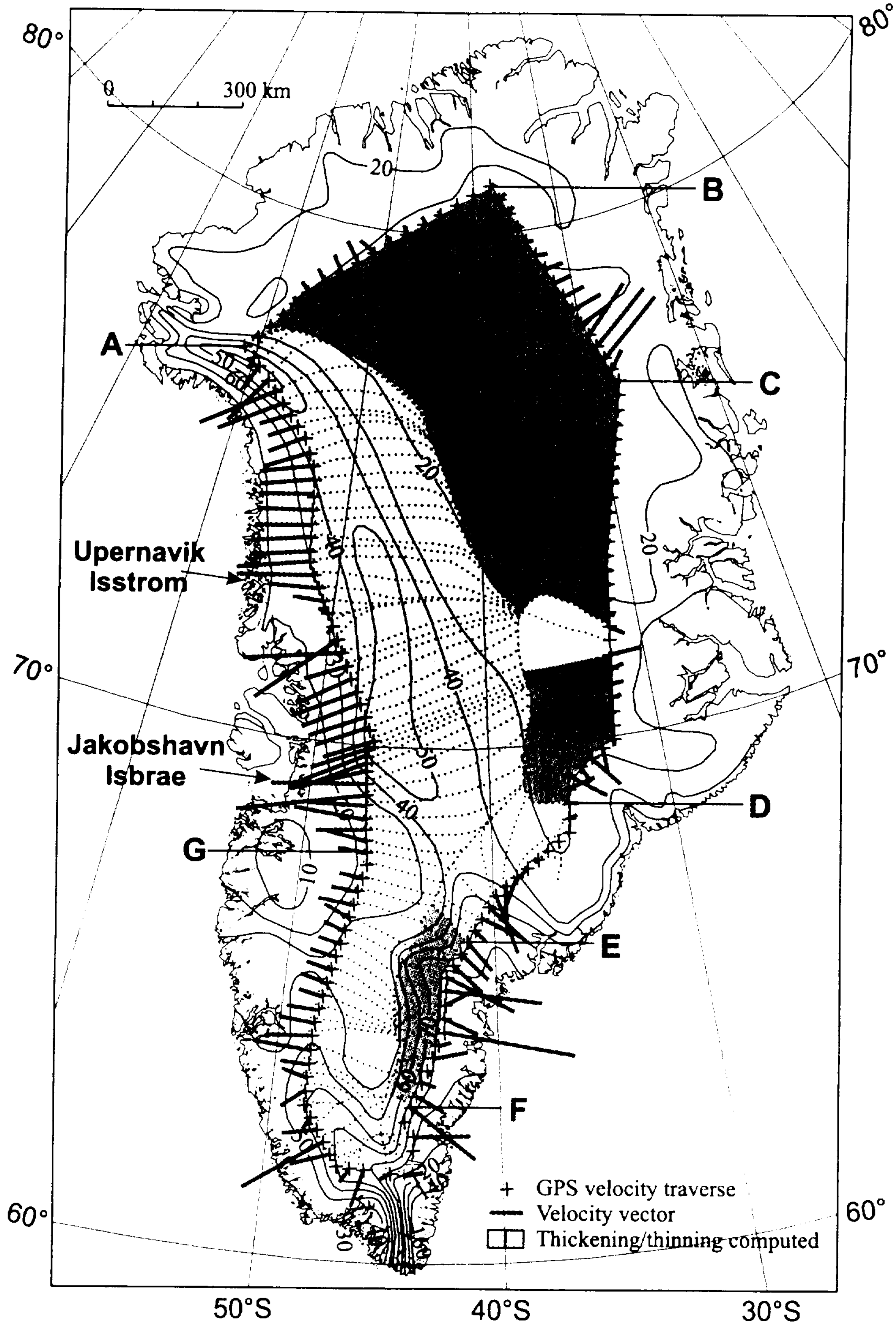


Figure 1. Thickening/Thinning and velocities along the traverse

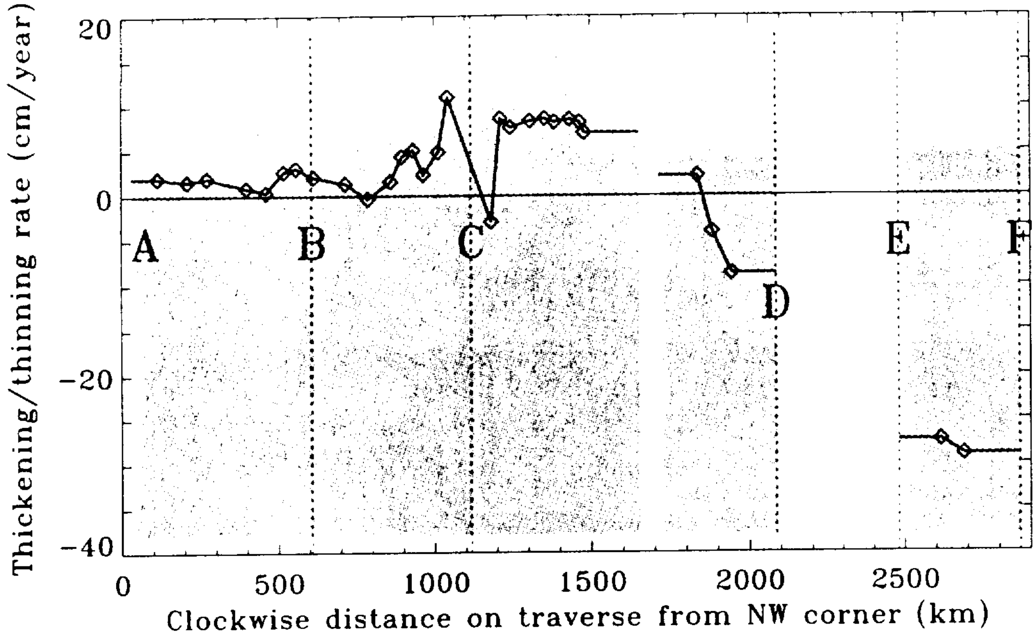


Figure 2. Thickening rates along traverse for sections shown in Fig. 1.

2 The northeast corner of the ice sheet (BC in Figure 1) appears to be thickening at a few cm/yr, with maximum thickening in the catchment basin of the northeast ice stream.

3 There is strong indication of thickening at about 7 cm/yr along most of the eastern side of the ice sheet (CD in Figure 1), with approximately equal thinning rates immediately north of D.

4 Thinning rates appear to be very large – about 30 cm/yr – in the high-accumulation region in the southeast corner of the ice sheet (EF in Figure 1). Within this region, the Ohmura and Reeh accumulation rates are between 40 and 90 cm ice/yr, so they would have to be grossly underestimated for the ice sheet to be in balance.

## Discussion

Before comparing these results with those from other approaches, it is useful to consider the temporal context of each approach. Our "indirect approach" to estimating mass balance compares total accumulation with total discharge. Accumulation estimates are from past data that generally represent averages over many years to decades, so we are comparing present-day ice discharge with past accumulation, and our results are probably representative of the net result of the past few decades. "Direct" approaches, such as comparison of precise altimetry surveys over periods of a few years, give an indication of the change in volume of the ice sheet over the survey intervals, and are thus a window into recent behavior. Uncertainties in the indirect approach are dominated by errors in the accumulation estimates, and in the direct approach by the effects of interannual variability of snow-accumulation rates. Finally, the "historical" approach takes proxy evidence from glacier moraines, trim lines etc, to infer ice-margin trends over decades to centuries or more.

Davis et al (1998) and Zwally et al (1998) have published estimates, from comparison of satellite radar-altimeter data, of ice thickening rates over southern Greenland. They broadly agree in concluding average thickening rates of between 2 and 4 cm/yr for the decade 1978-1988 for ice lying above the 1700-2000 meter contours, but they differ over temporal and spatial details. Davis et al (this report) give a figure describing spatial distribution of thickening rates which can be compared directly with our results:

- North of D between latitudes 70N and 71.5N, where we estimate thickening of about 2 cm/yr, they have thinning of about 3 cm/yr. Within our collective errors, these results are in agreement. But, inland of D (68.8N, 35.7W), where we estimate thinning of 8 cm/yr, they have thickening of about 3 cm/yr. The difference exceeds our collective errors, and suggests that local snow accumulation may be above the Ohmura and Reeh values.
- In our region EF, where we estimate thinning of about 30 cm/yr, they have very few estimates and these are close to the ice ridge. They range from 0 to 18 cm/yr thinning. Our results refer to the entire region from the ridge down to the 2000-m contour, more than double the area analyzed by Davis et al, and our larger thinning rates may indicate that thinning rates increase towards the coast. On the other hand, they may simply be a result of Ohmura and Reeh underestimating present-day accumulation rates over this region. Indeed, model studies by Bromwich et al (In Press) suggest that atmospheric conditions are compatible with southern Greenland accumulation rates significantly higher than the Ohmura and Reeh values.

**Future plans**

Over the coming year, we plan to complete the mass-balance analysis around the entire ice sheet, using thickness data provided by S. Gogineni's group at U Kansas, and to compare our results with all available other estimates, including those from the repeat airborne laser flights by W. Krabill's group at NASA/Wallops Flight Facility. We will use an improved version of the Ohmura and Reeh accumulation estimates, incorporating PARCA and other available recent measurements. In addition, we shall derive a set of mass-balance estimates using accumulation rates from D. Bromwich's most recent water-vapor balance calculations.

Apart from uncertainties in accumulation rate, errors in our analysis are caused mainly by errors in R, the ratio of column-averaged to surface ice velocity. These are from P. Huybrecht's model simulation of the ice sheet (personal communication, 1995), and we have assumed them to be accurate to 3%. In recent work, we have been assessing the possibility of using our observed velocities, together with values of ice thickness and surface slope, to infer basal temperature, sliding velocity, and melting rate at traverse stations that have higher velocities and surface slopes. Early results suggest that this approach may yield values of R for these stations that are more closely constrained by actual ice-sheet conditions.

**References**

Davis, C.H., C. A. Kluever, and B.J. Haines, 1998. Elevation change of the southern Greenland ice sheet, *Science*, 27 March 1998, Vol. 279, pp. 2086-2088.

Ohmura, A., and N. Reeh, 1991: New precipitation and accumulation maps for Greenland. J. Glaciol., 37, 140-148.

Thomas, R. H., B. Csatho, S. Gogineni, K. C. Jezek, and K. Kuivinen. Thickening of the western part of the Greenland ice sheet. *J. Glaciol.*, in press.

Zwally, H.J., A.C. Brenner, J.P. DiMarzio, 1998, Technical comment: growth of the southern Greenland ice sheet, *Science*, Vol. 281, 28 August 1998, p. 1251.

# Local Rates of Ice Sheet Thickness Change

*Gordon Hamilton Byrd Polar Research Center, The Ohio State University, Columbus, OH 43210*
*hamilton@iceberg.mps.ohio-state.edu*

## Objectives

Local rates of ice thickness change (mass balance) are being measured at several sites on the Greenland Ice Sheet. Results will be used to identify regions of the ice sheet where large changes are occurring, the causes of which can be investigated fully in future studies. The results will also be useful for interpreting elevation changes detected by repeat airborne and spaceborne altimetry.

## Method

The coffee-can method is used to measure local rates of ice thickness change. This method entails measuring the vertical velocity of markers set beneath the surface ("coffee cans") with precise GPS surveys repeated a year or more apart. Adjustments for vertical motion due to downslope flow and firn compaction are applied. Vertical velocities are compared with the local, long-term rate of snow accumulation obtained from core stratigraphy (e.g. Anklin and others, submitted) or gridded maps of accumulation (Ohmura and Reeh, 1991). The difference between the two quantities is the rate of thickening or thinning.

Results obtained using the coffee-can method have several advantages over traditional techniques for measuring mass balance. First, the results have small uncertainties. One-sigma uncertainties are typically about 0.02 m $a^{-1}$ for sites where accumulation rate is obtained from core stratigraphy; uncertainties are slightly larger for sites where accumulation rate is taken from Ohmura and Reeh's (1991) gridded map. Second, the results are significant over the period for which accumulation rate is measured. For sites where cores have been obtained, this timescale is between 50-800 years (Anklin and others, submitted). Third, the measurements are quick and easy to conduct. One day of work is required to install a new site and subsequent visits require only 1-2 hours to service the markers.

## 1998 work

No new coffee-can sites were installed during the 1998 field season. Five of the existing twelve sites (Figure 1) were re-occupied: Saddle (65.99975°N, 44.49987°W); South Dome (63.15019°N, 44.82369°W); Summit/GISP2 (72.57533°N, 38.45667°W); CC07/Daugaard-Jenssens Gletscher (71.88763°N, 32.05777°W); and Crawford Point (69.88194°N, 46.97889°W). In addition, three 2000-meter traverse stations were re-occupied (F024, F031 and F033).

Dual-frequency Ashtech Z-12 GPS receivers collected 12 hours or longer of data at each coffee-can site. Data were post-processed with the GIPSY-OASIS II software package using JPL precise satellite orbit and clock solutions. Very good-quality positions were obtained. 1-$\sigma$ uncertainties are about 0.01 m each for horizontal and vertical components.

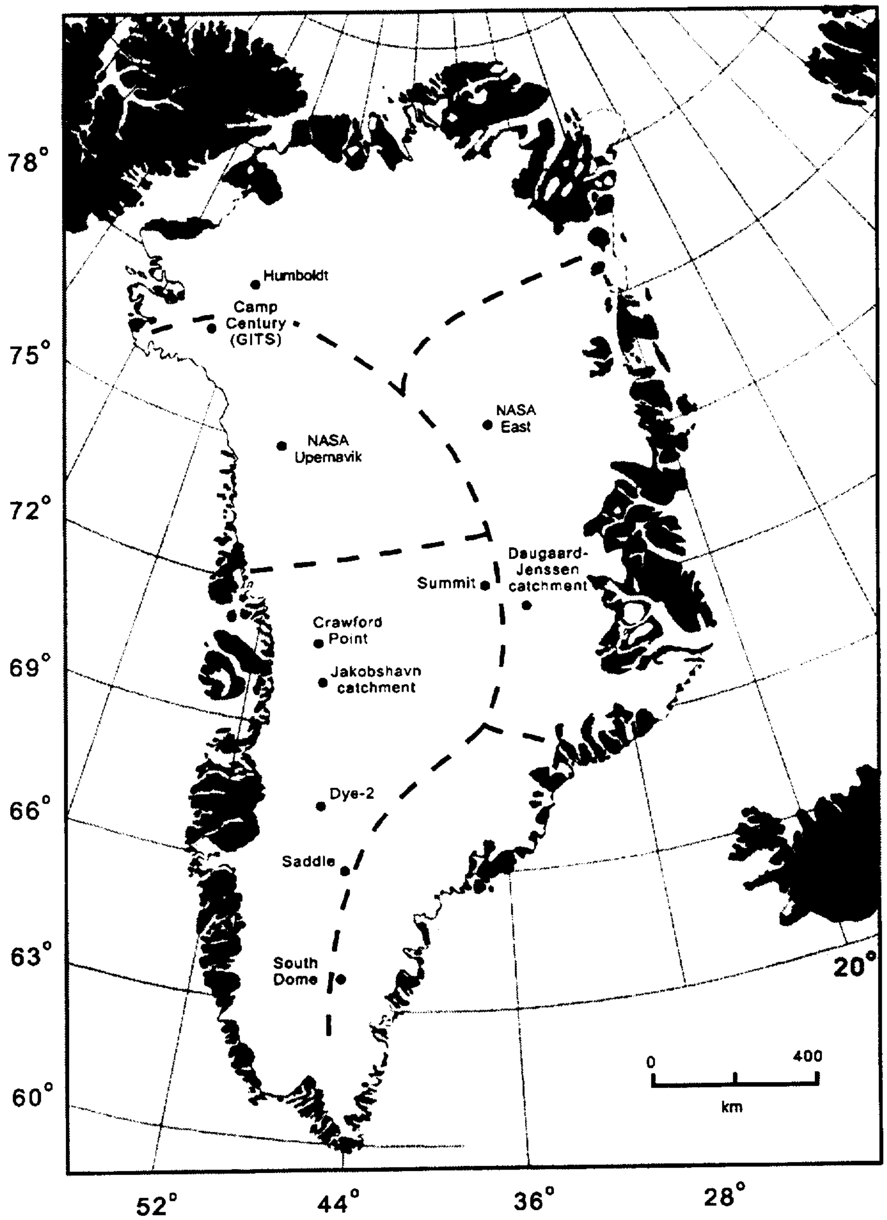


Figure1. Map of the Greenland ice sheet showing major coffee-can sites (circles) and major drainage divides (dashed lines).

## Results

As of this writing, accumulation rates from core stratigraphy are not available for sites at South Dome, the Saddle and CC07. Results for South Dome and the Saddle are pending analyses by Roger Bales and Ellen Mosley-Thompson. In the meantime, I calculate rates of ice thickness change for these sites using accumulation rates from Ohmura and Reeh's (1991) gridded map. Accumulation rates for Summit and Crawford Point are available from core stratigraphy.

Summit appears to be thickening slightly, at a rate of 0.039 (0.024) m $a^{-1}$ (the expression in parentheses is the standard deviation or 1-$\sigma$). Crawford Point also appears to be thickening at a rate of +0.153 (0.142) m $a^{-1}$, although the uncertainty on the result is rather large because of relatively poor core quality. Preliminary results show that CC07 (Daugaard Jenssen) is thinning (-0.391 (0.109) m $a^{-1}$), the Saddle is thickening (0.284 (0.112) m $a^{-1}$) and South Dome is thickening (0.310 (0.107) m $a^{-1}$). Note that rates of thickness change for the latter three sites have large uncertainties. These will decrease substantially when the new PARCA accumulation rates are used in the calculations (the rates of thickness changes will also likely change).

The results described here are in general agreement with thickness changes measured by satellite radar altimetry (Davis and others, 1998a and 1998b). Exact values are expected to be different, because results quoted here apply locally (5-10 km scale) whereas radar altimetry results are averaged over 50 km by 50 km cells.

## Planned work for 1999

A modest program is proposed for the 1999 field season. This includes reoccupation of coffee-can sites at NASA-East and Humboldt Glacier. These sites remain the only ones without repeat measurements. Other work includes deployment of one or more automatic coffee-can systems that will link short-term fluctuations in snow surface elevation (due to variable snow fall and firn compaction) as measured by laser altimeters with long-term rates of ice thickness change as measured by regular coffee-can markers. The automatic coffee-can instruments will be deployed at sites beneath planned airborne laser altimetry flightlines.

## Data availability

GPS tracking data from ice sheet coffee-can sites can be made available for ftp. Files are between 8 and 72 hours in duration, with a 30-second sampling interval. Ashtech Z-12 receivers were used and both native binary and rinex file formats are available. Contact GSH (hamilton@iceberg.mps.ohio-state.edu).

## References

Anklin, M., R.C. Bales, E.M.-Thompson and K. Steffen. submitted. Annual accumulation at two sites in Northwest Greenland during recent centuries. *JGR Atmospheres*.

Davis, C.H., C.A. Kluever and B.J. Haines. 1998a. Elevation change of the southern Greenland Ice Sheet. *Science*, 279, 2086-2088.

Davis, C.H., C.A. Kluever and B.J. Haines. 1998a. Growth of the southern Greenland Ice Sheet (technical comment). *Science*, 281, 1251-1252.

Ohmura, A. and N. Reeh. 1991. New precipitation and accumulation maps for Greenland. *Journal of Glaciology*, 37, 140-148.

# Absolute Gravity and GPS Measurements in Greenland

*J. Wahr, Dept of Physics and CIRES, Campus Box 390, U of Colorado, Boulder, CO 80309*

*T. van Dam and D. Robertson, Geosciences Laboratory, National Ocean Service, NOAA and CIRES, Campus Box 216, Boulder, CO 80309*

*K. Larson, Dept of Aerospace Engineering, Campus Box 390, U of Colorado, Boulder, CO 80309*

*O. Francis, Obs Royal de Belgique, Ave Circulaire 3, Bruxelles B-1180, Belgium*

## Objectives

Our objective is to use GPS and absolute gravity measurements made on bedrock along the edge of the Greenland ice sheet, to help detect ongoing changes in ice thickness. A change in ice load will deform the earth, and so cause vertical motion of the earth's crust. By measuring that motion we can put constraints on the change in ice mass averaged over a few hundred km of the observation point. By combining the GPS and absolute gravity measurements, it should eventually be possible to separate the secular effects of ongoing changes in ice from the earth's visco-elastic response to past ice variability. This project has been a joint effort between the University of Colorado (CIRES, Physics, and Aerospace Engineering), NASA, NOAA, and the Royal Observatory of Belgium.

## Method and Present Status

We installed permanent GPS receivers at Kellyville (just outside of Kangerlussuaq) in the summer of 1995, and at the Kulusuk airport in the summer of 1996. These two sites are located at about the same latitude but directly across the ice cap from one another. Data from Kellyville are transmitted to us daily via an internet connection. The Kulusuk data are initially archived in Kulusuk, and sent to Boulder at roughly three-week intervals. The data from both receivers are publically available at an anonymous FTP site.We have also visited each site with an absolute gravimeter on an annual basis: Kellyville during each summer of 1995-1998, and Kulusuk during 1996-1998. Gravity site occupations were 1-2 weeks in each case.

The GPS measurements alone are incapable of distinguishing between the secular effects of ongoing changes in ice mass, and the earth's viscous response to any changes in ice that might have occurred over the last several thousand years. Wahr et al, (1995) found, however, that by combining the GPS results with measurements of changes in gravity, it should be possible to separate those two effects.

$$\Delta = -u - A\delta g$$

Where A=6.5 mm/μgals, is reasonably independent of the earth's viscous response to past changes in ice – no matter what the viscosity profile or ice history. Viscous effects are about 10 times smaller (relative to the effects of present-day loading) in $\Delta$ than they are in $u$ alone.

We have been analyzing the GPS and gravity data as they arrive. The GPS observations are analyzed using the GIPSY/OASIS II software developed at JPL (Zumberge et al., 1997). After data editing, the carrier phase and pseudorange observations from both GPS frequencies are linearly combined in such a way to remove nearly all the effects of the ionosphere. We use GPS orbits, earth orientation, and clock products produced by JPL's independent analysis of 40+ globally distributed, continuously operating GPS receivers. The remaining parameters which must be estimated are station position, tropospheric refraction, and receiver clock parameters.

Figure 1 shows the GPS results for the daily-averaged vertical positions at both Kellyville and Kulusuk. The values have an rms about the best-fitting straight line of about 12 mm at Kellyville, and about 13 mm at Kulusuk. Our solutions show a significant subsidence of 7.7 $\pm$2.6 mm/yr at Kellyville, a less significant subsidence of 6.1 $\pm$ 5.1 mm/yr at Kulusuk, and no significant seasonal displacements at either location. To estimate these uncertainties, we assumed a de-correlation time of 15 days.

The gravity data (not shown) have been analyzed using the software provided by the instrument manufacturer: Micro-G. Tidal amplitudes at Kellyville were independently deduced using 200 days of spring gravimeter data from Kangerlussuaq, provided by M. Scheinert and R. Dietrich (personal communication). The results at both locations are corrected for tides and atmospheric pressure loading. Because the gravity data are made only once per year, there are not yet enough data to be able to infer a meaningful trend at either location.

## Interpretation of GPS Data

The observation time required to separate the viscous effects from the effects of present-day secular ice variability, will depend on how often we visit a site with the gravimeter, but is likely to be on the order of a decade from the inception of the experiment. So, it is too early to reach definitive conclusions about ongoing changes in ice.

The GPS secular rate of subsidence at Kellyville, however, is substantially larger than we expected. (So is the preliminary secular rate at Kulusuk, but the estimated uncertainty there is also large.) When we use Tushingham and Peltier's (1991) Ice3G model for the melting of Pleistocene ice prior to 4000 years ago, and convolve with visco-elastic Green's functions from Han and Wahr (1995), we estimate a viscous uplift at Kellyville of 3.5 $\pm$ 2 mm/yr. The $\pm$ 2 mm/yr uncertainty represents the effects of errors in the earth's viscosity profile. If we remove this uplift from the GPS secular subsidence value, we obtain a residual subsidence of 11.2 $\pm$ 3.3 mm/yr. If the Ice3G model is correct, then this subsidence would have to be due to a combination of ongoing changes in ice and of the earth's viscous response to any changes in ice that might have occurred during the past 4000 years

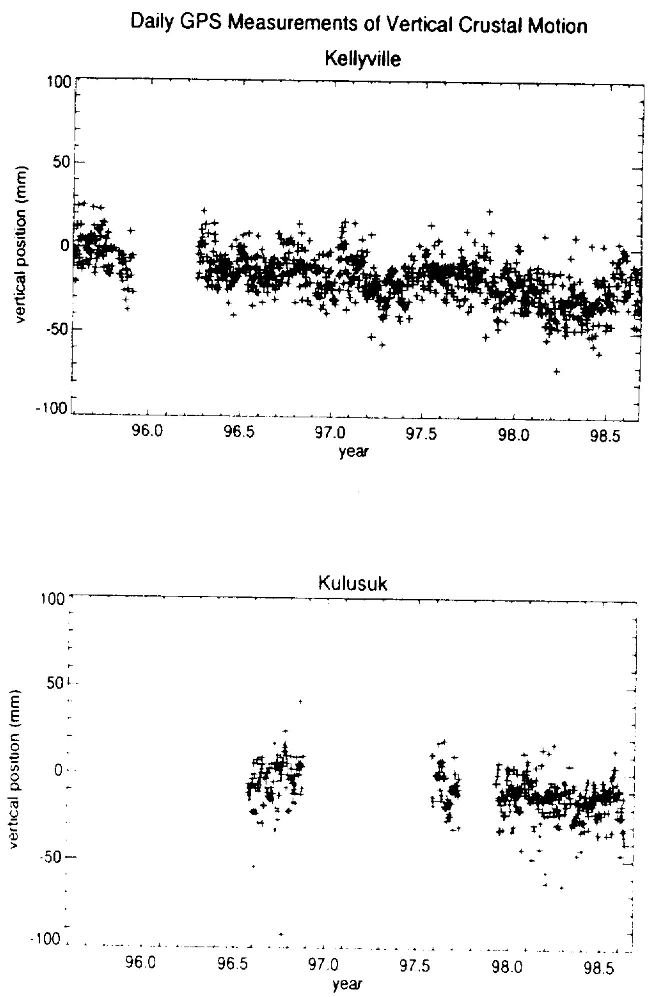


Figure 1. Daily GPS Measurements of Crustal Motion

We have little idea of what those past changes in ice might be. The 1995 IPCC report (Warrick et al., 1996) concludes that Greenland's contribution to sea level rise over this past century has been somewhere in the range of $\pm$ 0.4 mm/yr. This corresponds to a $\pm$80 mm/yr change in ice. As an upper bound, we accordingly assume that the average rate of change in ice thickness over the past 4000 yrs was somewhere in the interval $\pm$80 mm/yr, and that this thickness change was uniformly distributed over the ice cap. Using this assumption, we calculate a present-day crustal subsidence at Kellyville caused by the changing ice over the past 4000 years, of $\pm$4 mm/yr, and we add this $\pm$4 mm/yr to the uncertainty of the GPS results. We thus conclude that the subsidence at Kellyville due to ongoing changes in ice is 11.2 $\pm$ 7.3 mm/yr.

This result is almost certainly too large. For example, 11 mm/yr of subsidence at the edge of the ice sheet would imply that the ice is thickening at a rate of about 50 to 100 cm/yr averaged over a few hundred km of Kellyville. This is at least a factor of 3 larger than the ice surface changes inferred from altimetric observations. Even the lower bound of 11.2-7.3 = 3.9 mm/yr would imply the ice is thickening at a rate of from 20 to 40 cm/yr, which is on the very upper end of existing altimetry solutions.

At the moment, our best guess as to the eventual interpretation of our results is that the spatial dependence of the melting Pleistocene ice on Greenland is not well represented in Ice3G. If, for example, the total amount of melting Greenland ice is correct in Ice3G, but if the bulk of that melting ice was concentrated more in the far north-eastern portion of Greenland, then Kellyville could conceivably be located in the forebulge of the crustal motion signal. If that were the case, then the melting Pleistocene ice would be causing subsidence at Kellyville instead of uplift, and so would be in better agreement with the GPS estimate. The accumulation of more gravity data will eventually allow us to separate the viscous part of the signal from the effects of ongoing changes in ice mass, and so resolve this question.

**Proposed 1999 Field Campaign**

We will continue to operate the GPS receivers at Kellyville and Kulusuk, and to archive, analyze, and interpret the data. We will visit both sites with the absolute gravimeter during the summer of 1999.

**References**

Han, D. and J. Wahr, The viscoelastic relaxation of a realistically stratified earth, and a further analysis of postglacial rebound, *Geophys. J. Int.*, 120, 287-311, 1995.

Tushingham A.M., Peltier W.R. 1991. Ice-3G: A New Global Model of Late leistocene Deglaciation Based Upon Geophysical Predictions of Post-Glacial Relative Sea Level Change *J.Geophys. Res.*, 96, 4497-4523

Wahr, John M., Han Dazhong, and Andrew Trupin, 1995. Predictions of Vertical Uplift Caused by Changing Polar Ice Volumes on a Visco-Elastic Earth, *Geophys. R. Lett.*, 977-980.

Warrick, R.A., C. LeProvost, M.F. Meier, J. Oerlemans, P.L. Woodworth, 1996. Changes in Sea Level, in Climate Change 1995. *The Contributions of WGI to the Second Assessment Report of the Intergovernmental Panel on Climate Change*, 572 pp, Cambridge University Press, Cambridge.

Zumberge, J.F., M.B. Heflin, D.C. Jefferson, M.M. Watkins, and F.H. Webb, 1997. Precise point positioning for the efficient and robust analysis of GPS data from large networks, *J. Geophys. Res.*, 102, 5005-5017.

# ACCUMULATION ESTIMATES FROM ICE CORES

*R. C. Bales, J. F. Burkhart, J. R. McConnell, B. Snider, Dept. of Hydrology and Water Resources, University of Arizona, Tucson, AZ 85721, roger@hwr.arizona.edu,*

## Objectives

The objective of the 1998 SHAllow COring (SHACO) field campaign was to elucidate questions regarding spatial variability of accumulation rates throughout the Greenland ice sheet. In the 1998 field season we were primarily concerned with an accumulation trend along the central-western portion of the ice sheet. In addition, data were needed to fill a large gap of information in the central and southern portions of the ice sheet. In order to achieve a spatially extensive data collection program, depth (temporal variation) was limited to 20-m so that a greater number of cores could be efficiently collected. Cores acquired under PARCA use multi-species chemical analyses of ice cores to develop accurate estimates of annual accumulation at various sites. The ice core data are also analyzed for the interannual variability of snow-accumulation rates, which is a major cause of short-period variability of ice sheet elevation, and must be understood before we can infer long-term trends in ice sheet volume from observed surface elevation changes. This year's results will offer a spatially distributed record for the purposes of developing a high-resolution accumulation map of the Greenland ice sheet.

## Prior Field Work

We have analyzed cores collected in 1995 at NASA-U (73.8°N, 49.5°W), Humboldt Glacier (78.5°N, 56.8°W) and Crawford Point (69.85°N, 47.12°W) (Figure 1). Annual layers were identified in the cores using multiple parameters: $H_2O_2$, $NH_4^+$, $Ca^{2+}$ and $NO_3^-$ (Arizona), and $\delta^{18}O$, and dust (Ohio State). Using all parameters together to define annual layers resulted in a 350-year record for the NASA-U core with no dating uncertainty. For the lower-accumulation Humboldt core the dating uncertainty is about 5 years over the 852-year period of record, with no uncertainty over the past 200 years. Average accumulation is 0.34 m water at NASA-U and 0.14 m at Humboldt. See Anklin et al. [1998] for details.

We have also analyzed cores collected in 1996 at GITS (77.1°N, 61.0°W) and TUNU (78.1°N, 34.0°W). Average accumulation (still preliminary) is 0.36m water at GITS and 0.11m water at the main TUNU site (paper in preparation).

In 1997, shallow firn cores were collected at eight sites (Figure 1) around the perimeter of the Greenland ice sheet at approximately the 2500-m elevation contour. At those shallow coring sites that were co-located with automatic weather stations, more than one core was collected in order to investigate issues of short-scale spatial variability in snow accumulation. Average accumulation at two sites in northwest Greenland (75-76°N) had average annual accumulation values of 0.32-0.36 m water equivalent, and two sites in west central Greenland (71-72°N) had values of 0.40-0.42 m water equivalent. All four sites had values that were only 70-80% of that estimated from prior data and call into question the accumulation "ridge" in western Greenland that is apparent in older data. Figure 2 gives a comparison of preliminary accumulation values from our 1995-97 cores with values from the accumulation map done by Ohmura and Reeh [1991]. Note that at about half of our sites the standard deviation encompasses the Ohmura and Reeh [1991] interpolated value, and at about half their value lies outside our range.

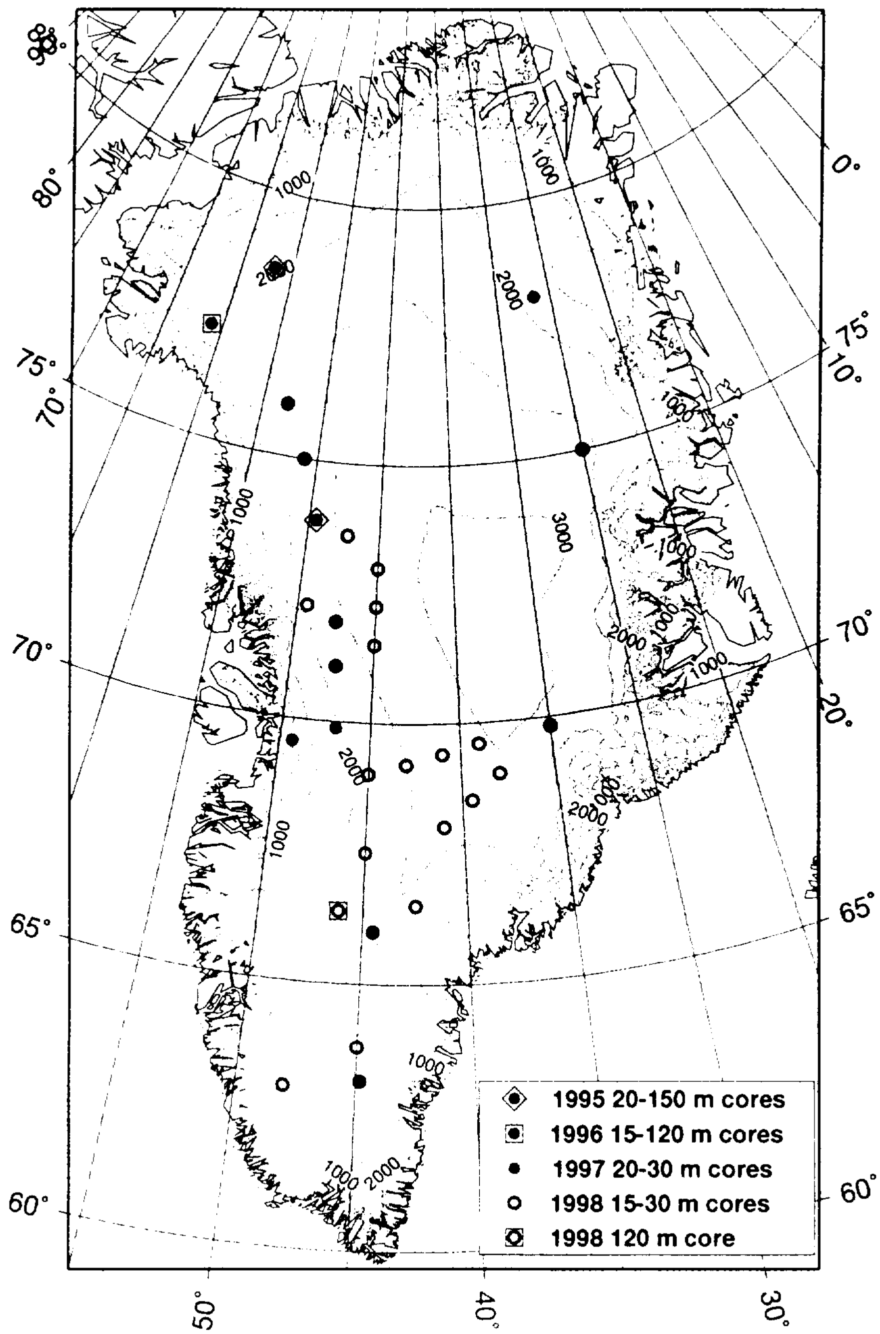


**Figure 1.** Locations of PARCA ice cores 1995-1998

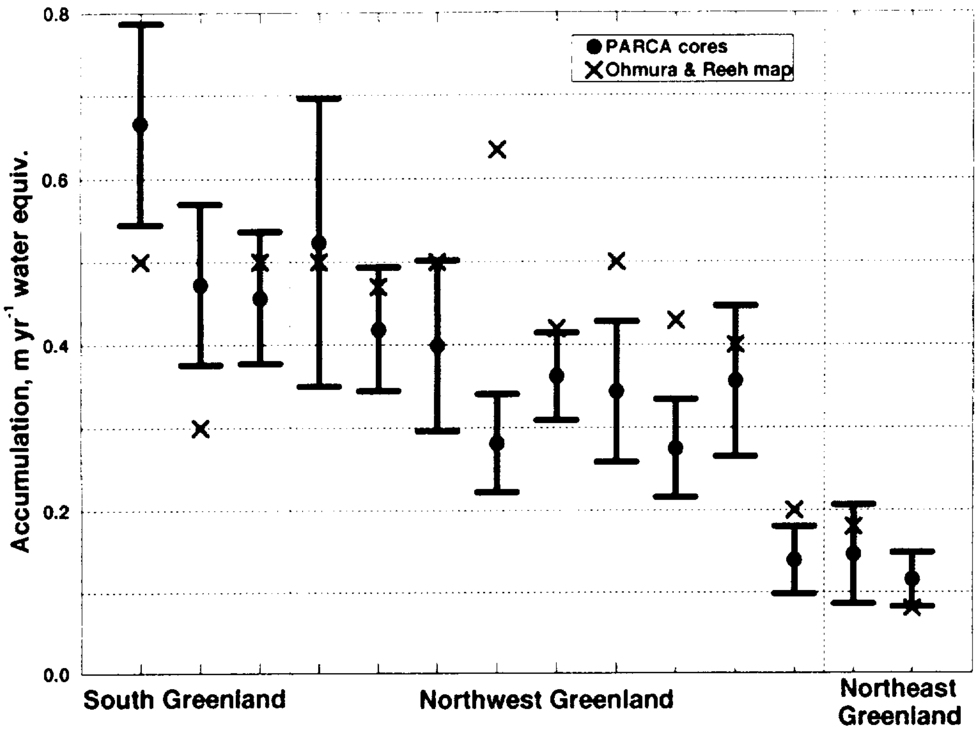


Figure 2. Comparison of recent and historical data (PARCA data preliminary)

**Work Done in 1998**

*Field Work:* During the months of April and May, eighteen shallow cores were collected on the Greenland ice sheet. The locations of the cores were selected to cover the suspect accumulation "ridge" and to fill data voids in the central and southern portion of the ice sheet. The primary focus of the 1998 field season was to collect cores in the region from 60-65° North and 35-45° West (Figure 1). Cores were collected by 2-3 person teams using the re-designed "Sidewinder II" 4-inch core drill, developed by Jay Kyne of PICO.

The results from the 1997 field season demonstrated the effectiveness of "commuter" coring. The 1998 field season was planned using this flight mode. Commuter coring uses a Twin-Otter to its fullest extent. All flights departed from Kangerlussuaq fully loaded with coring equipment, fuel, and emergency gear. Core drilling, weighing, and packing takes no more than 4 hours at each site. Upon return the plane is once again full with the weight of the ice replacing the weight of the fuel. In general, cores up to 20-m were collected from two separate locations in a single day. A total of 233-m of core was collected with only ten flights. All cores from the 1998 field season were stored in aluminum bags in order to prevent contamination and allow better preservation of reactive chemical species.

*Laboratory Analyses:* The shallow cores were sent from Kangerlussuaq, Greenland to the Byrd Polar Research Center at Ohio State University. In August the 4-inch cores were cut, and segments sent to the University of Arizona. Along with the SHACO cores, we are also analyzing a 20-m and a 120-m core from the Raven (66.38°N, 46.18°W) site that was collected by Ellen Mosely-Thompson of The Ohio State University.

Table 1. NASA 1998 Shallow Core Information, as of Sept. 30, 1998.

| Site | Latitude (°N) | Longitude (°W) | No. Cores (Depth (m)) | Status |
|---|---|---|---|---|
| 69_45 | 69.0 | 45.0 | 2(18.6, 5.1) | Ongoing |
| 692_43 | 69.2 | 43.0 | 1(17.6) | Ongoing |
| 694_41 | 69.4 | 39.0 | 1(11.7) | Ongoing |
| 696_39 | 69.6 | 39.0 | 1(12.2) | Ongoing |
| 68_41 | 68.0 | 41.0 | 1(12.2) | Ongoing |
| 675_45 | 67.5 | 45.0 | 1(12.1) | Ongoing |
| 685_395 | 68.5 | 39.5 | 1(11.9) | Ongoing |
| 69_38 | 69.0 | 38.0 | 1(12.2) | Ongoing |
| 665_425 | 66.5 | 42.5 | 2(2.8, 20.5) | Done |
| 638_45 | 63.8 | 45.0 | 1(14.8) | Done |
| 63_48 | 63.0 | 48.0 | 1(15.0) | Done |
| 722_494 | 72.2 | 49.4 | 1(15.25) | Done |
| 736_472 | 73.6 | 47.2 | 1(12.24) | Done |
| 73_45 | 73.0 | 45.0 | 1(14.6) | Ongoing |
| 71_45 | 71.0 | 45.0 | 1(12.0) | Ongoing |
| 722_45 | 72.2 | 45.0 | 1(12.1) | Ongoing |

From a 3.5x3.5 cm longitudinal cut, a 2-cm diameter core is continuously melted and analyzed using a flow-through analytical system. Our current analytes include $Ca^{+2}$, $NO_3$, $NH_4$, $H_2O_2$, and HCHO. Currently our system is configured such that the vertical resolution is 0.02 m, with some variation resulting from dispersion in the system.

## Results

At present we have cores that will provide accurate accumulation estimates for 29 locations on the ice sheet. Combined with the 36 points from the German traverse in North Greenland plus recent cores (e.g. GISP2), there are over 65 points with accurate accumulation estimates for the past 1-3 decades. From the Ohmura and Reeh compilation (about 250 points on the ice sheet), only about 50 points are based on a record that is 10 years or longer (Figure 3). To get an idea of the uncertainty associated with short records, we sampled different record lengths from the most recent 200 years of the NASA-U and Humboldt cores. For a record length of 1 year, the range is ±50-120% of the mean (Figure 4). For a record length of 10 years this drops to ±15-22%. The corresponding standard deviations for 1 and 10 years are ±25-30 and ±7%, respectively. For the PARCA cores we have aimed for record lengths of at least 10 years, and preferably at least 20 years. Note, however that the standard deviation drops off much more slowly after 10 years as compared to 20 years. It thus appears that the combined PARCA and German data, together with a subset of the historical data used by Ohmura and Reeh, should provide a much more accurate accumulation map than has been produced in the past.

Based just on the 1995-98 cores, our preliminary data call into question the accumulation ridge in the western part of the ice sheet that appears on the Ohmura and Reeh accumulation map. Note our means on Figure 2 versus the Ohmura and Reeh values. Especially striking is the Northwest Greenland site with 0.28-m accumulation (Figure 2), which lies near a reported 0.63-m accumulation point on the 1912 Koch-Wegner traverse. Our preliminary data suggest that Ohmura and Reeh's map overestimates accumulation in this portion of the ice sheet by 20-30%. The result is 3-5% less accumulation on the ice sheet as a whole as compared to Ohmura and Reeh's map. Our plan is to work with the AWI group to develop an updated accumulation map that combines PARCA and AWI data, pending completion of analysis of the 1998 cores.

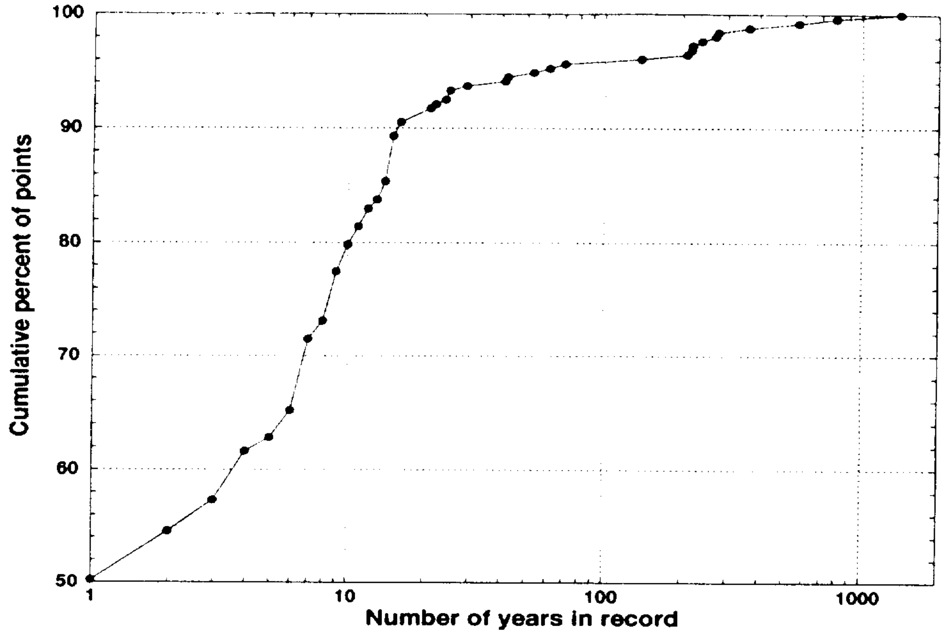


Figure 3. Cumulative distribution of points from Ohmura and Reeh with respect to years in record.

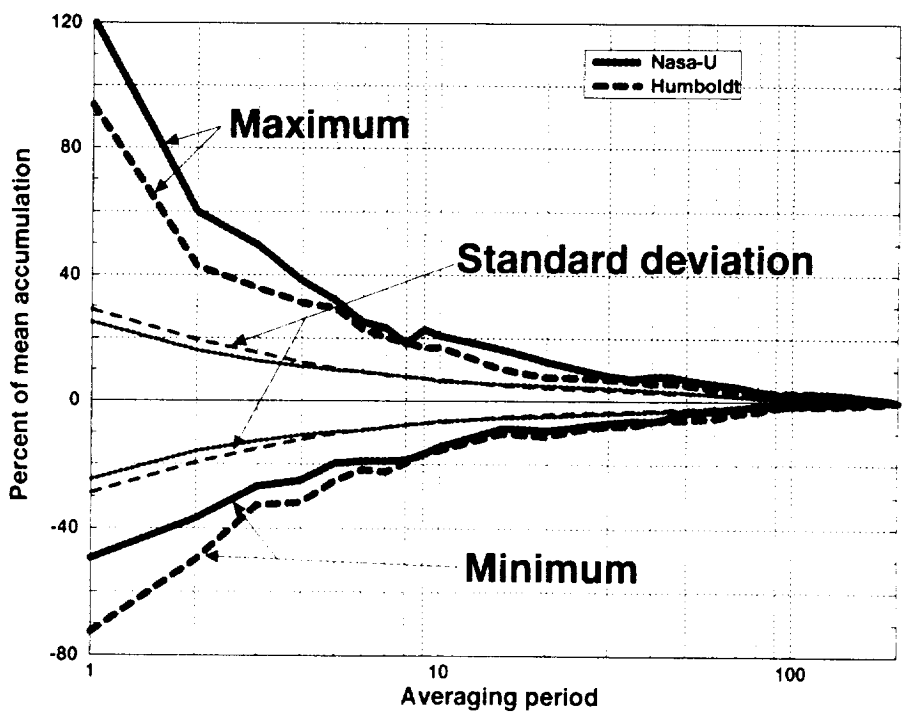


Figure 4. Mean and Standard Deviation information for NASA-U and Humboldt Cores for multiple years of averaging

**Plans for 1999-2000**

Our work involves a combination of 10-20 year cores to establish the recent accumulation on the ice sheet, and 200+ year cores to establish the long-term fluctuations. It is now apparent that gaps in the historical accumulation data compiled by Ohmura and Reeh (1991) are larger than has been assumed, bringing up the need to continue the shallow 10-20 year cores.

For cores of approximately 150-m depth, along with 20-m cores in the vicinity to estimate spatial variability, candidate locations are:

- South Greenland (1 core): South Dome or 63.8°N, 45°W
- West-central Greenland (1-2 cores): 70°N, 45°W and 72°N, 46°W vicinity and possibly 68.5°N, 41°W vicinity

Candidate locations for shallow (20-m) cores to fill in questions concerning accumulation high points are:

- Northwest Greenland (3-5 cores): 76.5°N, 55°W vicinity
- West Greenland (2-3 cores): 72°N, 46°W to 73°N, 47°W vicinity
- Southeast Greenland (1-3 cores): 70°N, 35°W vicinity
- South Greenland (1-3 cores): South Dome (63°N, 45°W) and Saddle (66°N, 44.5°W) vicinity

Final site selection will depend on the results from the in-progress analyses of the '98 cores.

*Data Availability & Dispersal*

The depth-age scale, density values, and year-by-year accumulation values for the NASA-U and Humboldt Glacier cores are available at http://www.hwr.arizona.edu/~Alpine/PARCA/parca.html. There is also a map and a detailed table of information for PARCA cores collected to date. We will add depth-age and accumulation data from other cores as it becomes available.

**Reference**

Ohmura, A., and N. Reeh. 1991. New precipitation and accumulation maps for Greenland. Journal of Glaciology, 37(125) pp.140-148.

# GREENLAND NET ANNUAL SNOW ACCUMULATION: TEMPORAL PERSPECTIVE AND SPATIAL CONSTRAINTS

*Ellen Mosley-Thompson Byrd Polar Research Center and Department of Geography, The Ohio State University, thompson.4@osu.edu*

## Introduction

The ice core analysis component of the PARCA Program is a joint effort by The Ohio State University (OSU), the University of Arizona (UA) and the University of Colorado-Boulder (CU). The primary objective is to use the well-preserved seasonal variations of various chemical and physical constituents in ice cores to reconstruct a combination of recent (last few decades) and longer (decades to centuries) histories of net accumulation from a broad spatial distribution of firn and ice cores from above 2000 meters elevation on Greenland. The OSU role in the PARCA Program is closely linked with that of the University of Arizona as both groups are engaged in the high resolution analysis of the chemical and physical properties of Greenland ice cores with the explicit goal of reconstructing annually resolved histories of net accumulation with minimal dating errors. OSU analyses include: (1) the concentrations of insoluble dust which exhibit a marked spring peak and winter minimum and serve as an excellent tool for dating Greenland ice cores; (2) the oxygen isotopic ratio ($\delta^{18}O$) also varies annually and in regions with higher accumulation ($\geq$ 0.25 m $H_2O$ or water equivalent) may be preserved for decades to hundreds of years; and (3) Beta radioactivity which provides critical 'known time stratigraphic horizons' that help verify and (in lower accumulation regions) help constrain the annual dating. The analytical procedures were discussed in the 1997 PARCA report and are not included.

**Table 1. Summary of OSU analyses for PARCA ice cores for 1995 Cores.**

| Core Name<br>**1995 Cores** | Lat.<br>N | Long.<br>W | Elev<br>(m) | Depth- m<br>Age at bottom | # Dust samples<br>Ave.>0.63μm<br>per ml samples | # $\delta^{18}O$ samples Ave.<br>$\delta^{18}O$ (‰) | Annual<br>Accumulation<br>(m w.e) |
|---|---|---|---|---|---|---|---|
| NASA-U<br>Core 1 | 73.8425 | 49.4953 | 2368 | 151.24 m<br>1645 AD | 3956 samples<br>17.246 dust | 3956 samp.<br>-30.91‰ | 0.332 m-dust<br>0.331 m $\delta^{18}O$<br>0.340 m @ |
| NASA-U<br>Core 2 | 73.8425 | 49.4953 | 2368 | 20.85 m<br>1965 AD | 441 samples<br>13.738 dust | 441 samples<br>-30.88 ‰ | 0.329 m @ |
| NASA-U<br>Core 3 | 73.8425 | 49.4953 | 2368 | 20.46 m<br>1965 AD | 400 samples<br>11.422 dust | 400 samples<br>-30.45‰ | 0.323 m @ |
| Humboldt<br>Main core | 78.5267 | 56.8306 | 1995 | 146.5 m<br>1143 AD | 4900 samples<br>19.756 dust | White | 0.148±.038m<br>* 0.140 m @ |
| Humboldt<br>Core 25 k North | 78.7387 | 57.2003 | 1995 | 21 m<br>1927 AD | 570 samples<br>13.845 dust | White | 0.144±0.041m @ |
| Humboldt<br>Core 25 km East | 78.5976 | 55.7659 | 1995 | 20.5 m<br>1929 AD | 551 samples<br>14.020 dust | White | 0.147±0.039m @ |
| Humboldt<br>Core 25 k South | 78.3148 | 56.4749 | 1995 | 20.7 m<br>1924 AD | 553 samples<br>13.481 dust | White | 0.136±0.041m @ |
| Humboldt<br>Core 25 k West | 78.4524 | 57.8826 | 1995 | 20.6 m<br>1924 AD | 554 samples<br>15.854 dust | White | 0.137±0.043m @ |

## Table 1 (continued). Summary of OSU analyses for PARCA ice cores for 1996/97 Cores.

| Core Name<br>1996 Cores | Lat N | Long W | Elev (m) | Depth- m<br>Age at bottom | # Dust samples<br>Ave >0.63µm per ml samples | # $\delta^{18}O$ samples Ave $\delta^{18}O$ (‰) | Annual Accumulation (m w.e) |
|---|---|---|---|---|---|---|---|
| GITS Core 1 | 77.8425 | 61.095 | 1910 | 21.8 m<br>1964 | 2585 samples<br>12,466 dust | 2585 samples<br>-29.19 ‰ | 0.343 m<br>based on dust 1996-1965 |
| GITS Core 2 | 77.8425<br>20 m fr Core 1 | 61.095 | 1910 | 120.5<br>1745 | 410 samples<br>15,963 dust | 410 samples<br>-29.30‰ | 0.344 m (dust)<br>1996-1965<br>0.340 m $<br>1996-1745 |
| Tunu - main Cores 1 & 2 | 78.0168 | 33.9939 | 2110 | 19m &<br>69m UA<br>≈ 1550 | NA yet | NA yet | NA yet -OSU<br>UA - 0.114m<br>(age: ≈1550) UA |
| Tunu - West Core W 25 | 78.0303 | 35.0639 | 2110 | 15 m<br>1918 | 586 samples<br>11,279 dust | NA yet | 0.074 m + |
| Tunu - West Core W 50 | 78.0394 | 36.1357 | 2110 | 15 m<br>1936-du<br>1937-ox | 403 samples<br>13,692 dust | 403 samples<br>-36.11‰ | 0.109 m + |
| Tunu - North Core N 25 | 78.3299 | 33.8884 | 2110 | 15 m<br>1925 | 474 samples<br>16,225 dust | 474 samples<br>-33.45 ‰ | 0.082 m + |
| Tunu - North Core N 50 | 78.4640 | 33.8414 | 2110 | 15 m<br>1932 | 613 samples<br>12,584 dust | 613 samples<br>-33.59 ‰ | 0.104 m + |
| Tunu - East Core 50 | 77.9780 | 31.8629 | 2110 | 15 m<br>1918 | 357 / 15 m<br>11,120 dust | 270 samples<br>*-30.7 ‰<br>to 1963 | 0.083 m + |
| Tunu - East Core 25 | 77.9996 | 32.9266 | 2110 | 15 m | ND / NA<br>for Beta | ND / NA<br>for Beta | 0.102 m + |
| Tunu - South<br>South 15<br>Really 7.5 km | 77.9589 | 34.0125 | 2110 | 15 m<br>1942 -du<br>1943- ox | 487 samples<br>13,114 dust<br>(1996-1942) | 487 samples<br>-35.2<br>(1996-43) | 0.122 m + |
| **1997 Cores** | | | | | | | |
| South Dome Core A | 63.1489 | 44.8167 | 2850 | 25m<br>1978 | 441 samples<br>7850 dust av | 441 s amples<br>-27.26‰ | 0.66 comb. @<br>OSU:0.653<br>UA: 0.673 |
| Saddle -<br>orig, N-Dye 3<br>60 km fr D3<br>Core A | 66.0006 | 44.5014 | 2631 | 20 m<br>1976 | 341 samples<br>9445 dust av | 341 samples<br>-27.47‰ | OSU den: 0.431 m; UA den: 0.462 m; 0.450 m-comb assumes dating ok |
| NASA East Core A | 75. | 29.9997 | 2631 | 20 m<br>≈ 1930 | 529 samples<br>11,549 dust | 529 samples<br>-33.96‰ | 0.136 m ** 1952 0.146 m<br>UA: 1951<br>0.140 m (1952) $ |
| South Tunu Core A | 69.5 | 34.5 | 2650 | 20 m<br>≈ 1974 | 435 samples<br>10.390 | 435 samples<br>-30.32 ‰ | 0. 422 OSU $<br>0.473 UA $ |
| 7551 | 75° | 50.9° | 2200 | 21.13 m<br>≈ 1965 | 526 samples<br>12,700 dust | 526 samples<br>-30.5 ‰ | 0.334 OSU $<br>0.325 UA $<br>0.33 comb $ |
| 7653 Core A | 76° | 53° | 2200 | 14.91 m<br>≈1978 | 320 samples<br>12,500 dust | 320 samples<br>030.17 ‰ | 0.332 OSU $<br>0.362 UA$ |

NOTES:
@ - official PARCA value
$ - tentative accumulation, pending OSU & UA final comparison
+ accumulation determined from the 1952 Beta Horizon, so value is 1952 to the surface
* data are preliminary from University of Arizona
NA-yet - not available yet - will be analyzed
NA - not available and will not be analyzed
White - responsibility of Jim White, Univ. Of Colorado
ND - not determined

**Spatial Variability of Accumulation**

The preceding report from the University of Arizona presents the locations (including a map) and basic physiographic information for the PARCA drilling sites so they are not repeated here. In addition to the annual layer identification and accumulation determination, the OSU data provide information about the atmospheric dust flux and isotopically inferred temperature trends which are of less concern to immediate PARCA objectives, but valuable for climate and paleoclimate investigations. Table 1 summarizes the information currently available from the OSU analyses for the cores collected between 1995 and 1997. Analyses of the 1998 cores have not yet begun. Note that accumulation averages denoted with $ are preliminary awaiting the OSU and UA final comparison of annual layers planned for the 1998 fall PARCA meeting. Table 1 also includes averages of dust concentrations and $\delta^{18}O$ for the length of record and are provided to illustrate spatial differences in other ice core constituents.

One focus of the OSU effort has been analysis of the spatial variability of net annual accumulation (henceforth $A_n$) within smaller regions by using the 'remote', shallow cores which have accompanied the longer cores from Humboldt (78°35'N; 57°13'W) and Tunu (78°N; 34°W). Knowledge of the spatial variability of $A_n$ is critical in assessing the significance of a single record. This is particularly important in light of PARCA's goal to characterize the entire ice sheet (above the 2000 m contour) with a limited number of observation points (ice cores, automatic weather stations, and coffee can experiments).

For the Humboldt site in NW Greenland, 4 remote cores were drilled 25 km from main base, one in each primary compass direction (N, S, E, W). Using multiple seasonal parameters, these cores were annually dated providing records extending into the 1920s (Table 1). Figure 1 illustrates the running average for each of the 5 cores (4 remote plus main) from 1994 to the end of the remote core records. The purpose of the successive running averages is to explore the length of time over which a single record must be averaged in order to approximate the regional average. Figure 1 illustrates that an averaging interval of approximately 40 years is necessary for the Humboldt region where accumulation is ≈0.140 mm we. As importantly, Figure 1 illustrates that averaging beyond 40 years does not improve convergence of the five $A_n$ histories to a single value. The five records converge to 2 different $A_n$ values (Fig. 1 and Table 1) suggesting that the region to the west and south of main camp lies in a different accumulation regime than the region to the north and east of main camp. These data illustrate the extent of regional $A_n$ variability in the Humboldt region.

Regional variability is greater in the Tunu region due, in large part, to the low $A_n$. Data in Table 1 illustrate $A_n$ values in a 7000 km$^2$ area surrounding Tunu region which vary by as much as 70%. No simple spatial pattern of $A_n$ emerges from these data which suggests that the 34-year averaging interval (1996 to 1963 [Beta horizon]) is insufficient to capture a regional $A_n$ record. The preliminary $A_n$ estimate (from UA chemistry only) on the 69-m Tunu core (≈1550 A.D.) is 114 mm we. The average $A_n$ from the seven ancillary (shorter) cores is 102 mm we (1996-1963) and 97 mm we (1996-1952). An interesting observation emerging from the use of two major Beta radioactivity horizons (1963 and 1952) is that $A_n$ during the 1950s appears to have been substantially below the mean for the last 40 years. This appears to be the case at nearly all the PARCA ice core sites, suggesting a large-scale decrease in $A_n$ during the 1950s.

**Importance of the Temporal Perspective**

The aforementioned observation raises an important issue for consideration by PARCA investigators: the need to establish a consistent time frame for comparison of regional accumulation data. The conclusions drawn about spatial changes in $A_n$ depend heavily upon the 'temporal frame of reference'. This is illustrated by data in Table 2 (a,b,c). Using Beta radioactive horizons only (Table 2a) leads to the conclusion that accumulation since 1963 has increased modestly in northwest Greenland (GITS and Humboldt), increased strongly in northeast Greenland (Tunu and Nasa-East) and decreased modestly in central Greenland on both sides of the divide (NASA-U, Summit, Site A). However, data in Table 2b illustrate that changing the temporal frame and using the first two-thirds of the 20$^{th}$ Century (1901-1963) as a basis for comparison leads to different conclusions about accumulation in the most recent 35 years. This view suggests zero to a very modest increase in $A_n$ in northwest Greenland (GITS and Humboldt, respectively). In northeast Greenland the earlier view that $A_n$ has increased changes to an apparent decrease accumulation (Tunu and Nasa-East). In central Greenland the area west of the divide (Summit and NASA-U) has experienced a very modest decrease in late 20$^{th}$ Century accumulation, while on the east (Site A) a significant reduction in accumulation is inferred. When viewed from an even longer perspective, 1750-1900 A.D., 20$^{th}$ Century accumulation shows no increase (Table 2c). It is important to note the limited number of cores and the potential danger of inferring regional changes from so few ice core records.

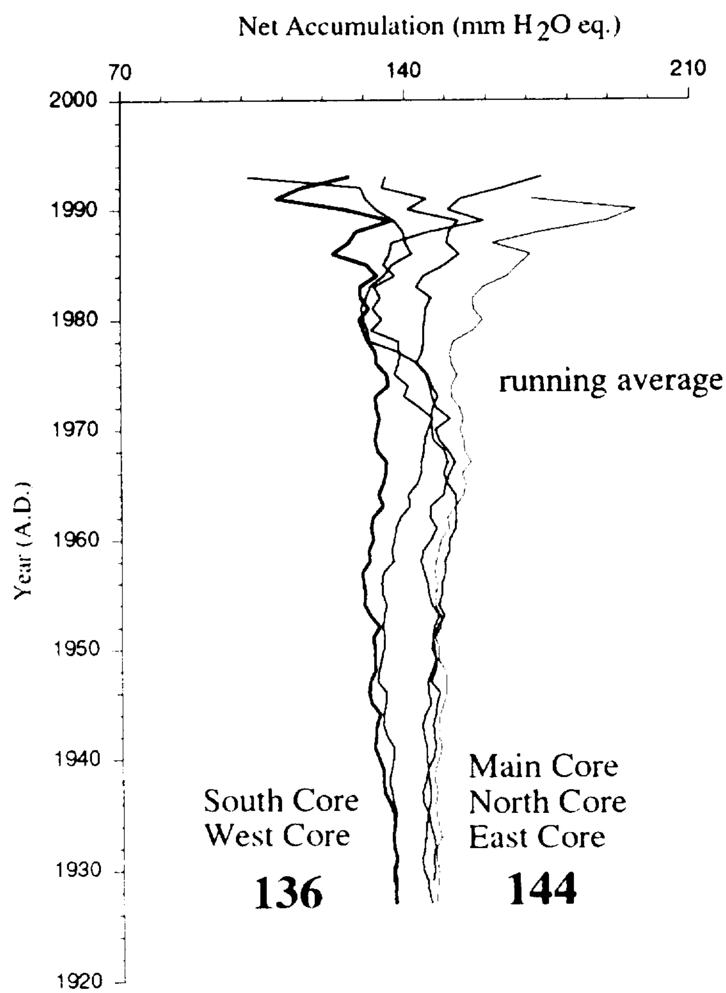


Figure 1. Net accumulation for various shallow cores at the Humboldt Site in Greenland.

**Table 2. Recent accumulation changes in Greenland from various temporal perspectives.**

a. Accumulation change is calculated using two known time stratigraphic markers: the 1963 and 1952 Beta radioactivity horizons produced by the Soviet and Castle tests, respectively. All accumulation data are in mm water equivalent (we).

| Location | $A_n$ since 1963 | $A_n$ (1952-1963) | % Change since 1963 |
|---|---|---|---|
| Humboldt | 152 | 139 | +9.4 |
| GITS | 345 | 323 | +6.8 |
| Tunu | 102 | 81 | +25.9 |
| NASA-East | 141 | 120 | +17.0 |
| NASA-U | 338 | 354 | -4.5 |
| Summit | 209 | 223 | -6.3 |
| Site A | 206 | 236 | -12.7 |

b. Accumulation change is calculated using $A_n$ since 1963 and $A_n$ from 1901 to 1962. This gives a perspective of the $A_n$ change in the last third of the 20th Century relative to the first 62 years.

| Location | $A_n$ since 1963 | $A_n$ (1901-1962) | % Change since 1963 |
|---|---|---|---|
| Humboldt | 152 | 143 | +6.3 |
| GITS | 345 | 344 | ~0.0 |
| Tunu | 102 | 121 | -14.0* |
| NASA-East | 141 | 155 | -9.0** |
| NASA-U | 338 | 347 | -2.6 |
| Summit | 209 | 216 | -3.2 |
| Site A | 206 | 336 | -38.7 |

c. Accumulation change is calculated using $A_n$ from 1901 to the present and $A_n$ from 1750 to 1900. This gives a perspective of 20th Century $A_n$ change relative to the previous 1.5 centuries.

| Location | $A_n$ (1901 to present) | $A_n$ (1750-1900) | % Change since 1900 |
|---|---|---|---|
| Humboldt | 146 | 148 | -1.3 |
| GITS | 344 | 356 | -3.3 |
| Tunu | 116 | 118 | -1.7* |
| NASA-U | 345 | 344 | ~0.0 |
| Summit | 215 | 220 | -2.7 |
| Site A | 300 | 417 | -28.0 |

* data are preliminary from UA

** interval used is 1932-1962; data are preliminary

## Considerations for 1999 Field Work

These results raise an important issue that should be addressed by PARCA investigators with regard to the acquisition of future ice cores and the limited resources available. If the priority is to characterize recent accumulation at many locations, then the focus will be on more short cores and fewer long records. In this mode of operation, attention to a common observational period becomes very relevant (as illustrated by data in Table 2). Core lengths should be adjusted to ensure acquisition of either (1) major time stratigraphic horizons such as the 1952 or 1963 Beta peak (the ideal scenario) or (2) some other time horizon which will be identified by layer counting and thus remain subject to interpretation (less ideal scenario). A few well-chosen deeper cores should be obtained to provide a longer temporal perspective for 20$^{th}$ Century changes. Hopefully, discussions with other PARCA investigators at the annual PARCA meeting, October 5-6, will highlight those regions where either a longer temporal perspective or a denser array of shorter records will be most beneficial.

## Raven Drill Test

During May 1998 a three-person OSU team (Ellen Mosley-Thompson, Victor Zagorodnov, and Eric Kline) spent nine days testing a re-designed electro-mechanical drill at the Raven Site. The support provided by PICO staff was outstanding. The team arrived in the afternoon of May 11 and left on the afternoon of May 20. During this time two cores, 120.87 and 20.5 m were obtained. The cores were returned frozen to OSU and will be analyzed in 1999 to contribute to PARCA objectives. UA has already obtained their samples from all 1998 cores, including the Raven cores.

The drill test highlighted the strengths and weaknesses of the OSU drill (Zagorodnov *et al.*, submitted). The weaknesses will be addressed in the intervening year and include the need for a better (more precise) penetration drive and removal of a reinforcement ring in the upper part of the inner barrel. The strengths of the drill include its reduced weight, shorter tower, smaller cable (8 mm Kevlar), and S-type design and chip removal system. The drill is easily set up, requires no extensive tethers, operates from the surface which eliminates the need for a pit, and it fits under our portable dome for all weather operation. A new, lighter weight dome is under construction.

## Planned Laboratory Analyses (1998-1999)

Beginning in November, OSU will have a Research Associate devoted full time to the analysis of the dust concentrations and size distributions in the Greenland cores. Over the next year all PARCA cores in hand will be analyzed for dust and $\delta^{18}O$ with the goal of annual resolution. In addition, OSU will conduct Beta radioactivity analyses on all cores (when appropriate) and sulfate analyses on selected sections for identification of suspected volcanic events which will contribute confidence to the dating by layer counting.

## Reference

Zagorodnov, V., L.G. Thompson and E. Mosley-Thompson, submitted. Portable system for intermediate depth ice core drilling. *J. Glaciol.*

# INTERDISCIPLINARY DETERMINATION OF ICE SHEET ACCUMULATION PATTERNS: COMBINED ATMOSPHERIC MODELING AND FIELD AND REMOTE SENSING STUDIES

*C.A. Shuman University of Maryland and R.A. Bindschadler, NASA Goddard Space Flight Center Mail Code 971, NASA Goddard Space Flight Center, Greenbelt, MD 20771, shuman@hardy.gsfc.nasa.gov*

## Introduction

This research is focusing on two related areas that are fundamental to the NASA PARCA program. The primary research area is the determination of the amount, rate, and timing of accumulation at distributed sites in the dry snow zone of Greenland and evaluation of these results in light of accumulation modeling results. The secondary research area is the calibration of the isotope "thermometer" at these ice sheet sites as well as the determination of long-term temperature trends in Greenland.

## Method

In the primary phase of this project we are using comparisons of high-resolution stable isotope ($\delta^{18}O$ and $\delta D$) profiles in snow pits to satellite brightness temperature trends to measure the amount, rate, and timing of accumulation for specific locations distributed over the Greenland ice sheet (see Figure 1). These results are then compared with the output from a high-resolution diagnostic-dynamic atmospheric model to validate sub-seasonal and annual estimates of accumulation (or precipitation minus evaporation, P-E) (NASA project with PI David H. Bromwich and Yufang Li) for the same locations. These data will improve our understanding of mass input to the ice sheet and aid inversion of ice core records to determine atmospheric characteristics. In addition, this research will assess the reliability of the atmospheric modeling approach to accumulation monitoring for ice sheet mass balance studies (see Figure 2). This will provide critical data for comparison to and validation of the hydrologic elements of global climate model results.

Additionally, through the collection and compilation of numerous high-resolution stable isotope profiles distributed across Greenland, a database will be compiled which can be used to assess this paleoclimate variable. Interpretation of stable isotope records has provided strong evidence of past climate change yet concerns remain about the accuracy of its interpretation. Completion of a decadal-length air temperature record from multiple automatic weather station (AWS) records and passive microwave emissivity modeling in central Greenland will facilitate interpretation of the isotope paleothermometer as well as provide a basis for recent climate variability and forcing in central Greenland. Additional temperature data from GC-Net AWS (Steffen et al., this report) will aid in this effort, and a collaboration has begun.

## Results

As illustrated in Figure 1, snow pit stable isotope profiles from a number of locations across Greenland are now being analyzed. The Alfred Wegner Institut (AWI) North Greenland Traverse (NGT) data from the NGT 38-45 sites are under analysis currently. Annual accumulation estimates from these data are within the expected range of values from this area. Isotope, density, and stratigraphic data from the two field sites successfully occupied in May 1997 are also under analysis, as are additional data from sites occupied during April and May 1998. The May 1997 snow pit records show evidence of lateral transport of significant accumulation, possibly due to katabatic flow, which may complicate atmospheric modeling estimates and paleoclimate interpretation. An additional field site is requested for the coming season, possibly in cooperation with an AWS servicing mission. The intent is to provide additional regional coverage as well as to allow direct comparison of the stable isotope record to the temperature record from the AWS.

The most recent samples are now at the University of Colorado's INSTAAR isotope laboratory and were obtained with the support of D. Winebrenner and R. Arthern (NASA researchers). The field sites visited during the 1998 season were selected to maximize expected accumulation variability in the Greenland Summit region as well as to allow integration of our results with those from the Summit "over-winter" studies. This collaboration with another PARCA group resulted from a mutual interest in understanding how passive microwave energy is emitted from the ice sheet and what can be determined from the resulting satellite brightness temperature data.

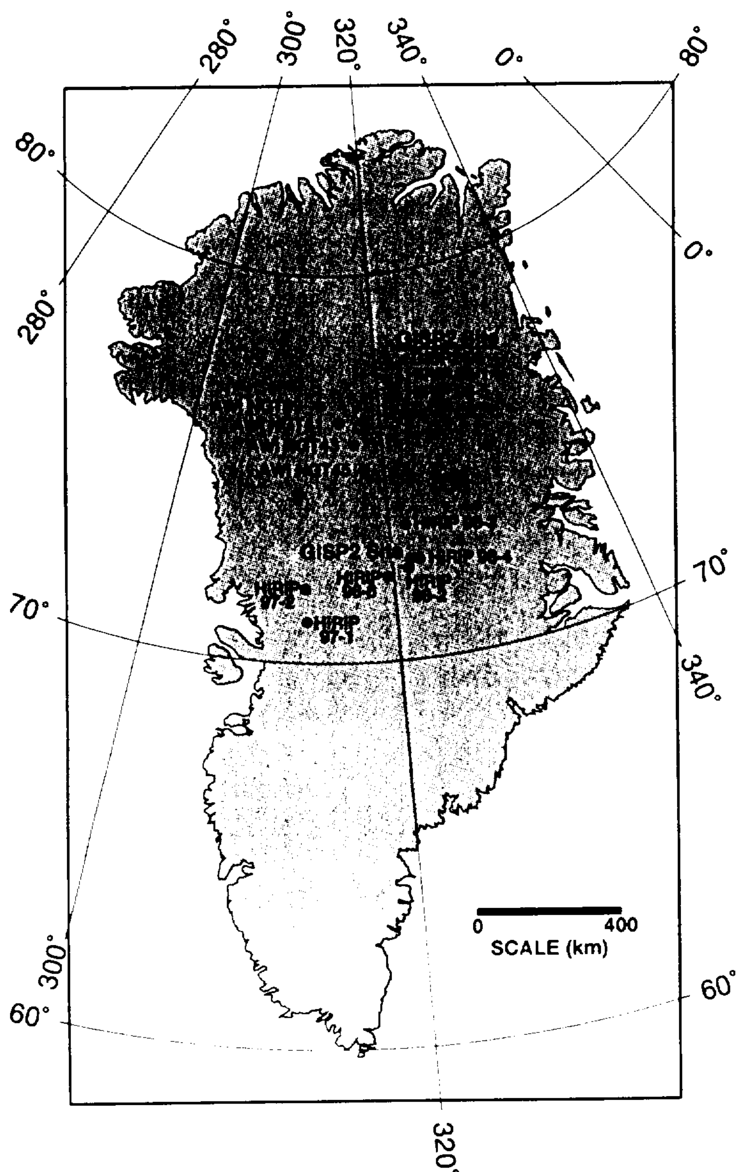


FIGURE 1 - Location map of sample sites available to this research. The AWI NGT sites were the only ones sampled with sufficient resolution (3cm) to be included in this study. The 1997 and 1998 field sites, as well as one from 1995 were all sampled at a resolution of at least 2cm for density and isotopes.

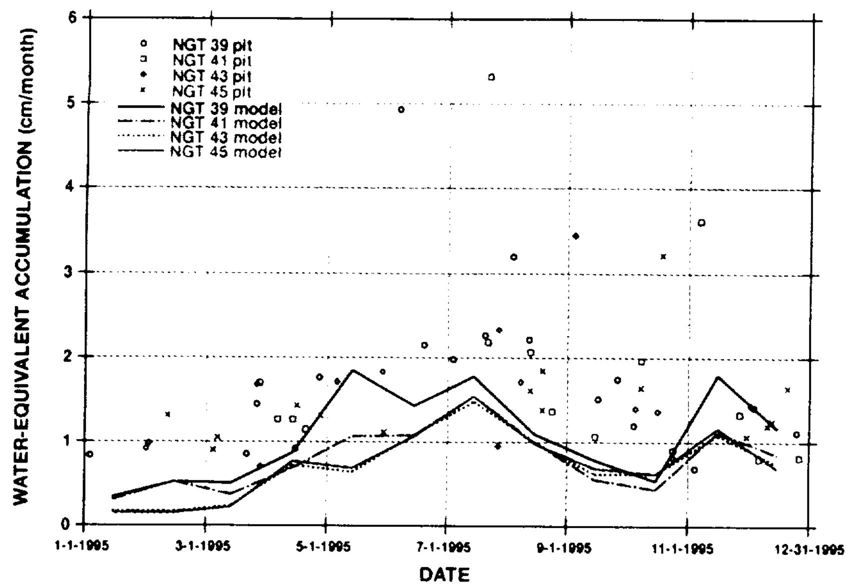


FIGURE 2 - Illustration of the sub-seasonal accumulation timing data available from the passive microwave - stable isotope comparison technique. Comparison of modeling output from Bromwich and Li to observed snow pit results (converted to reflect timing during 1995) from the NGT sites indicates a strong similarity in input timing but magnitudes differ by more than 50%.

FIGURE 3 - Composite decadal-length temperature record for the Greenland Summit region. The record is a composite of three AWS (C. Stearns, U. Wisconsin data) and is completed using passive microwave data from the same locations. This record shows the impact of the Mt. Pinatubo cooling and may contain information on the North Atlantic Oscillation (NAO).

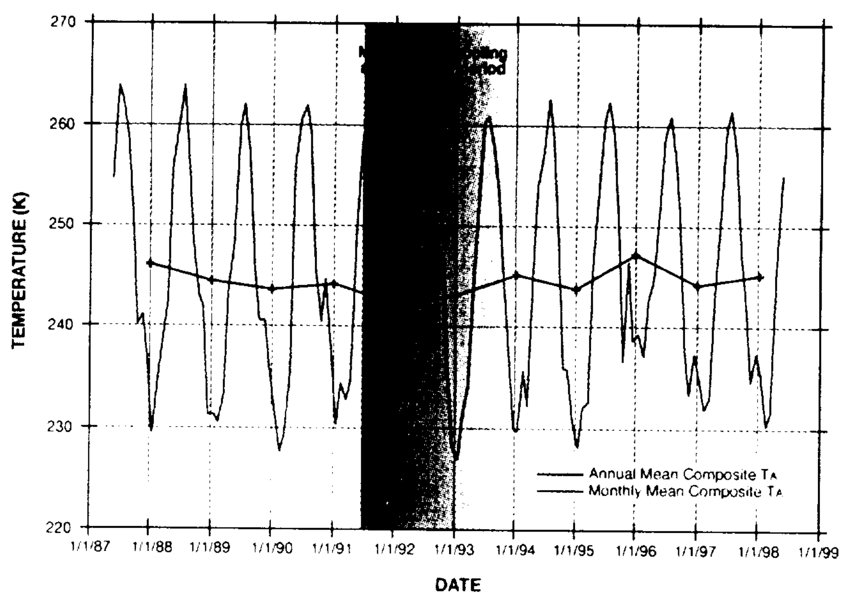

# GREENLAND ICE SHEET CLIMATOLOGY: GC-NET STATUS AND APPLICATIONS

*K. Steffen, J. E. Box, J. Weber and J. Estupinen, Cooperative Institute for Research in Environmental Sciences, University of Colorado, Boulder, koni@seaice.colorado.edu*

## Objectives

Climatological observations and surface energy balance studies are the keys to the understanding of the surface processes linked with ice sheet mass balance. Long-term climate records at different sites on the ice sheet are needed for the assessment of the snowpack energy and mass balance of the accumulation zone and to gain more complete information of the spatial variation of climate over the ice sheet.

The Greenland Climate Network (GC-Net) was established in spring 1994 with the emphasis on monitoring climatological and glaciological parameters at various location on the ice sheet over a time period of at least 5-10 years. The objectives of the GC-Net automatic weather station (AWS) network are:

- Assess daily, annual and interannual variability in accumulation rate, surface climatology and surface energy balance at selected locations on the ice sheet where high sensitivity of the ice sheet mass balance to climate anomalies is predicted from modeling results.
- Assess accurate surface elevation, location, and near-surface density at the AWS location with the option to revisit the locations in order to get temporal information for dynamic ice sheet modeling.
- Model the surface energy balance based on atmospheric and cyrospheric interactions, using the Greenland climate network of AWS stations as input parameters. In a first attempt, the surface energy balance of the western part of the ice sheet will be modeled, using the current AWS network.

## GC-Net Status

During the 1998 field season, 11 of 15 AWS were visited for maintenance and calibration. The AWS team was on the ice sheet April 18$^{th}$ through June 6$^{th}$ with 25 field days devoted to AWS work. AWS data sets collected in the field during the 1998 field season have replaced those transmitted data sets. The GC-Net archive has been brought up to date with a single common format for all station data. Compared with last year's 17 station years, there are now 28 station years of GC-Net measurements processed and available for use.

The ARGOS satellite data retrieval now updates automatically. Other steps in the data processing system have been refined and/or automated. The quality control procedures have been refined. More comprehensive documentation is available on station data sets. A HTML-based file server is in operational use internally.

We experienced one station failure at Crawford Pt. (CP1) on Julian day 309 1997. CP1 was reactivated day 150 1998. Fortunately, the Crawford Point 2 (CP2) station was running while CP 1 was out. CP 2 is 6 km from CP 1. Regression between the overlap of CP1 and CP 2 data was established to reconstruct the missing CP1 data. No other station failures occurred unless unknown failures have occurred at stations where we don't have up to date transmissions.

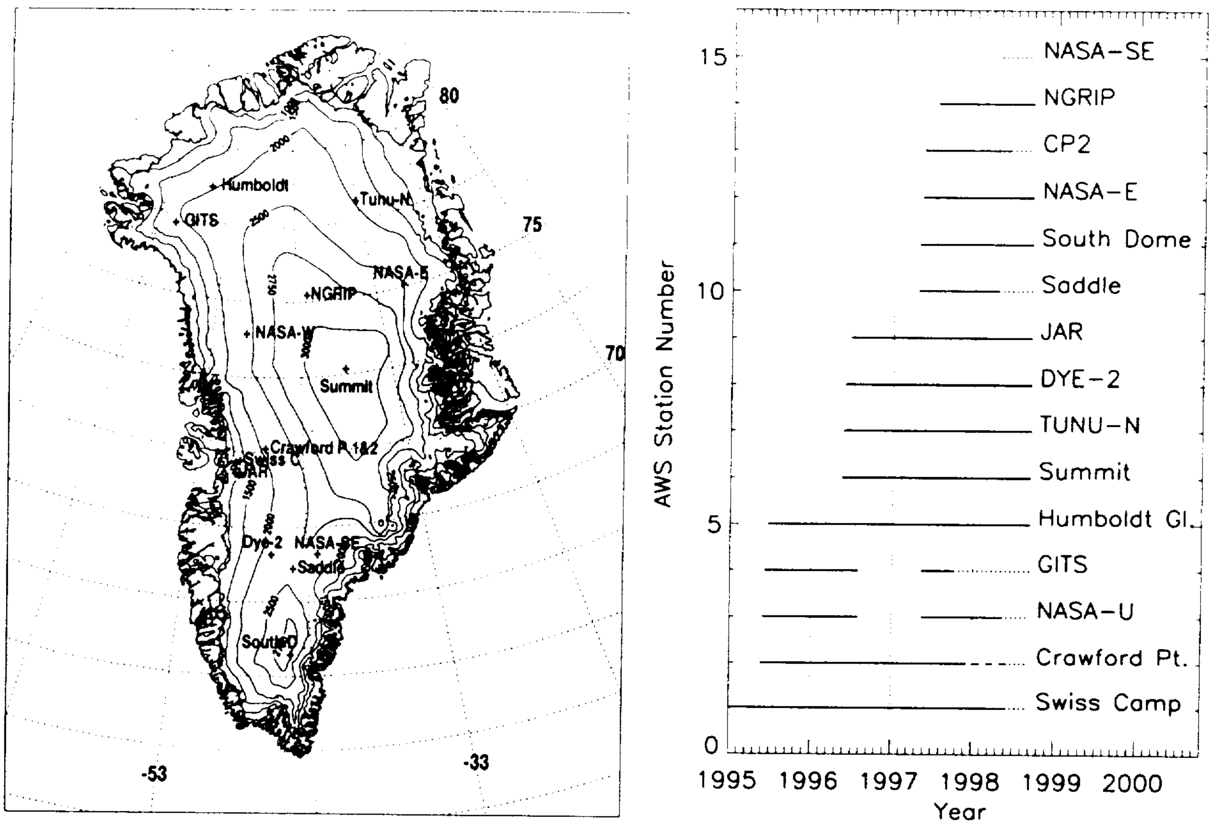


Fig. 1: The distribution of automatic weather stations on the Greenland ice sheet is shown in the left figure, as part of the Program for Arctic Regional Climate Assessment (PARCA) Greenland Climate Network (GC-Net). On the right the GC-Net timeline is given. The dotted line represents uncertain AWS status due to no satellite data link. The dashed line represents reconstructed Crawford Pt. data

*Quality Control Advances*

Knowledge of whether quality control procedures have been applied to the AWS data is important for data users. An identifier code has been included with each AWS dataset to allow the user to identify whether a given hourly data point has been synthesized, as in the case for interpolation, and which filter rejected the data point in question. Synthetic values comprise between 1% and 10% of the entire data volume by station.

*Annual, Monthly, and Daily Averages now Available*

AWS data have been averaged on annual, monthly, and daily time-scales. Annual averages have been set to rely on at least 90% of one year. Daily averages rely upon a 95% available data threshold. Three levels of monthly means are now available. One level is based upon a 95% available data threshold (in other words, at least 95% of the available hourly measurements are required for a mean value to be output). A less conservative 90% (availability) monthly data product is also available. A third data set called "reconstructed" provides monthly mean values at the 90% level with data gaps reconstructed (see next paragraph).

*Regression Reconstruction*

Linear regressions were performed on each AWS monthly mean parameter between each and every station in the GC-NET. For many of the parameters the explained variance between stations was sufficiently high that the empirical regression could be used to fill in missing monthly data. The third level of monthly mean data available includes the 'real' measurements as well as simulated monthly mean data based upon the empirical regression between all GC-Net stations that qualify above a conservative significance threshold. The simulated values allow a more continuous monthly time series where the available measurements did not pass the 90% available data thresholds as well as an extension of available records beyond their duration's at that site. For example, the explained variance in monthly mean air temperature between DYE-2 and Saddle is 99.8%. DYE-2 AWS has been measuring for 1 year more than Saddle. Hence, where DYE-2 data are available, the empirical function can be used to construct a time series for Saddle when it was not in operation. Another threshold of at least 10 months is required for the regression to be able to fill in data gaps.

The main purpose, however, is to fill in data gaps where station measurements did not pass quality control procedures more than 90% of the time each month. A significance threshold was set for each parameter, for example air temperature, an explained variance of 95% is required, for wind speed and 85% threshold was assigned, for relative humidity 90% was required.

*Future Work*

- Complete automation of data retrieval and processing of AWS satellite transmissions.
- Spatial covariance analysis.
- Non-linear interpolation of missing data based upon autocorrelation significance thresholds.
- Spatial interpolation by kringing method.
- Revised tower design.

**Results**

*Estimating Surface Height Change from Sonic Height Measurements*

Linear regression was used to estimate annual rate of surface height change at each of 12 AWS. At accumulation zone AWS sites, the linear model explained between 91 and 99 % of the hourly variance. Low fit-quality is observed at lower elevations due to ablation. Linear fit residuals allow for calculation of error/variance for sonically-derived surface height change.

| **AWS** | **dh/da 1 [m yr$^{-1}$]** | **dh/da 2 [m yr$^{-1}$]** | **$r^2$ 1** | **$r^2$ 2** | **years 1** | **years 2** | **std.1 [m]** | **std.2 [m]** |
|---|---|---|---|---|---|---|---|---|
| Sw. Camp | 0.12 | 0.1 | 0.62 | 0.6 | 1.93 | 1.93 | 0.3 | 0.3 |
| Cr. Pt. | 1.34 | 1.36 | 0.98 | 0.98 | 3.02 | 3.02 | 0.17 | 0.17 |
| NASA-U | 1.18 | 1.16 | 0.96 | 0.96 | 2.15 | 2.15 | 0.08 | 0.08 |
| GITS | 1.32 | 1.14 | 0.99 | 0.91 | 1.68 | 0.78 | 0.08 | 0.08 |
| Humboldt | 0.47 | 0.48 | 0.98 | 0.97 | 3.23 | 3.23 | 0.06 | 0.07 |
| GISP 2 | 0.63 | 0.62 | 0.99 | 0.99 | 2.32 | 2.32 | 0.05 | 0.05 |
| TUNU-N | 0.42 | 0.37 | 0.96 | 0.96 | 2.34 | 2.34 | 0.05 | 0.05 |
| DYE-2 | 0.91 | 0.91 | 0.98 | 0.98 | 2.31 | 2.31 | 0.09 | 0.08 |
| JAR | -0.37 | -7.24 | 0.18 | 0.9 | 2.24 | 0.31 | 0.52 | 0.22 |
| Saddle | 1.24 | 1.29 | 0.96 | 0.96 | 0.99 | 0.99 | 0.07 | 0.07 |
| S Dome | 1.86 | 1.86 | 0.97 | 0.97 | 1.39 | 1.39 | 0.14 | 0.14 |
| NASA-E | 0.38 | 0.42 | 0.92 | 0.95 | 1.37 | 1.37 | 0.04 | 0.04 |
| Cr. Pt. 2 | 1.69 | 1.66 | 0.94 | 0.95 | 1.05 | 1.05 | 0.13 | 0.12 |
| NGRIP | 0.5 | 0.51 | 0.96 | 0.97 | 1.19 | 1.19 | 0.04 | 0.03 |

Monthly surface height changes for 14 GC-Net stations are featured below. Pronounced summer ablation is evident at the Swiss Camp (1150 m) and at JAR (960 m). At other AWS in the accumulation zone: a springtime minimum is observed at Humboldt, the minimum is observed during summer at Saddle. Deflation will minimize the accumulation signal.

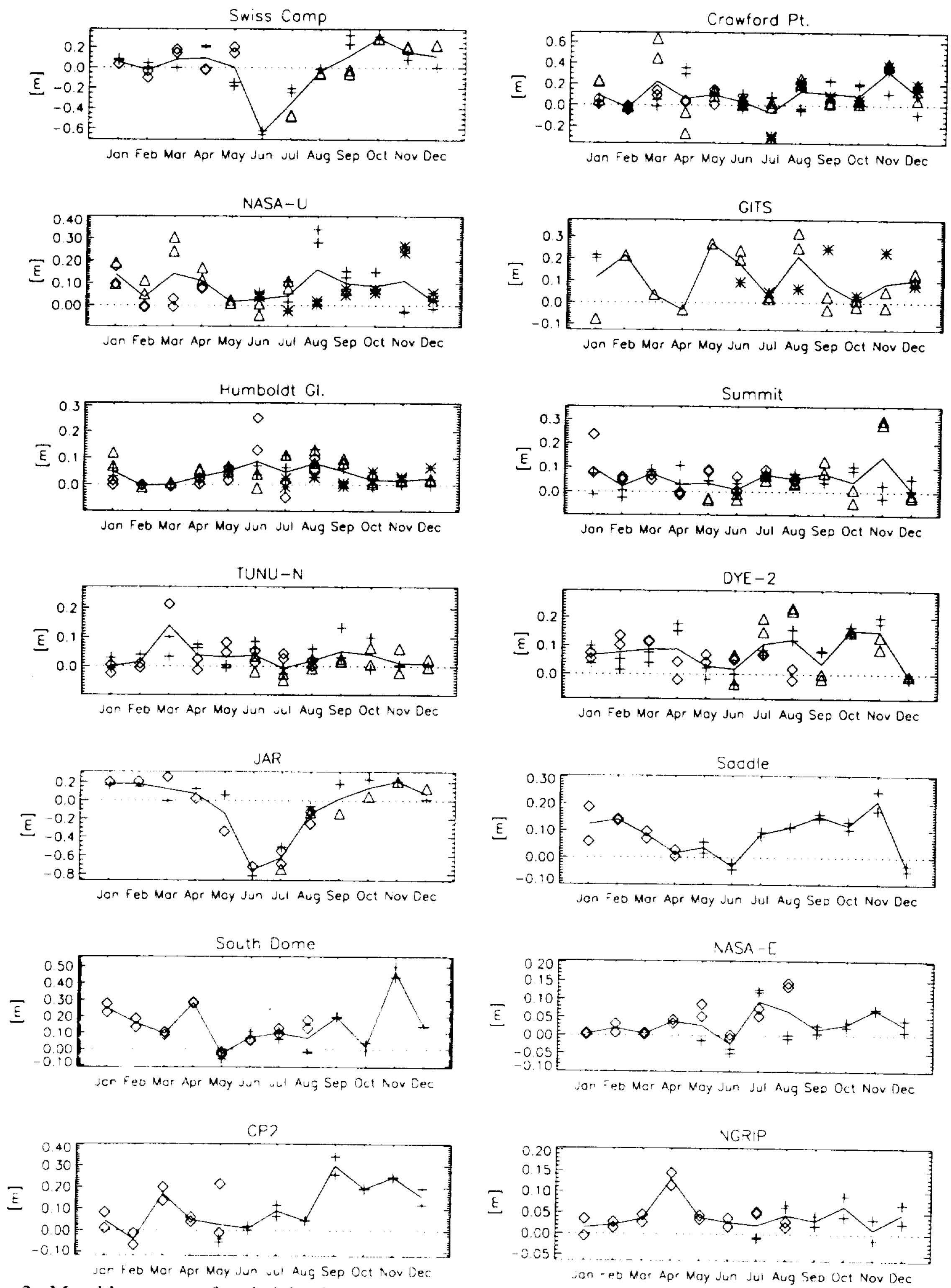


Fig. 2: Monthly mean surface height change: * - 1995, Δ - 1996, + 1997, ◊ 1998, ___ - average.

*Climate Variations at the Swiss Camp: 1991-1998*

The climate record at the Swiss Camp is continuous since April 1991, which makes it the ıongest continuous meteorological record on the Greenland ice sheet. The monthly mean air temperatures are shown in Figure3. The interannual variability of air temperatures is large, with decreasing annual amplitudes towards present. The mean annual air temperature has increased by 1° C per year, from -16° to -11° C between 1992 and 1997. The highest summer temperatures were recorded for the month of July, with no clear summertime trend over the seven years. This is not surprising, since the air temperatures cannot increase significantly above 0° C over a snow/ice surface. Summer temperatures were below normal for 1991 and 1992 due to the cooling effect of the aerosol loading in the stratosphere induced by the Mt. Pinatubo eruption. The coldest winter temperatures were recorded for the month of March, with a significant increase in springtime temperatures between 1993 and 1996. The winter temperatures showed the interannual strongest fluctuations, with a mean increase of 1.2° C/a for February and 0.6° C/a for the month of March.

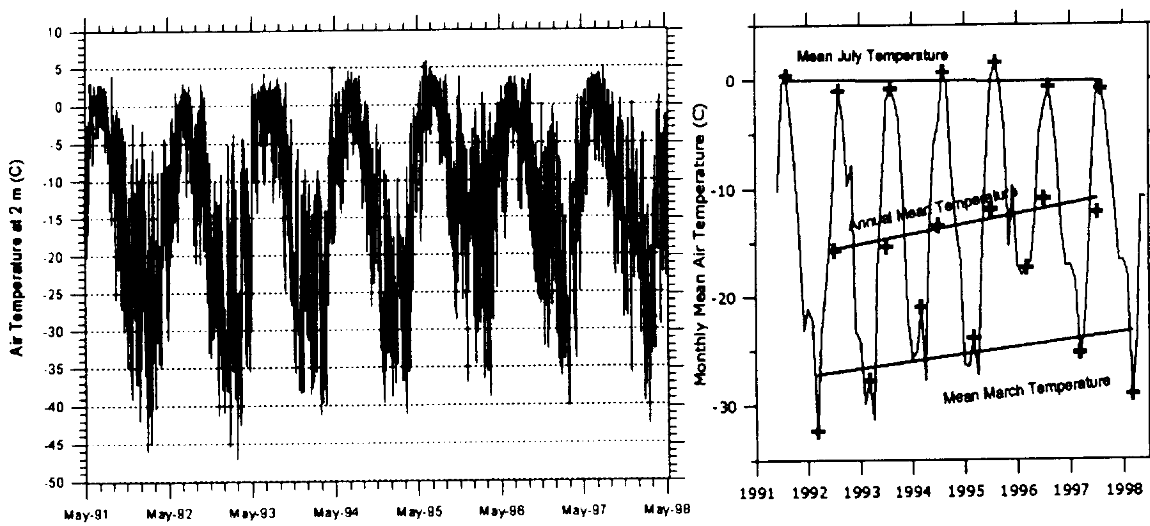


Fig. 3: Hourly and mean monthly air temperatures for the Swiss Camp (ETH/CU AWS) for 1991-1998. A linear regression line is shown for the July mean temperature, March mean temperature and annual mean temperature.

*Comparison of NCEP and GC-Net Pressure Fields*

Table 2: Variance and standard deviation of daily mean station atmospheric pressure and pressure values derived by a logarithmic regression of NCEP daily geopotential height values of the 500, 600, 700, 850, 925, and 1000 millibar levels. Given the station elevation, a pressure value for that location can be derived from the slope of the regression line. Confidence of fit of the regression line is 99.7 % to 99.9%.

| Station | Standard Dev. (mb) (1996) | Variance (mb) (1996) | Standard Dev. (mb) (1997) | Variance (mb) (1997) |
|---|---|---|---|---|
| Swiss Camp | 2.1 | 4.4 | 2.1 | 4.3 |
| Crawford Point | 2.5 | 6.0 | 2.5 | 6.0 |
| NASA West | 2.4 | 5.5 | 2.6 | 6.6 |
| GITS | 2.8 | 7.8 | 2.5 | 6.2 |
| Humboldt | 1.9 | 3.5 | 2.2 | 5.0 |
| Summit | 2.2 | 4.8 | 2.3 | 5.5 |
| Tunu | 4.0 | 16.2 | 2.8 | 8.1 |
| DYE2 | 2.6 | 7.0 | 4.3 | 18.1 |
| JAR | 2.2 | 5.0 | 2.2 | 4.8 |

*Blowing Snow Mass Fluxes*

Estimates of blowing snow mass fluxes for Greenland were made by assimilating GC-Net observations. An empirical relationship between elevation and annual blowing snow mass flux ($r^2$=0.78) was employed. The model results showed that the redistributed snow mass of $10*10^{10}$ kg equals 17% of the annual accumulation. The snow mass flux of the ice margins was $2*10^{10}$ kg, or 4% of the annual accumulation, which is in accordance with earlier estimates form the 1970's. Sublimation may limit the redistribution of snow significantly since single ice crystals in turbulent suspension survive less than 10 minutes before they are sublimated. Largest blowing snow mass fluxes were found at the low elevations of the Greenland ice sheet due to increased katabatic winds (Fig. 4). At high elevations strong summertime insolation and low barometric pressure also augment sublimation. The graphs are based on a 0.5° grid of interpolated GC-Net station data (weighted by distance) of annual blowing snow mass flux and wind direction.

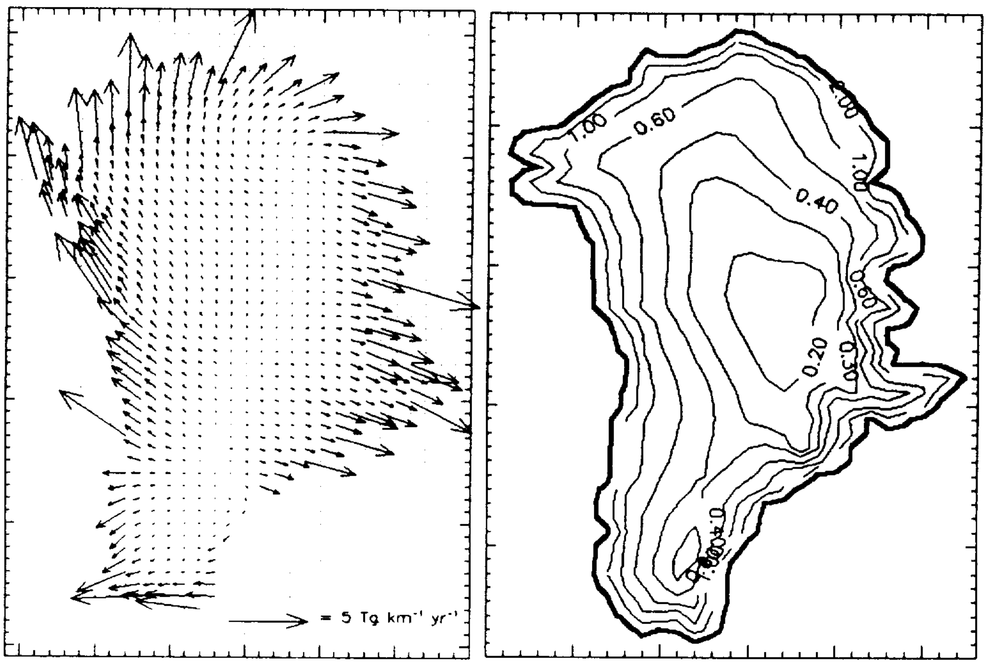


Fig. 4: (Left) Annual vectors of blowing snow transport for the Greenland ice sheet. (Right) Estimates of total blowing snow mass flux (Tg $km^{-1}$ $yr^{-1}$).

*Increased UV-Radiation over the Greenland Ice Sheet*

Enhanced UV cloud transmission was measured over snow surfaces at the Swiss Camp. Cloud attenuation of total radiation is twice that of UV radiation, whereas in mid-latitudes the attenuation ratio is 1.2. Consequently, higher UV cloud transmission over large snow covered surfaces will expose individuals at a higher UV risk.

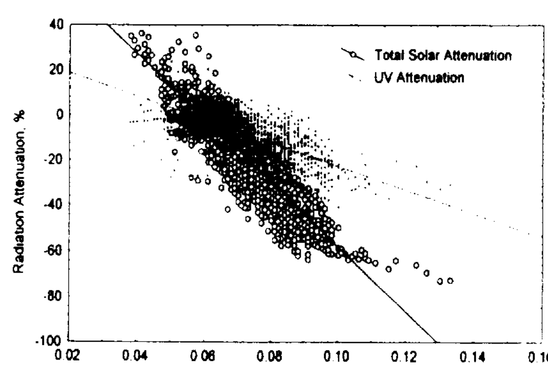


Fig. 5: Attenuation of total solar and UV radiation as a function of the UV to total solar radiation ratio. A positive attenuation indicates a radiation enhancement above clear skies due to clouds

*Faceted Crystal Growth due to Katabatic Storm Events*

Faceted snow crystals were found under wind crusts at the Tunu-N location (Fig. 1). These crusts appear to originate during winter. Snow and air temperatures from the Tunu-N AWS suggest that the katabatic storms are responsible for the wind crust and the faceted layers. The approximated temperature gradients for the top snow cover (5-14 cm in depth) show values in excess of 50 K $m^{-1}$ (a 5 K gradient over 10 cm) for periods of high wind (Fig. 6). The gradient even exceeds 100 K $m^{-1}$ on Nov. 11, 1996, assuming a 3-4 K error in snow surface temperature approximation (colder snow surface during low wind). Also large negative temperature gradients in excess of 100° K $m^{-1}$ were found to be caused by atmospheric warming during katabatic storms, resulting in a reversal of the water vapor flux. The snow temperature at 1 m depth varied only by ±1° C over the period of 8 days as shown in Figure 6, hence large temperature gradients (negative as well as positive) are limited to the top snow layer. This simple approximation suggests that snow temperature gradients in excess of the critical gradient (~25 K $m^{-1}$) necessary for faceted crystal development can occur during katabatic storms, and after the storms with subsequent radiative cooling. In addition to its climatological significance in the snow record, understanding the formation of these layers is especially important to the interpretation of microwave satellite observations of firn.

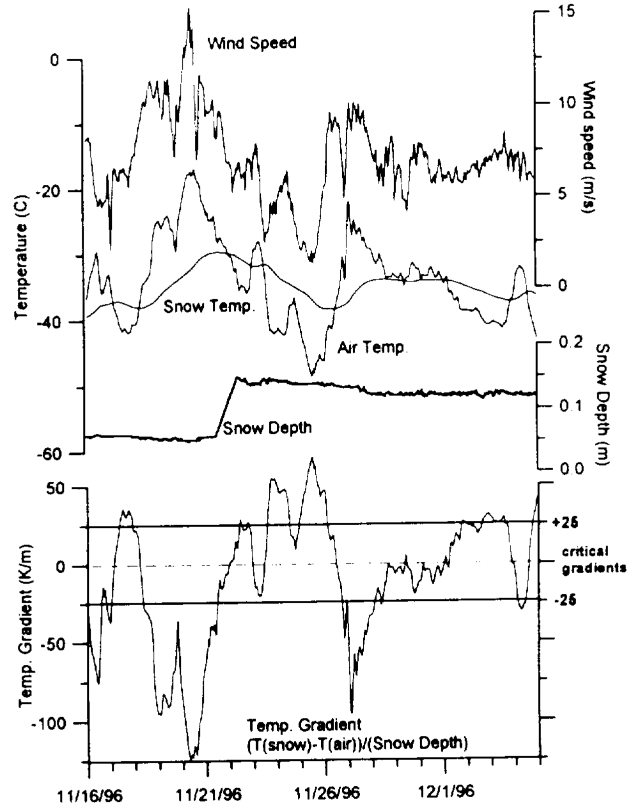


Fig. 6: Hourly automatic weather station record of wind speed, air and snow temperatures, and snow height for Tunu-N in north-east Greenland (Fig. 1). The zero level for the snow height represents the summer 1996 height, and the position of the first snow temperature thermistor. The temperature gradient in the top snow layer exceeds the critical value of 25 K $m^{-1}$ necessary for faceted crystal development several times

## Data Availability

To construct a list of data users, we will distribute GC-Net data on a request basis only. Send us email (jbox@seaice.colorado.edu or koni@seaice.colorado.edu) with your request and we will provide the data in a timely manner.

## Proposed Field Work 1999

- Any station that is revisited next field season will be converted to a new mast design that will allow more timely extension. Further, re-calibration of all sensors, net radiometer servicing, and leveling of all radiometers will be done. In addition, snow pit data will be collected.

- New Nunatak station to represent low elevation climate as part of elevation transect (JAR region)
- Additional SE station to fill data gap around 72° N along the eastern side of Greenland (former location Tunu-S)
- NASA/GSFC Lidar installation for monitoring aerosol and clouds on an annual basis at the Swiss Camp
- Atmospheric kite experiment: profile measurements of temperature, humidity, radiation and aerosol concentration in the first 1-2 km to study the boundary layer structure during katabatic storm events.
- Ground-penetrating radar transect between Swiss Camp and Crawford Point to monitor layering in the firn.

***Priority list of AWS maintanenence***

| *Site* | *Tasks* | *Time on Site Needed* | *Priority* |
|---|---|---|---|
| GITS | Extension.<br>New Transmitter.<br>Firn Temperature String. | 2-3 days | High |
| NASA-U | Extension.<br>New Transmitter.<br>New Firn Temperature String. | 2-3 days | High |
| Saddle | Extension.<br>Transmission reset 1998 did not work. | 2-3 days | High |
| NASA-SE | Extension.<br>Transmitter. | 1-3 days | High |
| SDOME | Extension.<br>1 x T/RH broken. | 2-3 days | High |
| JAR | New tower foundation.<br>TC Air out. | 1* day | High |
| CP 1 and 2 | Extend one tower | 2* days | Medium |
| Swiss Camp | Reset transmission . | 2* days | |
| Summit | Extension. | 2-3 days | Medium |
| NASA-E | 1 x T/RH broken | 1 day | Medium |
| Humboldt | Not Visited since 1996.<br>2 x T/RH broken | 1 day | Medium |
| Tunu-N | Might be something in way of wind direction sensors or a processing problem.<br>more noisy firn TC measurements after 1998 visit? | 2-3 hours | low |

* to be performed as part of Swiss Camp traverse work

# INTERPRETING AIRCRAFT-DERIVED ICE SHEET ELEVATION CHANGES USING CLIMATE STATION DATA

*Waleed Abdalati, Laboratory for Hydrospheric Processes, NASA Goddard Space Flight Center, Code 971 Greenbelt, MD 20771, waleed@intrepid.gsfc.nasa.gov*

*Jason Box and Konrad Steffen, Cooperative Institute for Research in Environmental Sciences, The University of Colorado, Boulder, CO 80309*

## Introduction

This year repeat elevation surveys in the southern half of Greenland were made using the Airborne Topographic Mapper (ATM). The intent of these surveys is to compare present elevations to those measured in 1993 and determine the magnitude and spatial distributions of thickening and thinning rates. In order to effectively interpret any observed changes, it is important to understand the processes that affect these changes. Moreover, because the surveys are made over a brief period (2-4 weeks) during the spring or summer, it is also important to understand the effects of seasonal and interannual elevation variability, in relation to the timing of these surveys.

Toward that end we are examining data from weather stations along the coast of Greenland along with data from GC-Net automatic weather stations (AWS's) on the ice sheet. The objectives are to assess: a) the importance of the timing of the flights in relation to natural processes that affect surface heights, namely accumulation and melt, and b) the temperature characteristics of the region in the five years that separated the two sets of surveys (1993-1998), in relation to the past 19 years.

## Approach

Using snow height data from the automatic weather stations, the deviation of the elevation about a linear slope was determined. The intent was to assess whether offsets in the timing of the resurveys can be adequately accounted for by linearly scaling the accumulation with respect to time. Such a relationship is important to reconcile surveys that occur at slightly different dates and also to account for variability of melt onset at the lower elevations. The information will also be important to the interpretation of Ice Cloud and Land Elevation Satellite (ICESat) observations. ICESat is currently planned to have a six month repeat cycle, so knowledge of interannual variability will be important. In order to eliminate partial-year effects in the analysis, or effects due to variability of melt onset, only data from each station for which a complete hydrological year was available were used. A hydrological year, for these purposes, is defined as the time beginning shortly after ice sheet melt is believed to have stopped and continuing through the next melt season. In this case it is defined as October 1st through September 30th. For stations in which more than one complete hydrological year of data is available, the results are averaged.

To study the temperature characteristics of the last five years and how they compared to the previous years, We examined data from 54 weather stations around the perimeter of Greenland. The data record, provided by Dennis Joseph, of the National Center for Atmospheric Research (NCAR) in Boulder Colorado cover the period from January 1, 1979 through May 31, 1998. By averaging the summer-month temperatures, June, July, and August, of each year, comparisons were made between the 1993-1997 summer temperatures, and the mean summer temperatures for the 1979-1997 time period. Only those stations with data values in each of the summer months for at least 13 years of the 19-year record were used in the comparison. This left 19 stations for the comparison (shown in Fig. 1). These stations cover each of the major climate zones identified by Ohmura and Reeh (1991).

**Results**

Figure 1 shows the mean annual accumulation rates and the standard deviations of the residuals about the linear trend (the accumulation rate is the slope of the trend). The results indicate that for the central higher elevation, the linear trend is a very good approximation. For AWS's at elevations at or above 2000 meters in elevation, the standard deviation of the residuals was less than or equal to 10 cm. This is about the accuracy of the ATM. The lower elevations, from the Swiss Camp to the Jakobshavn ablation region, where there was a net decrease in height for the period examined, show more variability – one third to half a meter. Thus timing of the surveys, in relation to the melt onset is important in these melt areas. However, by fitting a trend to only the summer values of elevation change, the residuals are significantly reduced ($\sigma$ = 16.5 cm).

It is important to note that for the westernmost station that is well into the ablation area, JAR, although the annual mass loss rate is 0.73 m/yr, the rate during the summer is 0.6 m per month. Thus in these high ablation areas, timing of the surveys in relation to melt is very important, but once known, the values can be corrected with reasonable precision. Still, an observed elevation change signal needs to be larger at the ice sheet edges to be significant to overcome the seasonal uncertainties.

The coastal temperature anomalies are shown in Figure 2. The results indicate that the entire east coast was significantly warmer during the observation period than it was over the longer term. The northern portions of the west coast were cooler, while the southern portions were relatively unchanged (when averaged spatially over the Ohmura and Reeh (1991) climate zones). These results suggest that the 1993-98 observed elevation differences in the west, with respect to temperature, are likely to be indicative of what has been ongoing for the last two decades. In the east, however, elevation changes are likely to be biased toward greater melting over the last five years, as a result of the warmer temperatures. Precipitation characteristics still need to be examined.

Data from these coastal and ice sheet weather stations are important to the understanding of observed elevation changes. By providing information on the climatological processes that affect these changes, they play a significant role in the interpretation of observed elevation changes. Such information is important to both ATM-derived elevation changes, as well as those that will be observed by GLAS in the future.

Future efforts will include the analysis of the passive microwave melt record to determine melt variability since 1993, and melt onset times in 1993 and 1998. In addition, comparisons need to be made to accumulation estimates over the 5-year time period. By combining the two, the relative importance of each in to the observed elevation changes can be assessed.

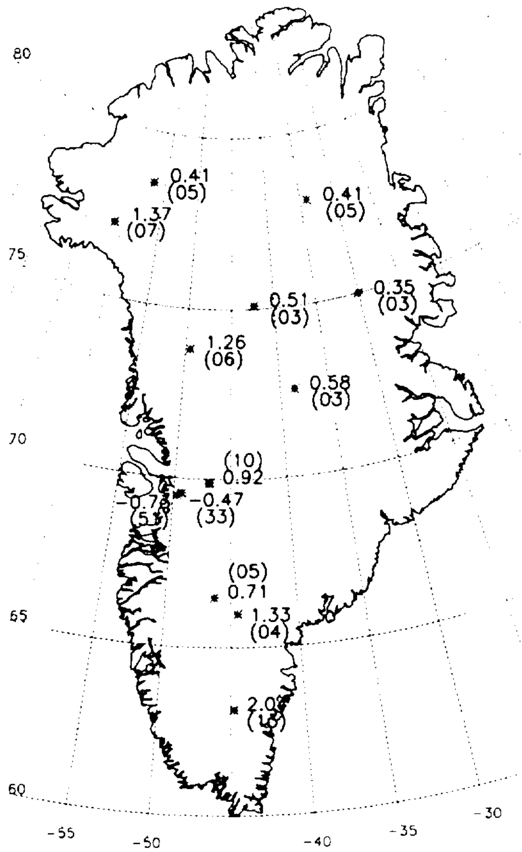


*Figure 1:* Mean annual elevation changes (in meters) as observed at the GC-Net AWS sites. In parentheses are the standard deviations (σ) in cm. after detrending. In the case of JAR, the westernmost station well into the ablation zone, σ can be reduced from 51 cm to 16.5, when only the ablation period is considered (taken to be May 15th – September 15th). Elevation changes average 60 cm per month during the summer months.

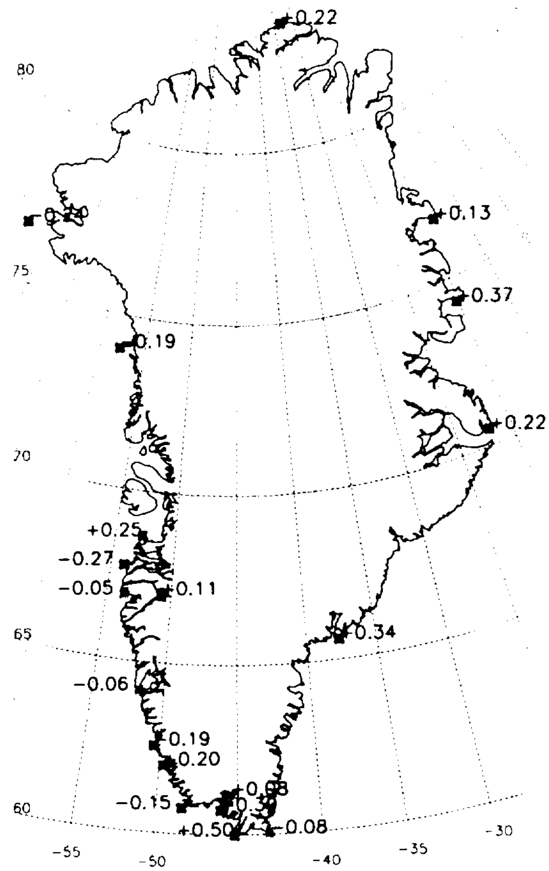


*Figure 2:* Deviation of average 1993-1997 summer (June – August) temperatures from the 1979-1997 mean. Positive values indicate that the period recent years were anomalously warm at the weather station site, while negative values indicate that the recent period was colder.

## Reference

Ohmura, A., and N. Reeh, 1991. New precipitation and accumulation maps for Greenland, *Journal of Glaciology*, **37**(125), 140-148.

# EVALUATION OF RECENT GREENLAND ICE SHEET PRECIPITATION STUDIES

*David H. Bromwich and Qiu-Shi Chen, Polar Meteorology Group, Byrd Polar Research Center, The Ohio State University, 1090 Carmack Road, Columbus OH 43210-1002, bromwich@polarmet1.mps.ohio-state.edu*

## Project objectives

Observations of precipitation over Greenland are limited and generally inaccurate. These limitations have given rise to the use of several different atmospheric methods for examining precipitation variability over Greenland. Atmospherically derived precipitation estimates typically rely on atmospheric numerical analyses in order to retrieve values. The high spatial and temporal resolution furnished by these methods provides a valuable climatological record that cannot presently be obtained from other sources. The various atmospheric methods presently available for precipitation retrieval over this Arctic ice sheet are examined in comparison to glaciological data and to each other (material adapted from Bromwich et al. (1998)). In addition, we compare the retrieved annual precipitation using the U.S. Navy 10 arc minute topographic data set with that obtained by using Ekholm (1996)'s topography.

The objective of this study is to develop an enhanced dynamic method for retrieving precipitation over Greenland from the atmospheric analyzed fields. Precipitation and accumulation over Greenland from 1979 to 1998 and their seasonal and interannual variations will be estimated by the enhanced method. How the atmospheric general circulation and weather systems control precipitation and accumulation over Greenland will also be studied.

## Spatial distribution of the mean annual precipitation over Greenland

The spatial distribution of the long-term accumulation field synthesized from glaciological data has previously been described by Ohmura and Reeh (1991) and Csathó et al. (1997). The distribution generally shows large values along the southeast coast with a significant elevation-related gradient to very small values in the interior. A region of some interest is along the western glacier margins near the 2400 m elevation contour. Previous syntheses have shown an orographically-related precipitation maximum extending from near Jacobshavn (approximately 70°N, 47°W) northwest to near Thule (77°N, 69°W). A major source of information for this feature has been measurements from the 1912 to 1913 Swiss Greenland Expedition; however, the region has been heretofore undersampled. The recent addition of cores from PARCA to the accumulation distribution has diminished this feature, although there remains a significant east-to-west gradient across the center of the ice sheet. Only relatively large values in close proximity to the location of the original measurements remain, rather than the continuous large-scale feature found in previous distributions. Nevertheless, values along the western half of Greenland north of 70°N are significantly larger than along the east coast.

Figure 1 shows the multi-annual spatial distributions of each of the atmospheric methods examined. All of the methods show two large-scale precipitation features for Greenland: essentially desertlike conditions for the northern ice sheet dome and very large values of 100 to 200 cm-yr$^{-1}$ along the southeast coastal region. The average spatial distribution of P-E derived from the atmospheric moisture budget using ECMWF (European Centre for Medium-range Weather Forecasts) operational analyses (Figure 1a) is very similar to the Csathó-PARCA depiction. Along the southeast coast, ECMWF moisture budget values are as large as 102 cm-yr$^{-1}$. This appears to be slightly low in comparison to the accumulation synthesis.

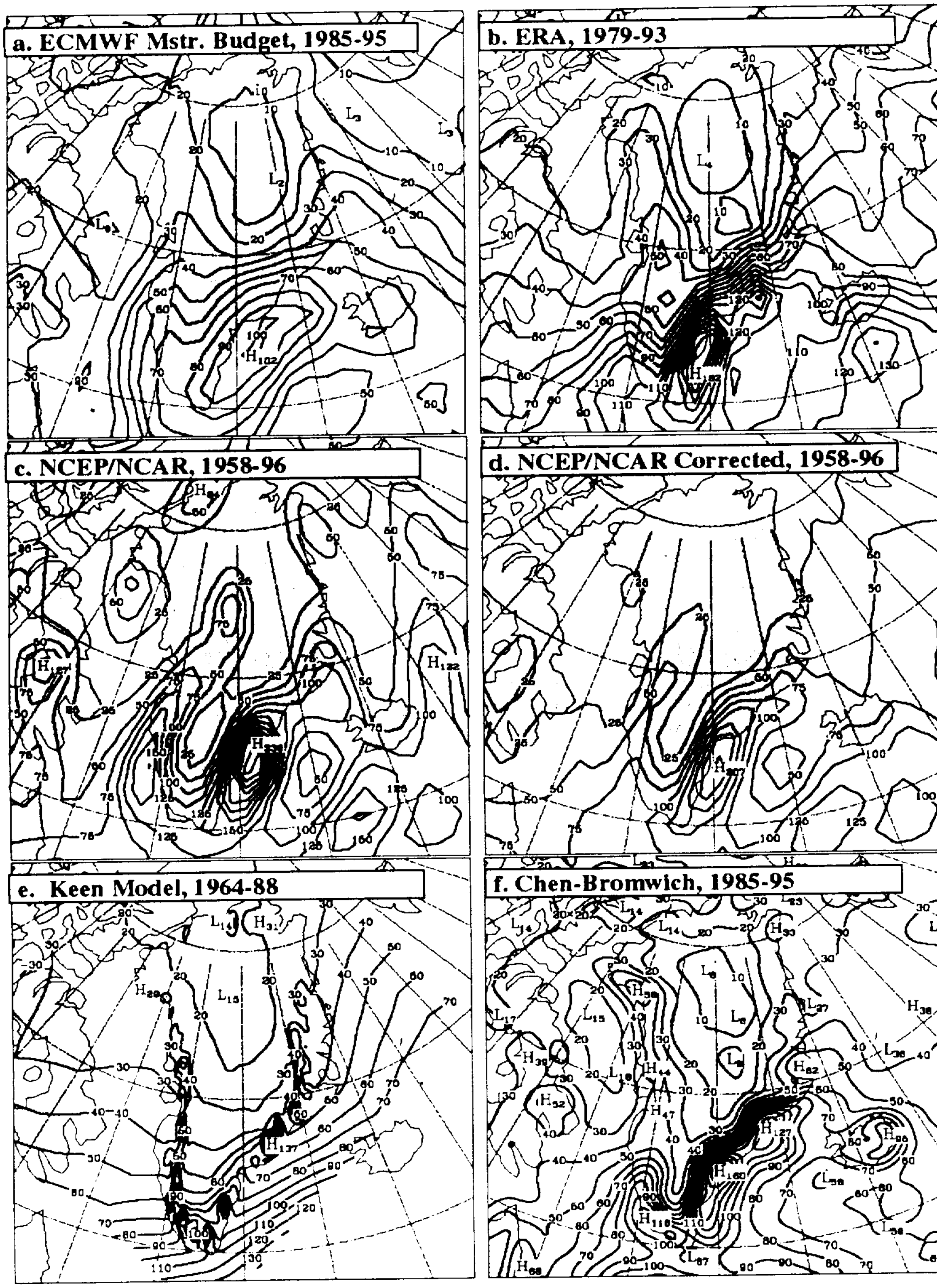


Figure 1. Average spatial disribution for various methods (a) P-E derived from he atmospheric moisture budget using ECMWF operational analyses for 1985-1995; (b) forecast precipitation from the ERA for 1979-93; (c) forecast precipitation from the NCEP/NCAR Reanalysis for 1958-96; (d) a corrected forecast precipitation climatology from the NCEP/NCAR Reanalysis for 1958-96; (e) precipitation using the Keen model, 1964-1988; and (f) precipitation from the Chen-Bromwich model for 1985-95. The contour interval is 10 cm-yr$^{-1}$ for (a), (b), (e), and (f), and 25 cm yr$^{-1}$ for (c) and (d).

However, there are difficulties with the accumulation data along the extreme coastal margins because of limited observations and complex topography. North of 70°N the spatial distribution is again very reasonable in a broad sense. At the highest elevations, however, the region covered by the 10 cm-yr$^{-1}$ contour is substantially larger than is supported by glaciological studies; average values for the interior are too low. The remaining five panels show precipitation, which has been estimated to be 8% greater than the depicted accumulation for the whole of Greenland (Ohmura and Reeh, 1991; Bromwich et al., 1993). The ERA (ECMWF Reanalysis) forecast precipitation shows values ranging from 182 cm-yr$^{-1}$ along the southeast coast to about 4 cm-yr$^{-1}$ in the interior. While the maximum values are not unreasonable in both location and magnitude, the minimum for the interior plateau is again too small. For example, the long-term average accumulation for Summit, which has been extensively sampled, is 22 cm-yr$^{-1}$ (Bolzan and Strobel, 1994), while ERA values averaged over 15 years are less than 50% of this value. A similar shortfall in ERA precipitation over polar glaciers has also previously been found for Antarctica (Stendel and Arpe, 1997). Not surprisingly, there is a greater amount of detail in the average forecast precipitation than in the lower-resolution moisture budget data. This is particularly true along the western coast.

Figure 1d shows the average distribution of the corrected NCEP/NCAR (National Centers for Environmental Prediction / National Center for Atmospheric Research) reanalysis forecast precipitation. The original spatial distribution, discussed previously (Chen et al., 1997), is shown in Figure 1c. A larger contour interval of 25 cm-yr$^{-1}$ is used for Figures 1c and 1d only to accommodate the large values. Erroneous higher-latitude maxima in the original NCEP/NCAR reanalysis precipitation data, which buttress Greenland near Thule and on the northeastern and northern coastlines, have been removed in Figure 1d. The correction identifies the bull's-eyes as spurious moisture sources and removes them in comparison to a diffusion-corrected moisture amount, subject to a temperature threshold. It is apparent from examination of the corrected field, however, that the problem is with the distribution, rather than the amount of atmospheric moisture. The corrected precipitation field, although an improvement in the spatial distribution, is overly dry in comparison to the original field and the ERA north of 70°N. This leads to a contrast between northern and southern Greenland that is greater than for other methods. Additionally, over central Greenland the temperature threshold of the correction does not allow for the complete removal of the spurious maximum that extends over the relatively colder regions of the high plateau. In general, neither of the two spatial depictions available from the NCEP/NCAR reanalysis appear to be promising.

Figure 1e shows the spatial pattern of the Keen model (Bromwich et al., 1993). The model uses NCEP operational analyses available on a polar stereographic grid that is diagonal to the view shown. The offshore values which increase to the south are in areas with minimal topographic forcing and are erroneous. Over the interior plateau the values shown are quantitatively superior to other methods. This is partially misleading, however, because the model was fitted to agree with glaciological data at Summit. Significant differences exist with other climatologies along the southern coastal regions. A maximum value in the Keen data of 137 cm-yr$^{-1}$ is found near the Denmark Strait. Along the west coast a continuous string of maxima occurring in close proximity to the coastline is not supported by the glaciological depiction.

Finally, Figure 1f shows the average spatial pattern of the Chen-Bromwich precipitation data. Both the Keen model and the Chen-Bromwich precipitation data have a significantly higher spatial resolution however; this is particularly apparent in the Chen-Bromwich distribution. Figure 1f is significantly busier than the other distributions. A resulting difference is the strong spatial gradient along the southeast coast, where the contour lines have merged together. Several maxima of up to 160 cm-yr$^{-1}$ are apparent along the southeast coastline. The values fall to less than 30 cm-yr$^{-1}$ only a short distance inland. Over the interior the spatial distribution is very similar to that of the ERA, which features two areas of less than 10 cm-yr$^{-1}$. Again, the values for the interior are small in comparison to the glaciological data. To an extent, the Chen-Bromwich precipitation data give the appearance of being a higher-resolution version of the ERAdata. A feature well captured by the Chen-Bromwich model is the precipitation maximum near Thule.

**Topographic errors and their effect on the mean annual precipitation over Greenland**

Several of the deficiencies in the spatial distributions are probably related to the topographic data employed in assimilation and modeling. Both the ECMWF and the NCEP use spectral versions of a global U.S. Navy 10 arc min digital elevation data set. Chen et al. (1997) also elected to use this data set for their study. Genthon and Braun (1995) have identified substantial errors of up to 1 km in the U.S. Navy data set over the Antarctic ice sheet. The topography of Greenland from the U.S. Navy 10 arc minute global data set and the modern data set of Ekholm (1996) are shown in shown in Figs. 2a and 2b, respectively. The Matrikelstyrelsen and Ekholm field is a realistic digital elevation data set synthesized from a variety of observations including satellite radar altimetry. The Navy depiction of the plateau region is found to erroneously extend too far to the south. Such an error is expected to have the effect of increasing orographic precipitation closer to the southeast coastline while reducing the total amount of moisture transported inland.

In order to check how the computed precipitation is affected by the topography, the distribution of the annual total precipitation for 1995 computed from the ω-equation method (Chen et al., 1997) based on the topography of Figs. 2a and 2b is presented Figs. 3a and 3b, respectively. Comparing Figs. 3a and 3b, it is seen that the precipitation amount in the central region near Summit, Greenland computed based on the topography of Fig. 2b is at least twice as large as that based on Fig. 2a. Furthermore the area within the 10 cm-yr$^{-1}$ contour in Fig. 3b is much smaller than that in Fig. 3a, and is close in areal extent and location to the 10 cm-yr$^{-1}$ contour shown by accumulation analyses. It is concluded that the anomalous topography near Summit in Fig. 3a does indeed affect the distribution of precipitation over the ice sheet.

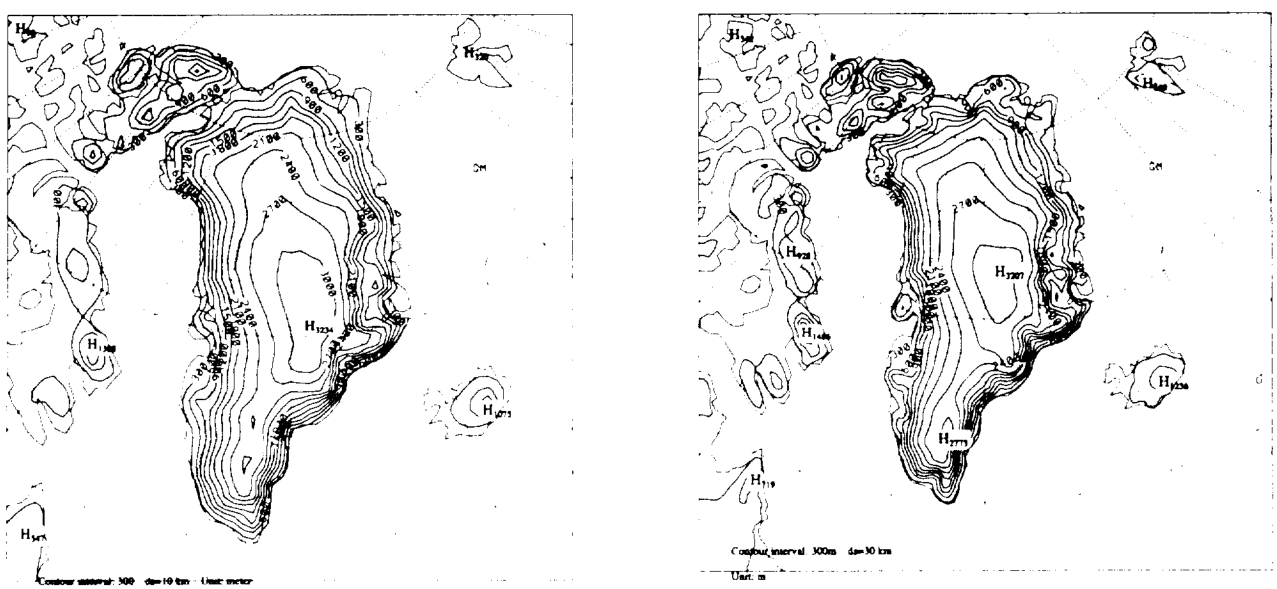

Figure 2. (a) The topography of Greenland and adjacent areas (in meters with a contour interval of 300 m); (b) same as (a) but based on Ekholm (1996). Notice the large difference over Greenland just to the south of 70°N.

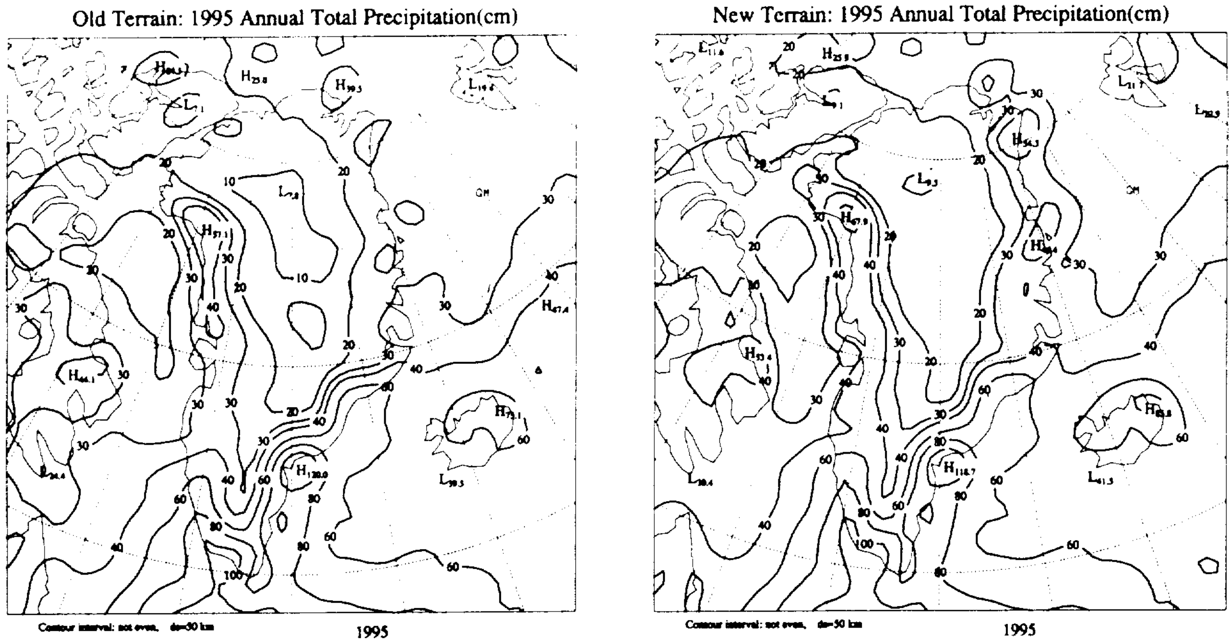


Figure 3 (a) The total precipitation for 1995 retrieved based on topography of Fig. 2a in cm with a contour interval of 20 cm, but 10 cm if smaller than 40; (b) Same as (a) but retrieved based on the topography of Ekholm (1996).

## Plans for 1999

From the above, it is seen that it is necessary to use the topography of Greenland based on the modern data set of Ekholm (1996) to retrieve precipitation. Cyclones are primarily responsible for precipitation formation over Greenland, including both the heavy and small precipitation amounts over the southern and central regions, respectively. Recently, the equivalent geopotoential $\phi_e$ in $\sigma$-coordinates was proposed (Chen and Bromwich, 1999). The equivalent geopotential $\phi_e(x,y,\sigma,t)$ can be used in $\sigma$-coordinates in the same way as $\phi_e(x,y,\sigma,t)$ is used in p-coordinates. In order to facilitate diagnosing the topographic effect on vertical motion, lee cyclogenesis and precipitation directly in $\sigma$-coordinates, a diagnostic method for using the equivalent geopotential $\phi_e$ is being developed. This method will be used to enhance the precipitation computation procedure of Chen et al. (1997), and to diagnose the effects of the Greenland Ice Sheet topography on the cyclone development and precipitation. Precipitation over Greenland from 1979 to 1998 and its seasonal and interannual variations will be computed. The relation of the precipitation over Greenland to the large scale circulation in the North Atlantic region including the North Atlantic Oscillation will also be studied.

## References

Bolzan, J.F., and M. Strobel, 1994: Accumulation rate variations around Summit, Greenland. J. Glaciol., 40, 56-66.

Bromwich, D.H., F.M. Robasky, R.A. Keen, and J.F. Bolzan, 1993: Modeled variations of precipitation over the Greenland Ice Sheet, J. Climate, 6, 1253-1268. Bromwich D. H., Bromwich, D.H., R.I. Cullather, Q.-S. Chen, and B. M. Csathó, 1998: Evaluation of recent precipitation studies for Greenland ice sheet. J. Geophys. Res., 130(D20), 26,007-26,024.

Chen, Q.-S., D. H. Bromwich and L. Bai, 1997: Precipitation over Greenland retrieved by a dynamic method and its relation to cyclonic activity. J. Climate, 10, 839-870.

Chen, Q.-S., and D. H. Bromwich, 1999: An equivalent isobaric geopotential height and its application to synoptic analysis and to a generalized $\omega$-equation in $\sigma$-coordinates .Mon. Wea. Rev. 127, (in press)

Csathó, B., H. Xu, R. Thomas, D. Bromwich, and Q.-S. Chen, 1997: Comparison of accumulation and precipitation maps of the Greenland Ice Sheet, Eos. Trans. AGU, 78(46), Fall. Meet. Suppl., F9.

Ekholm, S., 1996: A full coverage, high-resolution, topographic model of Greenland computed from a variety of digital elevation data. J. Geophys. Res., 101(B10), 21,961-21,972.

Genthon, C., and A. Braun, 1995: ECMWF analyses and predictions of the surface climate of Greenland and Antarctica, J. Climate, 8, 2324-2332.

Ohmura, A., and N. Reeh, 1991: New precipitation and accumulation maps for Greenland. J. Glaciol., 37, 140-148.

Stendel, M., and K. Arpe, 1997: Evaluation of the hydrologic cycle in reanalyses and observations. Tech. Rep., 52 pp., Max-Planck-Inst. für Meteorol., Hamburg.

# DEVELOPMENT OF GREENLAND GIS DATABASE SYSTEM (GGDS)

*Bea Csathó , Changjoo Kim, and John Bolzan, Byrd Polar Research Center, The Ohio State University, Columbus OH, 43210 csatho@ohglas.mps.ohio-state.edu)*

*Robert Thomas, EG&G Services, NASA Wallops Flight Facility, Code 972, Wallops Island, VA 23337*

## Introduction

An important component of the PARCA program is the 'traditional' mass-balance investigation (Thomas et al., in press). To obtain the mass balance the difference between the snow accumulation and the ice discharge is computed for the interior of the ice sheet. The input data of the analysis are the ice velocity and ice thickness measured along the 2000-meter elevation contour, digital accumulation maps, digital flowlines passing through the velocity stations, etc. The large data volume and complexity of the data set necessitated the introduction of a spatial database system. We have started to develop the Greenland GIS Database System (GGDS) in 1998. GGDS contains various geophysical and glaciological data collected on the Greenland ice sheet. Since the errors of the mass balance computations are dominated by the uncertainty in the accumulation rate, different accumulation and precipitation models have been included in GGDS, such as the Bender (1984) and the Ohmura and Reeh accumulation maps (1991). To take advantage of the information from the recent German and PARCA ice cores a new accumulation map has been compiled by using universal kriging (Csatho et al., 1997). Additional enhancements to this depiction are expected with the improved spatial coverage of glaciological observations supplied by the PARCA investigation. The current status of GGDS is reported here.

## Greenland GIS Database System (GGDS)

GGDS has been constructed by using Arc/Info and ArcView software (both from ESRI). Access97 from Microsoft serves as the Relational Database Management System (RDBMS). GGDS allows the user to interactively display and query geological, glaciological, and geophysical information by defining an area of interest, querying selected spatial and temporal databases, and searching for and returning geo-referenced information that intersects the user-defined area of interest.

The following data sets have already been entered into GGDS:

- Digital Elevation Model and land-cover (Ekholm, 1996).
- Accumulation and precipitation data. Details about these data sets are given in Section 3.
  - Accumulation and precipitation maps (raster data).
  - Ice cores and pits (point data).
- Ice velocity along the 2000-meter contour line from repeat GPS measurements (Thomas et al., in press).
- Gravity data and precise elevations from differential GPS at the ice velocity stations (Roman et al., 1997).
- Flowlines passing through ice velocity stations (Thomas and Csatho, in this report).
- Boundary of major climate regions of Greenland (Bromwich et al., in press).
- 10-meter temperature map of the ice sheet.

Other data, such as ice thickness from ice penetrating radar measurements, location of AWS and local mass balance measurements ('coffee can' stations) are currently being added to the database.

## Description of Accumulation Data Sets

An important component of the ice sheet mass balance is snow accumulation. Observations of snow accumulation are limited in space and time, and the available data are of mixed quality, were obtained over a long period and are far from uniformly distributed over the ice sheet.

*Raster data*

- Bender and Ohmura and Reeh accumulation maps. The latest observed accumulation maps of Greenland have been published by Bender (1984) and by Ohmura and Reeh (1991). For our applications these manual accumulation maps were digitized and converted into raster data sets by using an interactive finite difference interpolation technique.
- PARCA-OSU97 accumulation map. This model, depicted in Fig. 1, is our recent compilation of the Ohmura and Reeh observations with the inclusion of a few recent measurements (Bolzan and Strobel, 1994, Friedmann et al., 1995, McConnell et al., 1997, Anklin et al., in press) by using kriging analysis. Universal kriging is a local optimal linear spatial prediction method, which also yields a measure for the estimation error at every point in the sample space. This accumulation map was created by universal kriging with quadratic drift. To capture the major variance of the variogram a 500 km neighborhood was considered for the interpolation, and a 10 km resolution interpolation surface was created. The differences between this compilation and the Ohmura and Reeh map resulted from the addition of the new observations and the use of an objective approach instead of the manual analysis. On the new map the minimum on the NE part of the ice sheet is extended further south toward the Summit area. The large NNW-SSE maximum between Camp Century and the Saddle has a more complicated structure. The northern part, south of Camp Century, is open toward the coast. The maximum between NASA-U and Crawford Point has become less pronounced.
- The Chen-Bromwich precipitation model. As an alternative to the long-term glaciological synthesis atmospheric methods are used for examining the spatial and temporal variability of the precipitation. This model for the 1985-95 period is retrieved by dynamic method (Bromwich et al., in press).

*Point data*

The accumulation data set includes the glaciological observations and gauge measurements used by Ohmura and Reeh (1991). For the 252 ice cores and pits the original references have been investigated to validate the accumulation rate and to obtain other relevant perameters. Recent ice cores and pits acquired by PARCA and European investigators are currently being added to GGDS (e.g., Bolzan and Strobel, 1994, Anklin, 1994, Friedmann et al., 1995, Fischer et al., 1995, Fischer, 1997, and personal communications from PARCA investigators).

Attributes of accumulation stations Each ice core or pit site is described by the following attributes (the name of the attribute in the RDBMS and the physical unit of the measurements are given in brackets):

- Point-ID (Station Id) consists of two parts. The first part includes the name of the investigator(s) or the field-campaign. The second part is the unique name of the location. Station Ids can be defined by users. [POINT-ID]
- Reference indicates the name of the main author and the year of the publication(s). [REFERENCE]
- Location of station gives the position in geographical system (latitude and longitude) and in the Universal Transverse Mercator (UTM) projection system (Easting and Northing). UTM Zone 24 with a central meridian of W34° is used. [(Lat(°), Lon(°), UTM-X(m), UTM-Y(m)].
- Elevation provides the surface elevation on the WGS-84 ellipsoid. [ELEVATION(m)]

- Annual mean surface temperature is provided if annual mean temperature was determined from long-term temperature record. [ANNUAL-TEMPER( $^{o}$C)]
- Period of annual mean temperature gives the start and end date of the temperature measurement. [DATE-A-TEMPER(mm/yy-mm/yy)]
- 10-meter temperature provides the temperature measured at 10 meter depth. [10M-TEMPER($^{o}$C )]
- Date of 10-meter temperature measurement. [DATE-10-TEMPER(mm/dd/yy)]
- 20-meter temperature provides the temperature measured at 20 meter depth. [20M-TEMPER($^{o}$C )]
- Date of 20-meter temperature measurement. [DATE-20-TEMPER(mm/dd/yy)]
- Mean annual accumulation rate in water equivalent. [ACCUM-WATER(cm/a)]
- Mean annual accumulation rate in ice equivalent. An ice density of 917 $kg/m^3$ is used for the conversion. [ACCUM-ICE(cm/a)]
- First year of measured accumulation rate.[START-ACCUM(year)]
- Last year of measured accumulation rate.[END-ACCUM(year)]
- Date of ice core collection or pit observation. [DATE-ACCUM(mm/dd)].
- Period of accumulation rate represents the number of years. [PERIODS-ACCUM(year)]
- Standard deviation of accumulation rate in ice equivalent.[STDV-ACCUM(cm/a)]
- Minimum accumulation rate in ice equivalent. [MIN-ACCUM(cm/a)]
- Maximum accumulation rate in ice equivalent. [MAX-ACCUM(cm/a)]
- Type of observation is either ice core or pit. [LAYER-TYPES]
- Core-lengths. [CORE-LENGTHS(m)]
- Pit-depths. [PIT-DEPTHS(m)]
- Snow facies zone provides information about the location of the station using the terminology of the original source, for example upper or lower end of slush zone or superimposed ice. [ZONES]
- Ramm profile gives the length of the Rammprofile. [RAMMPROFILE(m)]
- Density profile gives the length of the density profile. [DENSITYPROFILE(m)]
- Density methods gives the type of the density measurement. [DENSITY-METHOD]
- Stratigraphy indicates if snow statigraphy is available or not. [STRATIGRAPHY]
- Comments. [COMMENTS]
- Quality index is based on the evaluation of the above attributes and it is determined by ice-core experts. [Q-INDEX]

## Current Research and Future Plans

After the reevaluation of the Ohmura and Reeh data set and the inclusion of all new PARCA cores, and other glaciological and geophysical data the database will be made available for the PARCA investigators. Our final objective is to create an internet-based system that supports searching, displaying, and retrieval of various data sets, including not only the ones presented in this report, but also remote sensing imagery and interpreted data, for example thickening/thinning rates or melt zones from passive microwave data.

## Data Availability

For information on data availibility please check the GGDS webpage:
http://polestar.mps.ohio-state.edu/ckim/GGS.html

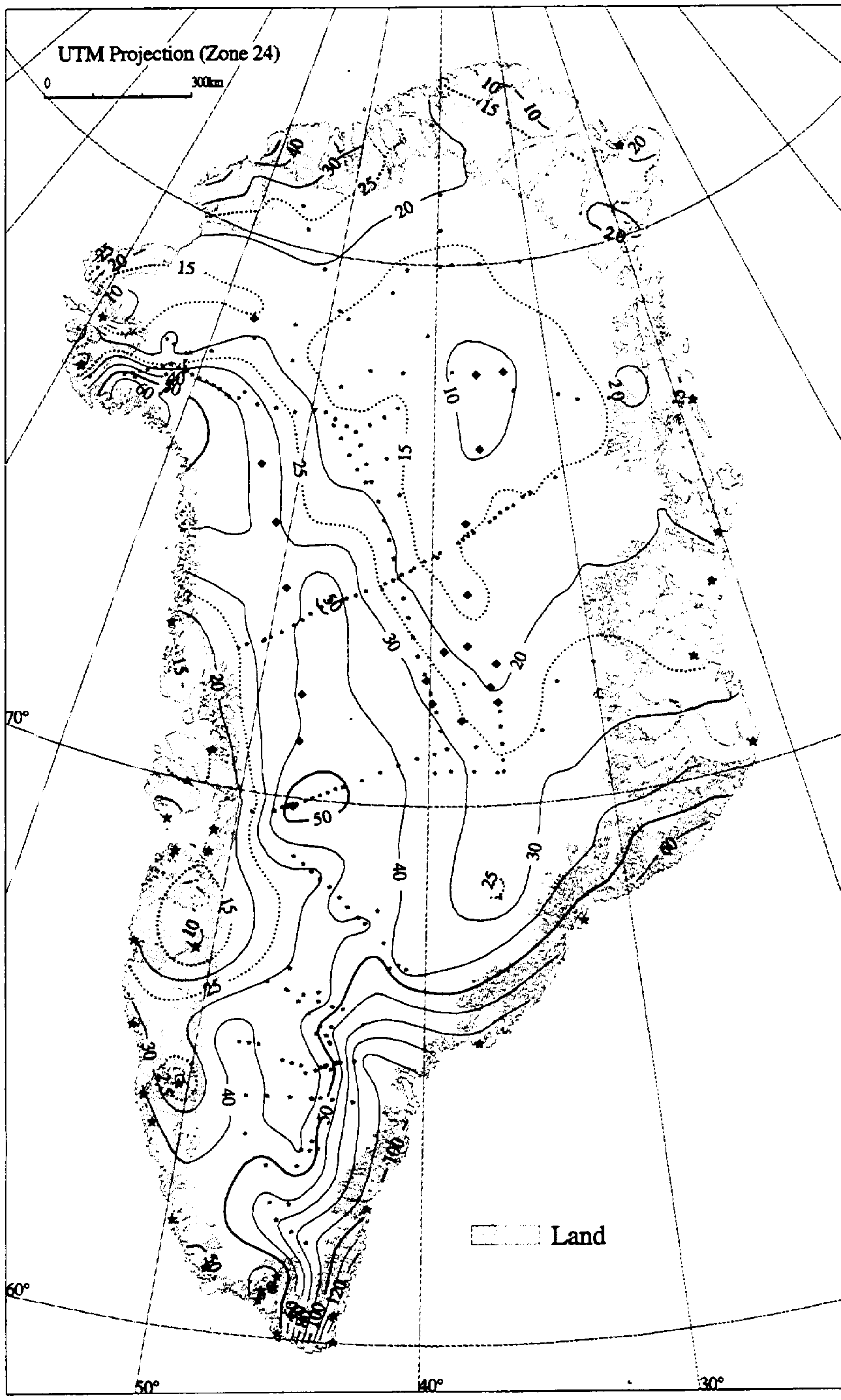


Figure 1. PARCA-OSU97 accumulation map. The map was compiled using a kriging analysis of a data sets that include all ice cores and pits (small stars) and meteorological stations (large stars) from Ohmura and Reeh, as well as a few new ice cores (diamonds). See text for details on the map compilation method and the data set.

**References**


Anklin, M., and B. Stauffer, 1994. Pattern of annual snow accumulation along a west Greenland flow line: no significant change observed during recent decades. *Tellus*, 46B, 294-303.

Anklin, M., R. C. Bales, E. Mosley-Thompson, and K. Steffen. Annual accumulation at two sites in northwest Greenland during recent centuries. *J. Geophys. Res.*, in press.

Bender, G., 1984. The distribution of snow accumulation on the Greenland ice sheet. MS Thesis, University of Alaska, Fairbanks, 110 p.

Bolzan, J. F., and M. Strobel, 1994. Accumulation-rate variations around Summit, Greenland. *J. Glaciol.*, 40(134), 56-66.

Ekholm, S., 1996. A full coverage, high-resolution, topographic model of Greenland computed from a variety of digital elevation data. *J. Geophys. Res.*, 101(B10), 21,961-21,972.

Fischer, H., D., Wagenbach, M. Laternser, and W. Haeberli, 1995. Glacio-meteorological and isotopic studies along the EGIG line, central Greenland. *J. Glaciol.*,41(139), 515-529.

Fischer, H., 1997. Räumliche Variabilität in Eiskernzeitreihen Nordostgrönlands, Rekonstruktion klimatischer and luftchemischer Langzeittrends seit 1500 A. D. PhD Dissertation, Ruprecht-Karls-Universität, Heidelberg, 135 p.

Friedmann, A., J. C. Moore, T. Thorsteinsson, J. Kipfstuhl, and H. Fischer, 1995. A 1200 year record of accumulation from northern Greenland. *Ann. Glaciol.*, 21, 19-25.

McConnell, J. R., R. C. Bales, B. Snider, and B. Matson, 1997. Accumulation estimates from ice cores. *PARCA Contributed Reports, Greenland Science and Planning Meeting*, October 15-16, 1997, Tucson, Arizona, 12-15.

Ohmura, A., and N. Reeh. 1991. New precipitation and accumulation maps for Greenland. *J. Glaciol.*, 37(125), 140-148.

Roman, D. R., B. Csatho, K. C. Jezek, R. H. Thomas, W. B. Krabill, and K. Kuivinen, 1998. Gravity values measured on the Greenland ice Sheet. BPRC Technical Report, 98-01, Byrd Polar Research Center, The Ohio State University, Columbus, Ohio, 39 pages.

Thomas, R. H., B. Csatho, S. Gogineni, K. C. Jezek, and K. Kuivinen. Thickening of the western part of the Greenland ice sheet. *J. Glaciol.*, Vol. 45, 148, 651-656.

# SOFTWARE DEVELOPMENT FOR VISUALIZATION AND ANALYSIS OF SCANNING LASER ALTIMETER DATA

*Sagi Filin, Department of Civil Engineering and Geodetic Sciences, OSU, and*
*Beata Csatho, Byrd Polar Research Center, OSU, csatho@ohglas.mps.ohio-state.edu*

## Introduction

Ice sheet elevation changes have been measured by repeat airborne laser altimetry in Greenland since 1991. The system, which has been mounted on a NASA P-3 aircraft, includes a scanning laser altimeter, Inertial Navigation System INS and differential GPS. During the postprocessing the measured data are converted into measurements of ice sheet elevation relative to the Earth ellipsoid (Krabill et al., 1995). Since laser scanner data sets are composed of a huge amount of points, obtaining the swath contour and locating overlapping areas between different swaths in an efficient way is not a simple task. To make this task more feasible NASA has developed an online database called GReenland Airborne Precision Elevation Survey (GRAPES). So far only data acquired prior to 1994 are included in GRAPES and the database system contains only the thinned version of the original data files. Our major goal is to develop software to access, display, and manipulate the individual laser swaths, to determine the overlap between several surveys, compute elevation changes, and to create DEMs and contour maps. Using the original binary data file as an input the user will be able to perform most of these tasks by using a single application. Until now we were focusing on the first part of the job, namely to provide tools for locating the laser swaths and their overlapping areas.

## Description of the software

Our main objective was to design and implement a tool that is:

- **Efficient** – For example the extraction of laser altimetry data in a given geographic window, plotting the contour of the swath etc., is performed without processing the whole data set first.
- **Machine independent** – It runs on any machine without being specific for a given operating system of machine.
- **Open architecture** – It is easy to maintain and to extend.
- **User friendly** – A Graphical User Interface (GUI) is used to enable the user to extract data and use other applications in a more intuitive way.

  Based on these criteria IDL programming language has been selected. IDL is commonly used in the current environment as well as in NASA. It runs on most platforms, therefore the applications are not system dependent and they should only be compiled before executing them. IDL provides a GUI development toolkit and thus does not require external packages. Finally, it includes advanced graphical analysis tools that can be used to develop further applications.

  The application performs the following tasks:

- **Extraction and graphical display of the laser data swath** – The preliminary graphical overview of the swath trajectory is an important tool for deciding whether the current file is of any interest or not, before extracting the whole data file.
- **Conversion from binary to ASCII format and coordinate conversion** – An operating system independent ASCII to binary conversion has been implemented with an option to transform the geographic positions (latitude, longitude) into a user selected projection system. Currently Universal Transverse Mercator (UTM) and polar stereographic projection systems are supported.

- **Manipulation of several laser files simultaneously** – There have been no tools available for quick and precise determination of the overlap between two or more laser swaths. We have developed a tool to compute and display the boundaries of the laser swaths, which enables the user to locate overlapping areas. Elevation data extracted from these areas will then be used as input for the computation of surface elevation changes.

## Details of the algorithms and techniques

*Data extraction:* The first task is the conversion of the files from binary format to ASCII. Besides the technical aspect of data conversion, the main obstacle is that each machine has its way to represent numerical data -- more specifically they place the most significant bit differently. The application has tackled this problem by first identifying the representation method and then choosing the appropriate data conversion strategy.

*Determination of the laser swath contour:* We define the swath contour as the polygon that bounds all the laser points in a given data file. However, extracting the perimeter from a large data file (files are often larger than 80 MB) may result in an unacceptably long processing time. The main two design issues here are the definition of swath contour and the development of an algorithm for it's efficient extraction.

The laser data footprints form a set of overlapping spirals on the ground. The shape of this pattern is a function of the laser scanning mechanism and the aircraft's motion. The two extreme points of each scanning cycle, with respect to the flight direction, are parts of the swath contour. There are usually 10-20 scans in each second, but the number of cycles necessary to form the swath's contour is negligible compared with the overall number of cycles within the flight. The swath contour can be computed by selecting an equally distributed subset of the cycles and by connecting their bounding points. This approach promises a reliable description of the contour, in contrast to other common contour extraction algorithms (such as the convex hull) that are far more computationally complex, and may not be as accurate.

The scanning cycle was determined by using the scan azimuth field attached to each laser point record. The skip interval is given as a fixed number of points that is equivalent to a selected time interval. After computing the bounding points of the first scan, a certain number of points are skipped, then the next scan is processed, etc. This process continues until the end of file is reached.

Several methods were considered for the computation of the extreme points, for example curve fitting by least squares, or a rigorous solution using the mathematical description of the shape of the spirals. Finally a method based on the determination of the centroids of the scan cycles was selected. The algorithm first computes the centroid of a single scan cycle, then searches for the two farthest points in opposite directions. The centroid is computed as the weighted mean of the horizontal positions of the laser points in the scan cycle, and the distances between the consecutive laser points are used as weights. Weighted averages are used since simple averaging did not work well in areas with gaps in the data. Data are sometimes missing because of the scattering of the laser beam from clouds, fog, water, etc. By using the distance between the consecutive points as a weight, the lower density of the laser data is compensated by their higher weights.

## Example

The example in Figure 1 shows the contour of the laser swath for a large data file. The contour has been extracted from the original binary data files that contain the positions in a geographic coordinate system (latitude and longitude). The flight segment was almost 30 km long, and the size of data file is approximately 50 Mbyte. The total processing time was about 6 seconds (PC with Pentium 133 MHz processor). The time interval between consecutive samples on the boundary was 10 sec.

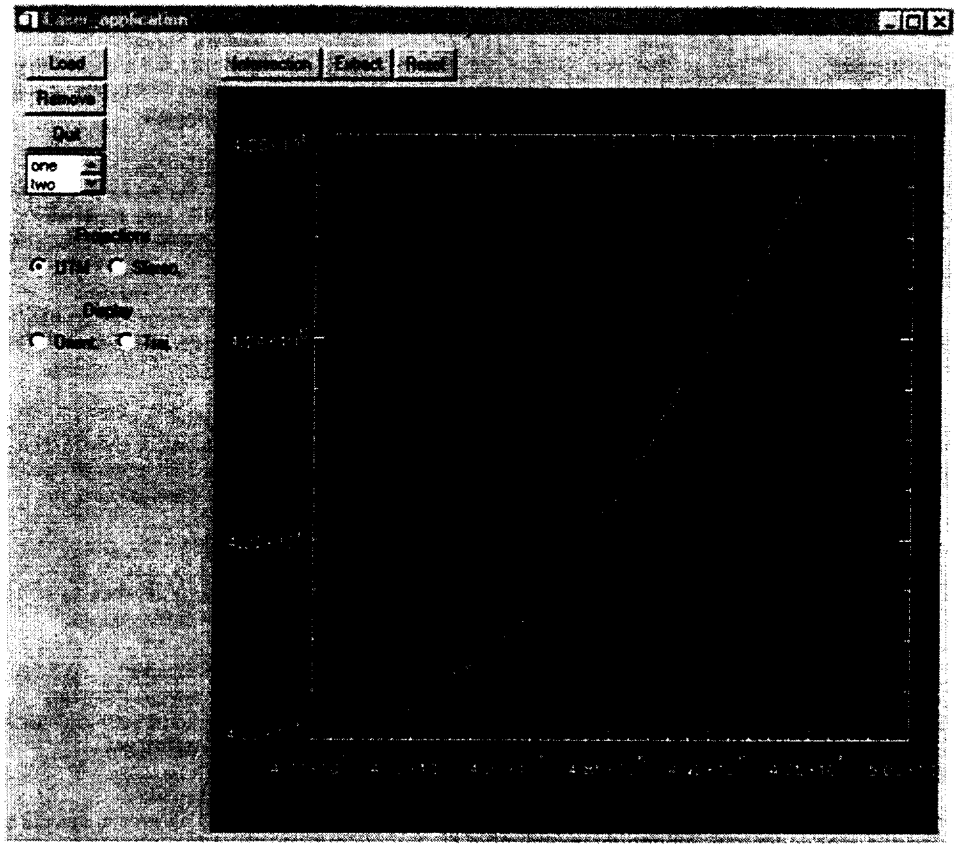


Figure 1. A prototype of the laser data application. The Graphical User Interface window shows the available functions. The plot is made in UTM coordinate system (units are in meters).

**Reference:**

Krabill, W. B, R. H. Thomas, C. F. Martin, R. N. Swift and E. B. Frederick, 1995. Accuracy of airborne laser altimetry over the Greenland ice sheet. *Int. J. Rem. Sens*, 16(7), 1211-1222.

# Appendix I: Meeting Participants

Waleed Abdalati
Laboratory for Hydrospheric Processes
NASA/Goddard Space Flight Center
waleed.abdalati@gsfc.nasa.gov

Torry Akins
Radar Systems and Remote Sensing Lab
University of Kansas
takins@rsl.ukans.edu

Mary Albert
U.S. Army Cold Regions Research
and Engineering Laboratory
malbert@hanover-crrel.army.mil

Robert Arthern
Applied Physics Laboratory
University of Washington
rja@apl.washington.edu

Phil Austin
PICO
University of Nebraska
sirgpico@unlinfo.unl.edu

Jo Baker
University of Michigan
BAKERJB@ZASU.SPRL.UMICH.EDU

Roger Bales
Dept. of Hydrology and Water Resources
The University of Arizona
roger@hwr.arizona.edu

Francois Baumgartner
Byrd Polar Research Center
The Ohio State University
baum@iceberg.mps.ohio-state.edu

Nicola Blake
The University of California Irvine
nblake@uci.edu

Jason Box
CIRES, Dept. of Geography
University of Colorado at Boulder
jbox@seaice.colorado.edu

David Bromwich
Byrd Polar Research Center
The Ohio State University
bromwich@polarmet1.mps.ohio-state.edu

Johnny Burkhart
Dept. of Hydrology and Water Resources
University of Arizona
johnny@hwr.arizona.edu

Brad Campbell
Purdue University

Major Shawn Clouthier
New York Air National Guard
sclouthier@nysch.ang.af.mil

SSgt Steven Cousineau
New York Air National Guard
Scotia, NY

Bea Csatho
Byrd Polar Research Center
The Ohio State University
csatho@ohglas.mps.ohio-state.edu

Lloyd Currie
Atmospheric Chemistry Group
NIST
lloyd.currie@nist.gov

Cliff Davidson
Dept. of Civil and Env. Engineering
Carnegie Mellon University
cliff@andrew.cmu.edu

Curt Davis
Depart. of Electrical Engineering
University of Missouri, Kansas City
curt@polar.cuep.umkc.edu

Jack Dibb
University of New Hampshire
jack_dibb@grg.sr.unh.edu

Linda Duguay
Office of Polar Programs
The National Science Foundation
lduguay@nsf.gov

Marijane England
PICO
University of Nebraska
mengland@unl.edu

Mark Fahenstock
University of Maryland
mark@fim.gsfc.nasa.gov

Earl Frederick
EG&G
NASA Wallops Flight Facility
earlb@osb.wff.nasa.gov

Prasad Gogineni
Code YS
NASA Headquarters
sgoginen@hq.nasa.gov

Gordon Hamilton
Byrd Polar Research Center
The Ohio State University
hamilton@ra.cfm.ohio-state.edu

Richard Honrath
Dept. of Civil and Env. Engineering
Michigan Technological University
reh@mtu.edu

Changjoo Kim
Byrd Polar Research Center
The Ohio State University
ckim@iceberg.mps.ohio-state.edu

Pannir Kanagaratnam
Radar Systems and Remote Sensing Lab
University of Kansas
pkanagar@rsl.ukans.edu

Bill Krabill
Laboratory for Hydrospheric Processes
NASA Wallops Flight Facility
krabill@osb.wff.nasa.gov

Jay Kyne
PICO
University of Nebraska
jkyne@unlinfo.unl.edu

Mike Ledbetter
Office of Polar Programs
The National Science Foundation
mledbett@nsf.gov

Justin Legarsky
Radar Systems and Remote Sensing Lab.
University of Kansas
legarsky@rsl.ukans.edu

Serdar Manizade
EG&G
NASA Wallops Flight Facility
manizade@osb.wff.nasa.gov

Chreston Martin
EG&G Services
martin@wasc2.wff.nasa.gov

Joe McConnell
Dept. of Hydrology and Water Resources
The University of Arizona
joe@hwr.arizona.edu

Ellen Mosley-Thompson
Byrd Polar Research Center
The Ohio State University
thompson.4@osu.edu

P.J. Oneill
PICO
University of Nebraska
poneill@unlinfo.unl.edu

Kim Partington
National Ice Center
NOAA
kparting@hq.nasa.gov

## Meeting Participants (continued)

Earl Ramsey
PICO
University of Nebraska
earl@arctic.net

Eric Rignot
Jet Propulsion Laboratory
eric@adelie.jpl.nasa.gov

Paul Shepson
Purdue University
PSHEPSON@chem.purdue.edu

Christopher Shuman
University of Maryland
shuman@hardy.gsfc.nasa.gov

Lt. Col. Bob Sittinger
New York Air National Guard
rsitting@@nysch.ang.af.mil

Pat Smith
PICO
University of Nebraska
sirgpico@unlinfo.unl.edu

John Sonntag
EG&G Services
sonntag@wasc1.wff.nasa.gov

Konrad Steffen
CIRES, Dept. of Geography
University of Colorado at Boulder
koni@seaice.colorado.edu

Sarah Sturges
PICO
University of Nebraska
sirgpico@unlinfo.unl.edu

Robert Swift
EG&G Services
NASA Wallops Flight Facility
swift@osb.wff.nasa.gov

Robert Thomas
EG&G
NASA Wallops Flight Facility
robert_thomas@hotmail.com

John Wahr
Dept of Physics and CIRES
University of Colorado at Boulder
wahr@lemond.colorado.edu

Dale Winebrenner
Applied Physics Laboratory
University of Washington
dpw@maxwell.apl.washington.edu

Anthony Wong
Radar Systems and Remote Sensing
Laboratory
University of Kansas
ywong@rsl.ukans.edu

James Yungel
EG&G
NASA Wallops Flight Facility
yungel@osb.wff.nasa.gov

Susan Zager
PICO
University of Nebraska
szager@unlinfo.unl.edu

Jay Zwally
Laboratory for Hydrospheric Processes
NASA/Goddard Space Flight Center
jay.zwally@gsfc.,nasa.gov

# Appendix II: PARCA Publications

92

94


Mote, T.L., 1998. Mid-tropospheric Circulation and Surface Melt on the Greenland Ice Sheet. Part I: Atmospheric Teleconnections. *International Journal of Climatology*, 18, 111-130.

Mote, T.L., 1998 Mid-tropospheric Circulation and Surface Melt on the Greenland Ice Sheet. Part II: Synoptic Climatology. *International Journal of Climatology*, 18, 131-146.

Rignot, E. 1998. Hinge line migration of Petermann Gletscher, north Greenland, detected using satellite-radar interferometry, *J. Glaciol.*, 44(148), 469-476.

Scambos TA; Fahnestock MA, 1998. Improving digital elevation models over ice sheets using AVHRR - based photoclinometry, *J. Glaciol.*, Vol 44, No. 146, 97-103

Shuman CA; Alley RB; Fahnestock MA; Bindschadler RA; White JWC; Winterle J; McConnell JR, 1998. Temperature history and accumulation timing for the snowpack at GISP2, central Greenland *J. Glaciol.*, Vol 44, Iss 146, pp 21-30

Serreze, M., J. Key, J. Box, J. Maslanik, and K. Steffen, 1998. A new monthly climatology of global radiation for the Arctic and comparison with NCEP-NCAR reanalysis and ISCCP-C2 field, *J. Climate*, 11, 121-136.

Stroeve, J., and K. Steffen, 1998. Variability of AVHRR-derived clear-sky surface temperature over the Greenland ice sheet, J. Appl. Meteorol., 37, 23-31.

Stroeve, J. and K. Steffen, 1998. Variability of AVHRR-derived Clear Sky Surface Temperature over the Greenland Ice Sheet, *Journal of Applied Meteorology*, Vol. 37, No. 1, 23-31.

Thomas, R. H., B. M. Csatho, S. Gogineni, K. C. Jezek, and K. Kuivinen, 1998. Thickening of the western part of the Greenland ice sheet. *J. Glaciol.*, **44**(148), 651-656.

van der Veen, C. J., W. B. Krabill, B. M. Csatho, and J. F. Bolzan, 1998. Surface roughness on the Greenland ice sheet from airborne laser altimetry. *Geophysical Research Letters*, Vol. 25, No. 20, pp. 3887-3890.

Wahr, J. and D. Han, 1998. Geodetic Techniques for Estimating Changes in Polar Ice, in *Dynamics of the Ice Age Earth; a Modern Perspective*, P. Wu ed., pages 497-508.

Zwally, H.J., A.C. Brenner, J.P. DiMarzio, 1998, Technical comment: growth of the southern Greenland ice sheet, *Science*, Vol. 281, 28 August 1998, p. 1251.


**1999**


Abdalati, W. and W.B. Krabill, W.B., in press. Calculation of ice velocities in the Jakobshavn Isbrae area using airborne laser altimetry, *Remote Sensing of Environment*.

Krabill, W.B., E. Frederick, S. Manizade, C. Martin, J. Sonntag, R. Swift, R. Thomas, W. Wright, J. Yungel, Rapid Thinning of Parts of the Southern Greenland Ice Sheet, *Science*.


**In press**

Davis, C.H., 1995. Synthesis of passive microwave and radar altimeter data for estimating accumulation rates of dry polar snow, *International Journal of Remote Sensing*, Vol. 16, No. 11, pp. 2055-2067.

Giovinetto, M.B., and H.J. Zwally, 1995. An assessment of the mass budgets of Antarctica and Greenland using accumulation derived from remotely sensed data in areas of dry snow. *Zeit. Gletsh.Glazial.*, 31, 25-37.

Joughin, I. R., D. P. Winebrenner, and M. A. Fahnestock. 1995. Observations of ice-sheet motion in Greenland using satellite radar interferometry. *Geophys. Res. Lett.*, 22(5), 571-574.

Krabill, W., R.H. Thomas, K.C. Jezek, K. Kuivinen, and S. Manizade, 1995, Greenland ice sheet thickness changes measured by laser altimetry, *Geophys. Res. Lett.* 22: (17) 2341-2344

Krabill, W.B., R.H. Thomas, C.F. Martin, R.N. Swift, and E.B. Frederick, 1995. Accuracy of airborne laser altimetry over the Greenland ice sheet, *International Journal of Remote Sensing*.

Mote, T.L., and M.R. Anderson, 1995: Variations in Melt on the Greenland Ice Sheet Based on Passive Microwave Measurements. *Journal of Glaciology*, 41, 51-60.

Rignot, E., Jezek, K.C., and Sohn, H.G., 1995. Ice flow dynamics of the Greenland ice sheet from SAR interferometry, *Geophys. Res. Lett.*, 22: (5) 575-578

Rignot, E., 1995. Backscatter model for the unusual radar properties of the Greenland ice sheet, J. Geophys. Res – Planets, 100: (E5) 9389-9400.

Rowe, C.M., M.R. Anderson, T.L. Mote, and K.C. Kuivinen, 1995: Indications of Melt in Near Surface Ice Core Stratigraphy: Comparisons with Passive Microwave Melt Signals over the Greenland Ice Sheet. *Annals of Glaciology*, 21, 59-63.

Shuman, C.A., R.B. Alley, S. Anandakrishnan, J.C.W. White, P.M. Grootes, and C.R. Stearns, 1995. Temperature and accumulation at Greenland Summit: Comparison of high-resolution isotope profiles and passive microwave brightness temperature trends. *J. Geophys. Res.*, 100(D5), 9165-9177.

Thomas, R.H., W.B. Krabill, E.B. Frederick, and K.C. Jezek, 1995. Thickening of Jakobshavn Isbrae, West Greenland measured by airborne laser altimetry. *Ann. Glaciol.*, 23:259-262.

Zwally, H.J., and M.B. Giovinetto, 1995. Accumulation in Antarctica and Greenland derived from passive-microwave data: a comparison with contoured compilations, *Ann. Glaciol.*, 21, 123-130.

**1996**

Bromwich DH, Du Y, Hines KM, 1996. Wintertime surface winds over the Greenland Ice Sheet *Mon. Weath. Rev.* 124: (9) 1941-1947.

Davis, C.H., 1996. Temporal change in the extinction coefficient of snow on the Greenland ice sheet from an analysis of Seasat and Geosat altimeter data," IEEE Transactions on Geoscience & Remote Sensing, Vol. 34, No. 5, pp. 1066-1073.

Davis, C.H., 1996. Comparison of ice-sheet satellite altimeter retracking algorithms, IEEE Transactions on *Geoscience & Remote Sensing*, Vol. 34, No. 1, pp. 229-236.

Joughin, I., D. Winebrenner, M. Fahnestock, R. Kwok, and W. Krabill. 1996. Measurement of ice-sheet topography using satellite radar interferometry. *J. Glaciology*, 42(140), 10-22.

Joughin, I., R. Kwok, and M. Fahnestock. 1996. Estimation of ice-sheet motion using satellite radar interferometry. *J. Glaciology*, 42(142), 564-575.

Joughin, I., S. Tulaczyk, M. Fahnestock, and R. Kwok. 1996. A mini-surge on the Ryder Glacier, Greenland observed via satellite radar interferometry. *Science*, 274, 1525-1530.

Kwok R; Fahnestock MA, Ice sheet motion and topography from radar interferometry, *IEEE Trans Geosci. And Rem. Sens.*, 1996, Vol 34, Iss 1, pp 189-200

Mote, T.L., and C.M. Rowe, 1996. A Comparison of Microwave Radiometric Data and Modeled Snowpack Conditions for Dye-2, Greenland. *Meteorology and Atmospheric Physics*, 59, 245-256.

Rignot, E., 1996. Tidal motion, ice velocity and melt rate of Petermann Gletscher, Greenland, measured from radar interferometry, *J. Glaciol*, 42: (142) 476-485.

Shuman CA; Fahnestock MA; Bindschadler RA; Alley RB; Stearns CR, 1996. Composite temperature record from the Greenland summit, 1987-1994: Synthesis of multiple automatic weather station records and SSM/I brightness temperatures, *J. Clim.* Vol 9, Iss 6, pp 1421-1428

Stroeve, J., M. Haefliger, and K. Steffen, 1996. Surface temperature fro ERS-1 ATSR infrared thermal satellite data in Polar regions, *J. Appl. Meteorol.*, 35(8), 1231-1239.

**1997**

Abdalati, W. and Steffen, K., 1997. Snow melt on the Greenland ice sheet as derived from passive microwave satellite data. *Journal of Climate*, Vol. 10, No. 2, pp. 165-175.

Abdalati, W. and Steffen, K, 1997. The effect of the Mt. Pinatubo eruptions on the Greenland ice sheet melt conditions. *Geophysical Research Letters*, Vol. 24, No. 14, pp. 1795-1797.

Allen C, Gogineni S, Wohletz B, Jezek K, Chuah T, 1997. Airborne radio echo sounding of outlet glaciers in Greenland, *Int. J. Rem. Sens.*, 18: (14) 3103-3107

Chen QS, Bromwich DH, Bai LS, 1998. Precipitation over Greenland retrieved by a dynamic method and its relation to cyclonic activity. *J. Climate* 10: (5) 839-870.

Dahl-Jensen D, Gundestrup NS, Keller K, Johnsen SJ, Gogineni SP, Allen CT, Chuah TS, Miller H, Kipfstuhl S, Waddington ED, 1997. A search in north Greenland for a new ice-core drill site, *J. Glaciol.* 43: (144) 300-306

Davis, C.H., 1997. A robust threshold retracking algorithm for measuring ice-sheet surface elevation change from satellite radar altimeters," *IEEE Transactions on Geoscience & Remote Sensing*, Vol. 35, No. 4, pp. 974-979.

Joughin I., M. Fahnestock, S. Ekholm, and R. Kwok. 1997. Balance Velocities for the Greenland Ice Sheet, *Geophys. Res. Lett.*, 24(23), 3045-48.

Nolin, A. and J. Stroeve, 1997. The Changing Albedo of the Greenland Ice Sheet: Implications for Climate Change, *Annals of Glaciology*, Vol. 25, 51-57.

Rignot, E., S.P. Gogineni, W.B. Krabill, and S. Ekholm, 1997. North and northeast Greenland ice discharge from satellite radar interferometry, *Science*, 276: (5314) 934-937 MAY 9 1997

Rignot, E., S.P. Gogineni, W.B. Krabill, and S. Ekholm, 1997. Mass balance of North Greenland – Response, *Science* , 278: (5336) 209-209

Shuman CA; Alley RB; Fahnestock MA; Fawcett PJ; Bindschadler RA; White JWC; Grootes PM; Anandakrishnan S; Stearns CR, 1997. Detection and monitoring of stratigraphic markers and temperature trends at the Greenland Ice Sheet Project 2 using passive-microwave remote-sensing data, *J. Geophys. Res – Oceans*, Vol 102, Iss C12, 26877-26886

Stroeve, J., and A. Nolin, 1997. The changing albedo of the Greenland ice sheet: implications for climate modeling, Ann. of Glaciol. 25, 51-57.

Stroeve, J., A. Nolin, and K. Steffen, 1997. Comparison of AVHRR-Derived and in-situ Surface Albedo over the Greenland Ice Sheet, *Remote Sensing of the Environment*, Vol. 62, N3, 262-276.

Wahr, John M. and Dazhong Han, 1997. Predictions of Crustal Deformation Caused by Changing Polar Ice on a Visco-Elastic Earth, *Surveys in Geophysics.*, 18, 303-312.

Zwally, H.J., and M.B. Gioviento, 1997. Annual sea level variability induced by changes in sea ice extent and accumulation on ice sheets: an assessment based on remotely sensed data, *Surveys in Geophysics*, 18: 327-340.

**1998**

Abdalati, W. and Steffen, K., 1998. Accumulation and hoar effects on microwave emission in the Greenland ice sheet dry snow zones. *J. Glaciol.*, 148, 523-531.

Anklin, M., R.C. Bales. E. Mosley-Thompson, and K. Steffen, 1998. Annual accumulation at two sites in northwestern Greenland during recent centuries, *J. Geophys. Res*. 103: (D22) 28775-28783

Appenzeller, C., T.F. Stocker, and M. Anklin, 1998 North Atlantic Oscillation dynamics recorded in Greenland ice cores, *Science*, **282**: (5388) 446-449.

Bentley, C.R. and J.M. Wahr, 1998. Satellite Gravity and the Mass balance of the Antarctic Ice Sheet, *J. Glaciol.*, 44(146), 207-213.

Bromwich, D. H., R. I. Cullather, Q-s. Chen, and B. Csatho, 1998. Evaluation of recent precipitation studies for the Greenland Ice Sheet. *Journal of Geophysical Research – Atmospheres*, 130: (D20) 26007-26024.

Davis, C.H., C. A. Kluever, and B.J. Haines, 1998. Elevation change of the southern Greenland ice sheet, *Science*, 27 March 1998, Vol. 279, pp. 2086-2088.

Davis, C.H., C.A. Kluever, and B.J. Haines, 1998. Response: growth of the southern Greenland ice sheet, *Science*, Vol. 281, 28 August 1998, p. 1251-51a.

Gogineni, S., T. Chuah, S. Allen, K. Jezek and R. K. Moore, 1998. An improved coherent radar depth sounder,, *Journal of Glaciology*, 148, 657-667.

Joughin I., R. Kwok, and M. Fahnestock. 1998. Interferometric estimation of three-dimensional ice-flow using ascending and descending passes. *IEEE Trans. Geosci. Rem. Sen.*, 36(1), 1998.

Jouzel, J., R.B. Alley, K.M. Cuffery, W. Dansgaard, P.Grootes, G. Hoffman, S.J. Johnsen, R.D. Koster,, D. Peel, C.A. Shuman, M. Stievenard, and J.W.C. White, 1998. Validity of the temperature reconstruction from water isotopes in ice cores, GISP2-GRIP Compendium Volume, *J. Geophys. Res*. 102(C12), 26471-26488.

Legarsky J, Wong A, Akins T, Gogineni SP, 1998. Detection of hills from radar data in central-northern Greenland, *J. Glaciol*, 44: (146) 182-184.

Mote, T.L., 1998. Mid-tropospheric Circulation and Surface Melt on the Greenland Ice Sheet. Part I: Atmospheric Teleconnections. *International Journal of Climatology*, 18, 111-130.

Mote, T.L., 1998 Mid-tropospheric Circulation and Surface Melt on the Greenland Ice Sheet. Part II: Synoptic Climatology. *International Journal of Climatology*, 18, 131-146.

Rignot, E. 1998. Hinge line migration of Petermann Gletscher, north Greenland, detected using satellite-radar interferometry, *J. Glaciol.*, 44(148), 469-476.

Scambos TA; Fahnestock MA, 1998. Improving digital elevation models over ice sheets using AVHRR - based photoclinometry, *J. Glaciol.*, Vol 44, No. 146, 97-103

Shuman CA; Alley RB; Fahnestock MA; Bindschadler RA; White JWC; Winterle J; McConnell JR, 1998. Temperature history and accumulation timing for the snowpack at GISP2, central Greenland *J. Glaciol.*, Vol 44, Iss 146, pp 21-30

Serreze, M., J. Key, J. Box, J. Maslanik, and K. Steffen, 1998. A new monthly climatology of global radiation for the Arctic and comparison with NCEP-NCAR reanalysis and ISCCP-C2 field, *J. Climate*, 11, 121-136.

Stroeve, J., and K. Steffen, 1998. Variability of AVHRR-derived clear-sky surface temperature over the Greenland ice sheet, J. Appl. Meteorol., 37, 23-31.

Stroeve, J. and K. Steffen, 1998. Variability of AVHRR-derived Clear Sky Surface Temperature over the Greenland Ice Sheet, *Journal of Applied Meteorology*, Vol. 37, No. 1, 23-31.

Thomas, R. H., B. M. Csatho, S. Gogineni, K. C. Jezek, and K. Kuivinen, 1998. Thickening of the western part of the Greenland ice sheet. *J. Glaciol.*, **44**(148), 651-656.

van der Veen, C. J., W. B. Krabill, B. M. Csatho, and J. F. Bolzan, 1998. Surface roughness on the Greenland ice sheet from airborne laser altimetry. *Geophysical Research Letters*, Vol. 25, No. 20, pp. 3887-3890.

Wahr, J. and D. Han, 1998. Geodetic Techniques for Estimating Changes in Polar Ice, in *Dynamics of the Ice Age Earth; a Modern Perspective*, P. Wu ed., pages 497-508.

Zwally, H.J., A.C. Brenner, J.P. DiMarzio, 1998, Technical comment: growth of the southern Greenland ice sheet, *Science*, Vol. 281, 28 August 1998, p. 1251.

**1999**

Abdalati, W. and W.B. Krabill, W.B., in press. Calculation of ice velocities in the Jakobshavn Isbrae area using airborne laser altimetry, *Remote Sensing of Environment*.

Krabill, W.B., E. Frederick, S. Manizade, C. Martin, J. Sonntag, R. Swift, R. Thomas, W. Wright, J. Yungel, Rapid Thinning of Parts of the Southern Greenland Ice Sheet, *Science*.

**In press**

Joughin I., M. Fahnestock, R. Kwok, P. Gogineni, and C. Allen. in press. Ice Flow of Humboldt, Petermann, and Ryder Glaciers, North Greenland. *J. Glaciol*

Long, D.G., and M.R. Drinkwater, in press. Cryosphere Applications of NSCAT Data, *IEEE Trans. Geosci. and Remote Sens.*

Steffen, K., Abdalati, W., and Sherjal, I., in press. Hoar development on the Greenland ice sheet. *Journal of Glaciology*.

# REPORT DOCUMENTATION PAGE

*Form Approved*
*OMB No. 0704-0188*



**1. AGENCY USE ONLY** *(Leave blank)*

**2. REPORT DATE**
April 1999

**3. REPORT TYPE AND DATES COVERED**
Technical Memorandum

**4. TITLE AND SUBTITLE**
Program for Arctic Regional Climate Assessment (PARCA)
Greenland Science and Planning Meeting

**5. FUNDING NUMBERS**
Code 971

**6. AUTHOR(S)**
Progam Scientist: Dr. Sivaprasad Gogineni
Project Scientist: Robert H. Thomas
Editor: Dr. Waleed Abdalati

**7. PERFORMING ORGANIZATION NAME(S) AND ADDRESS (ES)**
Laboratory for Hydrospheric Processes
Goddard Space Flight Center
Greenbelt, Maryland 20771

**8. PEFORMING ORGANIZATION REPORT NUMBER**
99E01109

**9. SPONSORING / MONITORING AGENCY NAME(S) AND ADDRESS (ES)**
National Aeronautics and Space Administration
Washington, DC 20546-0001

**10. SPONSORING / MONITORING AGENCY REPORT NUMBER**
TM–1999–209205

**11. SUPPLEMENTARY NOTES**
Gogineni: Dept. of Electrical Engineering and Computer Science, The Univ. of Kansas, Lawrence, KS 66045
Thomas: EG&G Services, Inc., NASA Wallops Flight Facility

**12a. DISTRIBUTION / AVAILABILITY STATEMENT**
Unclassified–Unlimited
Subject Category: 48
Report available from the NASA Center for AeroSpace Information,
7121 Standard Drive, Hanover, MD 21076-1320. (301) 621-0390.

**12b. DISTRIBUTION CODE**

**13. ABSTRACT** *(Maximum 200 words)*

The Program for Arctic Regional Climate Assessment (PARCA) is a NASA-sponsored initiative with the prime objective of understanding the mass balance of the Greenland ice sheet. In October 1998, PARCA investigators met to review activities of the previous year, assess the program's progress, and plan future investigations directed at accomplishing that objective. Some exciting results were presented and discussed, including evidence of dramatic thinning of the ice sheet near the southeastern coast. Details of the investigations and many of the accomplishments are given in this report, but major highlights are given in the Executive Summary of the report.

**14. SUBJECT TERMS**
PARCA, Greenland, ice sheet

**15. NUMBER OF PAGES**
94

**16. PRICE CODE**

| 17. SECURITY CLASSIFICATION OF REPORT | 18. SECURITY CLASSIFICATION OF THIS PAGE | 19. SECURITY CLASSIFICATION OF ABSTRACT | 20. LIMITATION OF ABSTRACT |
|---|---|---|---|
| Unclassified | Unclassified | Unclassified | UL |